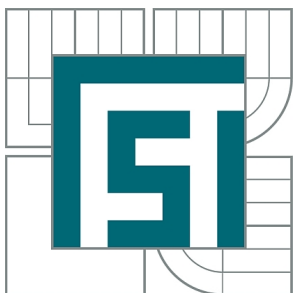


VYSOKÉ UČENÍ TECHNICKÉ V BRNĚ

BRNO UNIVERSITY OF TECHNOLOGY



FAKULTA STROJNÍHO INŽENÝRSTVÍ
LETECKÝ ÚSTAV

FACULTY OF MECHANICAL ENGINEERING
INSTITUTE OF AEROSPACE ENGINEERING

MODIFIKACE LETOUNU EV-55 PRO PŘISTÁNÍ NA VODNÍ HLADINĚ

EV-55 AIRCRAFT MODIFICATION FOR WATER LEVEL LANDING

DIPLOMOVÁ PRÁCE

MASTER'S THESIS

AUTOR PRÁCE

AUTHOR

Bc. JAN ŠPONER

VEDOUCÍ PRÁCE

SUPERVISOR

Ing. Ladislav Chybík

BRNO 2013

Vysoké učení technické v Brně, Fakulta strojního inženýrství

Letecký ústav

Akademický rok: 2013/14

ZADÁNÍ DIPLOMOVÉ PRÁCE

student(ka): Bc. Jan Šponer

který/která studuje v **magisterském studijním programu**

obor: **Stavba letadel (2301T039)**

Ředitel ústavu Vám v souladu se zákonem č.111/1998 o vysokých školách a se Studijním a zkušebním řádem VUT v Brně určuje následující téma diplomové práce:

Modifikace letounu EV-55 pro přistání na vodní hladině

v anglickém jazyce:

EV-55 aircraft modification for water level landing

Stručná charakteristika problematiky úkolu:

Pro současný letoun EV-55 zpracujte návrh modifikací nutných pro přistání na vodní hladině. Zhodnoťte varianty plováků nebo člunu a vybranou variantu rozpracujte do konstrukčního návrhu a proveďte pevnostní analýzu.

Cíle diplomové práce:

Pro současný letoun EV-55 předběžně navrhnete hydroplán s variantou plováky nebo variantu létající člun a navržené varianty kvantitativně porovnejte.

Pro vybranou variantu stanovte zatížení a proveďte pevnostní analýzu.

Během práce postupujte dle pokynů vedoucího DP.



[Handwritten signature]

[Handwritten signature]

Seznam odborné literatury:

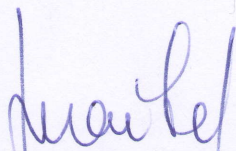
- [1] Stavební předpis CS-23 a FAR part 23
- [2] Konstrukční podklady společnosti Evektor, s.r.o.
- [3] David B. Thurston, Amphibian Aircraft Design, Business Aircraft Meeting, Wichita, Kansas, April 2 – 5, 1974
- [4] J. Tichý, P. Patek, Teória lodě, Slovenská technická univerzita v Bratislavě, 2006
- [5] E. F. Bruhn, Analysis and Design of Flight Vehicle Structures, Jacobs Pub, 2nd Edition, 1973

Vedoucí diplomové práce: Ing. Ladislav Chybík

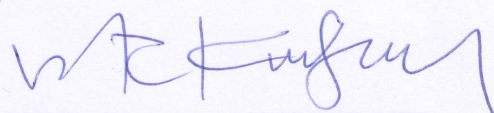
Termín odevzdání diplomové práce je stanoven časovým plánem akademického roku 2013/14.

V Brně, dne 18.11.2013





doc. Ing. Jaroslav Juračka, Ph.D.
Ředitel ústavu



prof. RNDr. Miroslav Doupovec, CSc., dr. h. c.
Děkan

ABSTRACT

Modification of the contemporary terrestrial version of EV-55 aeroplane for the possibility of water level landing is considered in this Masters Thesis. The aim is to find a design solution which does not lead to significant structural modifications in the airframe and meet Certification Specification 23 (CS 23). Weight analysis of the modified aeroplane is made and the water loads determined in accordance with CS 23. The connecting frame is designed in accordance with water loads and stress analysis for each element and fastener is performed. These values are compared with ground loads. Finally, flight performance, such as maximal horizontal speed, rate of climb, range and endurance are determined.

KEYWORDS

seaplane, hydroplane, float, hydrostatic, hull, EV-55 Outback, Evektor, NASTRAN, strut

ABSTRAKT

Diplomová práce se zabývá modifikací stávající pozemní verze letounu EV-55 pro možnost přistání na vodní hladině. Snahou je najít takovou variantu, která nepovede k výrazným konstrukčním zásahům do draku letounu a bude vyhovovat stavebnímu předpisu CS 23, zejména požadavkům týkající se plovatelnosti a stability na vodě. Je proveden hmotový rozbor modifikované verze a s tím související omezení hmotové obálky a rozsahu centráží. Zatížení od vody je spočítáno v souladu s CS 23. Pro toto zatížení je následně navrženo konstrukční řešení uchycení plováků k trupu a provedena pevnostní kontrola jednotlivých prvků a spojovacích uzlů. Tyto hodnoty jsou dále porovnány s pozemními případy zatížení a stanoveny součinitele rezerv. V závěru jsou spočítány letové výkony: maximální horizontální rychlost, stoupavost, dolet a vytrvalost.

KLÍČOVÁ SLOVA

hydroplán, plovák, hydrostatika, trup, EV-55 Outback, Evektor, NASTRAN, vzpěra

DECLARATION

I declare that I have elaborated my master's thesis on the theme of "EV-55 aircraft modification for water level landing" independently, under the supervision of the master's thesis supervisor and with the use of technical literature and other sources of information which are all quoted in the thesis and detailed in the list of literature at the end of the thesis.

As the author of the master's thesis I furthermore declare that, concerning the creation of this master's thesis, master's thesis, I have not infringed any copyright. In particular, I have not unlawfully encroached on anyone's personal copyright and I am fully aware of the consequences in the case of breaking Regulation § 11 and the following of the Copyright Act No 121/2000 Vol., including the possible consequences of criminal law resulted from Regulation § 152 of Criminal Act No 140/1961 Vol.

Brno

.....

(author's signature)

I would like to thank all my family who supported me while studying at the University. My thanks also has to go to the employees of the analysis and simulation department of Evektor company who were my mentors throughout creating of this work.

CONTENTS

1	Nomenclature	11
2	Objective	17
2.1	Used procedure	17
3	Introduction	18
3.1	History of seaplanes	18
3.2	Manufacturing time line	18
3.3	General requirements	19
4	General technical description of EV-55 aeroplane	20
4.1	Overview	20
4.2	Wing	20
4.3	Fuselage	20
4.4	Landing gear	20
4.5	Flight performance	22
5	Theoretical background	23
5.1	Basic terms	23
5.2	Basic parts of a float	23
5.3	Hydrodynamic characteristics of a float	24
5.3.1	Boat hull	24
5.3.2	Flying boat hull	24
5.3.3	Seaplane Float	25
5.4	Hydrodynamic drag of the float	26
6	Meeting the regulations	27
7	Conceptual design	32
7.1	Introduction	32
7.2	EV-55 as a flying boat	32
7.2.1	The pros and cons of a flying boat	35
7.3	EV-55 as a float seaplane	36
7.3.1	The pros and cons of a float seaplane	37
7.4	Conclusion	37

8	Competitive seaplanes	39
8.1	Graphs	39
9	Coordination system	42
9.1	The aeroplane coordination system	42
9.2	The float coordination system	42
9.3	Mutual position of ACS and FCS	42
9.4	The centre of gravity coordination system	43
10	Shape of the float	44
10.1	Determination of the float shape	44
10.2	Important angles	44
11	Hydrostatic calculations	45
11.1	A Volume	45
11.2	Stability	45
11.2.1	Conditions of equilibrium	45
11.2.2	Stable condition	46
11.3	Lateral and vertical position of the floats	48
11.4	Longitudinal position of the floats	51
11.5	Waterline position	51
11.6	Waterline position when using full thrust	56
11.7	Reed's diagram	57
12	Weight breakdown	60
12.1	Weight of the floats	60
12.2	Terrestrial version of EV-55	62
12.2.1	Moment of inertia	62
12.3	Seaplane version of EV-55	63
12.3.1	Moment of inertia	66
12.4	Ratio of distance	68
13	Speed corrections	69
13.1	Lift curve correction	69
13.2	Weight correction	69
13.3	Centre of gravity correction	70
14	Water loads	72
14.1	Symmetrical step landing case	72
14.2	Symmetrical bow landing case	74
14.3	Symmetrical stern landing case	77

14.4	Unsymmetrical landing case	79
14.5	Take-off case	80
14.6	Hydrostatic drag	81
14.7	Summary	82
15	Attachment Points	84
15.1	Front attachment points	84
15.2	Aft attachment points	86
16	Stress analysis	87
16.1	Ultimate load	87
16.2	General description	91
16.3	Finite Element Method - description	92
16.3.1	FEM model of the floats	94
16.3.2	FEM model of the struts	94
16.3.3	FEM model of the horizontal beams	95
16.3.4	RBE2 and RBE3 elements	96
16.3.5	Main leg beams and shear wall	96
16.4	Finite Element Method - results	98
16.4.1	Reaction forces - Connection Points CP1, CP2 and CP3	98
16.4.2	Front Frame	100
16.4.3	Aft Frame	112
16.5	Attachment points at the fuselage - front frame	120
16.6	Attachment points at the fuselage - aft frame	122
16.6.1	Front landing gear spar	122
17	Flight Performance	129
17.1	Drag	129
17.1.1	Floats	129
17.1.2	Struts	129
17.1.3	Summary	132
17.2	Drag polar	132
17.3	Maximal horizontal speed	135
17.4	Climbing performance	139
17.5	Range and Endurance	141
17.5.1	Payload configurations	143
17.5.2	Range	145
17.5.3	Endurance	148
18	Conclusion	151

Bibliography	155
List of appendices	163
A Competitive seaplanes	164
B K_1 factor graphs	165
C Summary of the water loads	168
D Complete weight breakdown	169
E Moments of inertia	171
F Input data-PBEAM elements-floats	172
G Input data - PROD and PBEAM elements - struts and horizontal beams	173

1 NOMENCLATURE

a	[m]	Distance between c.b. and c.g.
a	[m]	Length of semi-major axis of the ellipse.
a	[m]	Vertical position of the floats
A, A_{wing}	[m^2]	Wing area
A_{br}	[m^2]	Projecting bearing area
A_{wp}	[m^2]	Area of the floatation waterplane
A	[m^2]	Area of the cross-section
b	[m]	Track of the floats
b	[m]	Righting arm
b	[m]	Horizontal distance between c.b. and c.g.
b	[m]	Length of semi-minor axis of the ellipse.
b_f	[m]	Length of the fuselage
$\overline{BB_1}$	[m]	Distance between buoyant forces before and after heeling
\overline{BM}	[m]	Metacentric radius
c	[1]	Wind gust coefficient
c	[m]	Distance between chine and keel of the float
$c.g.ref$	[m]	Reference c.g. position
$c.g.comp$	[m]	Computed c.g. position
C	[PAX]	Passengers
C_D	[1]	Drag coefficient
$C_{add,total}$	[1]	Total additional drag coefficient
$C_{D,ellipse}$	[1]	Drag coefficient of the ellipse cross-section
$C_{D,int,A}$	[1]	Interference Drag coefficient between strut and wall related to the wing area
$C_{D,int,t}$	[1]	Interference Drag coefficient between strut and wall related to the thickness
$C_{D,float}$	[1]	Drag coefficient of the float related to the main rib
$C_{D,float,A}$	[1]	Drag coefficient of the float related to the wing area
$C_{D,floats,A}$	[1]	Drag coefficient of the floats related to the wing area
$C_{D,strut,A}$	[1]	Drag coefficient of the strut related to the wing area
$C_{D,strut,total}$	[1]	Total drag coefficient of the strut
$C_{D,struts,A}$	[1]	Drag coefficient of the struts related to the wing area
C_L	[1]	Lift coefficient
C_{Lref}	[1]	Maximum lift coefficient at the desired c.g.
C_{Lcomp}	[1]	maximum lift coefficient at the computed c.g.

C_{TO}	[1]	Empirical seaplane operations factor
C_1	[1]	Empirical seaplane operations factor
d	[m]	Distance between point of the thrust force and c.g.
D	[m]	Diameter of the pin
D_F	[N]	Form drag
D_{FR}	[N]	Friction drag
D_{HD}	[N]	Hydrodynamic drag force
D_{HS}	[N]	Hydrostatic drag force
e	[m]	Distance between c.g. and acting point of hydrostatic force
E	[MPa]	Young's modulus
EAS	[m · s ⁻¹]	Equivalent Air speed
F_b	[N]	Buoyant force
F_{bru}	[MPa]	Ultimate tensile strength of lug
F_{crit}	[N]	Critical compressive force
F_{MLi}	[N]	Force at Main Leg from FEM model
F_{Ri}	[N]	Force at Rod from FEM model
F_{RwA}	[N]	Water reaction force for symmetrical step landing
$F_{RwA,x}$	[N]	Water reaction force in x-direction for symmetrical step landing
$F_{RwA,y}$	[N]	Water reaction force in y-direction for symmetrical step landing
$F_{RwA,z}$	[N]	Water reaction force in z-direction for symmetrical step landing
F_{RwB}	[N]	Water reaction force for symmetrical bow landing
$F_{RwB,x}$	[N]	Water reaction force in x-direction for symmetrical bow landing
$F_{RwB,y}$	[N]	Water reaction force in y-direction for symmetrical bow landing
$F_{RwB,z}$	[N]	Water reaction force in z-direction for symmetrical bow landing
F_{RwC}	[N]	Water reaction force for symmetrical stern landing
$F_{RwC,x}$	[N]	Water reaction force in x-direction for symmetrical stern landing
$F_{RwC,y}$	[N]	Water reaction force in y-direction for symmetrical stern landing
$F_{RwC,z}$	[N]	Water reaction force in z-direction for symmetrical stern landing
$F_{RwD,y}$	[N]	Water reaction force for unsymmetrical landing

$F_{RwD,x}$	[N]	Water reaction force in x-direction for unsymmetrical landing
$F_{RwD,y}$	[N]	Water reaction force in y-direction for unsymmetrical landing
$F_{RwD,z}$	[N]	Water reaction force in z-direction for unsymmetrical landing
F_{RwE}	[N]	Water reaction force for take-off case
F_x	[N]	Force in x-direction of appropriate coordination system
F_y	[N]	Force in y-direction of appropriate coordination system
F_z	[N]	Force in z-direction of appropriate coordination system
g	$[m \cdot s^{-2}]$	Gravitational acceleration
g	[mm]	Distance between lugs
G	[MPa]	Shear modulus
$\overline{gg_1}$	[m]	Distance between c.g. position of volumes dV_1 and dV_2
\overline{GM}	[m]	Metacentric height
\overline{GZ}	[m]	Distance between buoyant force and weight
h	[m]	Distance between flanges
H	[m]	Altitude
H_a	[m]	Waterline position on aft scale
H_f	[m]	Waterline position on front scale
I_x	$[m^4]$	Moment of inertia of floatation waterplane
I_y	$[m^4]$	Moment of inertia of floatation waterplane
$I_{x.c.g.}$	$[kg \cdot m^2]$	Moment of inertia of aeroplane to the c.g. coordination system
$I_{y.c.g.}$	$[kg \cdot m^2]$	Moment of inertia of aeroplane to the c.g. coordination system
$I_{z.c.g.}$	$[kg \cdot m^2]$	Moment of inertia of aeroplane to the c.g. coordination system
I_{xG}	$[kg \cdot m^2]$	Moment of inertia of aeroplane to the global coordination system
I_{yG}	$[kg \cdot m^2]$	Moment of inertia of aeroplane to the global coordination system
I_{zG}	$[kg \cdot m^2]$	Moment of inertia of aeroplane to the global coordination system
I_{x0}	$[m^4]$	Moment of inertia of floatation water-plane to its x_f axis

J	$[kg \cdot m^2]$	Torsional constant
J_y	$[kg \cdot m^2]$	Moment of inertia of cross-section to its coordination system
J_z	$[kg \cdot m^2]$	Moment of inertia of cross-section to its coordination system
J_1	$[kg \cdot m^2]$	Minimum moment of inertia of the lug
K	[1]	Constant for twin-float seaplane
$KEAS$	$[kn]$	Equivalent Air speed in knots
$KTAS$	$[kn]$	True Air speed in knots
K_1	[1]	Empirical hull station weighing factor
l	$[m]$	Length of the float
l	$[m]$	Length of the strut
l_t	$[m]$	length of the tail
l_a	$[m]$	Aft length of the float
l_f	$[m]$	Front length of the float
l_1	$[m]$	Length of the lug
L	$[m]$	Length of the element
$m_{acc+struts}$	$[kg]$	weight of struts and accessories
M	$[Nm]$	Righting moment
M_{wind}	$[Nm]$	Wind gust acting moment
MAC	$[m]$	Mean aerodynamic chord
m_{LW}	$[kg]$	Design landing weight
m_{MLW}	$[kg]$	Maximum Landing Weight
m_{MTOW}	$[kg]$	Maximum Take-off Weight
M_T	$[Nm]$	Moment created by thrust force
m_{TOW}	$[kg]$	actual take-off weight of the seaplane
n	[1]	Number of the struts
n_{wA}	[1]	Water reaction factor for symmetrical step landing
n_{wB}	[1]	Water reaction factor for symmetrical bow landing
n_{wC}	[1]	Water reaction factor for symmetrical stern landing
n_{wD}	[1]	Water reaction factor for unsymmetrical landing case
n_{wE}	[1]	Water reaction factor for take-off case
P	$[N]$	Force at the lug
P_{bru}	$[N]$	Allowable ultimate load for shear-bearing failure
P_{ava}	$[W]$	Power available

P_{engine}	$[W]$	Power of the engine
P_{req}	$[W]$	Power required
P_{tu}	$[N]$	Allowable ultimate load for transversal shear-bearing failure
P_u	$[N]$	Allowable ultimate load for axial tension failure
r_{xb}	$[1]$	Ratio of distance for bow landing
r_{xs}	$[1]$	Ratio of distance for stern landing
$R.F.$	$[-]$	Reserve factor
R_m	$[MPa]$	Tensile strength
$R_{p0.2}$	$[MPa]$	Yield strength
S	$[m^2]$	Wing area
t	$[mm]$	Thickness of the strut
t_1, t_{lug}	$[mm]$	Thickness of the lug
t_2	$[mm]$	Thickness of the lug
T	$[N]$	Thrust
TAS	$[m \cdot s^{-1}]$	True Air speed
T_{ava}	$[N]$	Thrust available
T_{req}	$[N]$	Thrust required
u	$[m \cdot s^{-1}]$	Speed of the wind
V	$[m^3]$	Immersed volume of the floats
V	$[m \cdot s^{-1}]$	Speed
V_f	$[m^3]$	Volume of the float
V_{CR}	$[m \cdot s^{-1}]$	Critical speed
V_{LOF}	$[m \cdot s^{-1}]$	Lift-off speed
V_{max}	$[m \cdot s^{-1}]$	Maximal horizontal speed
V_{ST}	$[m \cdot s^{-1}]$	Observed stalling speed
V_{S0}	$[m \cdot s^{-1}]$	Stall speed in landing configuration (Flaps 38°)
$V_{S0_{weight}}$	$[m \cdot s^{-1}]$	Corrected stall speed in landing configuration (Flaps 38°)
V_{S1}	$[m \cdot s^{-1}]$	Stall speed in specific configuration (Flaps 0°, 20°)
$V_{S1_{weight}}$	$[m \cdot s^{-1}]$	Corrected stall speed in specific configuration (Flaps 0°, 20°)
V_{TAS}	$[m \cdot s^{-1}]$	True Air speed
w	$[m \cdot s^{-1}]$	Climbing speed
w	$[m]$	Width of the flange
w	$[m]$	Width of the lug
w_{max}	$[m \cdot s^{-1}]$	Maximal climbing speed
W	$[N]$	Weight of the aeroplane
W_E	$[kg]$	Empty weight

W_f	[N]	Weight of the floats
W_S	[kg], [lb]	Standard weight
W/S	[kg · m ⁻²]	Wing Loading
W_T	[kg], [lb]	Aeroplane weight at the stall
$x_{c.g.}, y_{c.g.}, z_{c.g.}$	[m]	Centre of gravity position
x_f, y_f, z_f	[m]	Coordinations for Float coordination system
x_G, y_G, z_G	[m]	Coordinations for Aeroplane coordination system
$x_{G-f}, y_{G-f}, z_{G-f}$	[m]	Distance between Aeroplane and Float coordination system
β	[°]	Angle of dead rise at the longitudinal station
η	[1]	Propeller efficiency
θ	[°]	Angle of heel
θ_{gust}	[°]	Angle between wind direction and lateral axis of the aeroplane
ρ	[kg · m ⁻³]	Density of fresh water, Density of air
ρ	[kg · m ⁻³]	Density of material
σ_B	[MPa]	Bending stress
σ_t	[MPa]	Tensile stress
$\bar{\sigma}$	[MPa]	Mises equivalent tensile stress
τ	[MPa]	Shear stress
ϕ	[°]	Angle of the float to the waterline in longitudinal direction
φ	[—]	Bending stiffness coefficient

Shortcuts:

ACS	Aeroplane coordination system
c.b.	Centre of buoyancy
c.g.	Centre of gravity
CS	Certification Specification
DOF	Degrees Of Freedom
FCS	Float coordination system
ISA	International Standard Atmosphere
LC	Load Case
RBE	Rigid Body Element
SL	Sea Level
SAVLE	System of automatic aeroplane computations
STOL	Short Take-off and Landing

2 OBJECTIVE

The objective of this master's thesis is to modify terrestrial version of EV-55 aeroplane to the seaplane. Evaluation between twin-float version and flying-boat modification is done. Construction design and stress analysis is required for selected modification.

2.1 Used procedure

Next steps are used during seaplane modification of EV-55 aeroplane.

A conceptual design - this is the first part that has to be done. There are several supposable options which could be used. They have advantages and disadvantages, as well. The selected option is developed later. The decision is based on current shape of the fuselage, water stability, drag and operational performances.

A shape - when the conceptual design is set, more accurate shape of a float or a hull is set. There is used cooperation with American company dealing with floats for seaplanes.

A volume - of the floats or a hull is set in accordance with CS 23.751 regulation and basic condition of buoyancy.

Weight - weight estimation is done in accordance with data found on Wipaire, Inc. web pages [25] and literature [18].

A float position - influences the stability of the seaplane and it is set in chapter 11 dealing with hydrostatic calculations.

A hydrostatic calculations - there is determined reasonable water stability on the basis of hydrostatic calculations and volume of the floats, water stability affected by wind and basic condition of buoyancy.

Water loads - during take-off and landing there are determined water loads in accordance with CS 23.525, CS 23.527, CS 23.529 and CS 23.531 regulations. Necessary computations are done in MATLAB and can be used for different input variables.

Attachment of the floats - tries to have minimal construction impact on the current version of the fuselage.

Struts layout - basic layout of the struts is done.

Stress analysis - in according to the geometry and layout of the struts, finite element methods to set the stress, needs to be done. After that, the reserve factors are determined for every construction element.

3 INTRODUCTION

This master's thesis is based on general requirement to be able to take-off and land with EV-55 Outback aeroplane on the water level. The main purpose of the thesis is to set necessary requirements that seaplanes should meet. Next main goal is to set appropriate seaplane configuration, which is going to be based on stability, CS-23 regulation, safety and present design of the fuselage. Set the load is obvious. After that, general design solution of the floats, struts and connection points will be set in according to load cases during landing and take-off.

3.1 History of seaplanes

The history of the seaplanes started in 1910. Probably the first take-off was made by French aviator Henri Fabre in Martinique, France. At the same time, Glenn H. Curtis and U. S. Navy started to collaborate on building and operating seaplanes of various types. At the beginning of the year 1911, he flew the first seaplane from the water in the United States.

First of all, the land-planes were converted to the seaplanes. The most critical part of the aeroplanes at the beginning of the aviation used to be engine. There were used engines that produced from 40 hp to 80 hp. It was not enough for successful take-off from water level with ordinary type of floats. Some investigation needed to be done. To decrease the drag, amphibians, flying-boats and single-floats seaplanes were tried. It had been shown, that main component of the drag during take-off, is the hydrodynamic drag. By appropriate shaping of the float, the hydrodynamic drag can be reduced. The substantial amount of research has been devoted to reduce the hydrostatic drag [16].

The first use of seaplanes was to carry payload from the coast to the patrol ships, photographing, observing, patrolling or for example mapping. Especially during First World War and Second World War, the seaplanes were used for scouting, fighting other aircraft, torpedoing, bombing or also for ground attack. Nowadays, the main purpose of the seaplanes is to carry passengers, cargo, mail, patients etc., especially to or from the hard accessible places on the World.

3.2 Manufacturing time line

The biggest production of the seaplanes was during First World War and also between the Wars. There were about 15 new types of seaplanes every year. At the end

of Second World War and especially after that there was rapid decrease of developing new seaplanes per year. Figure 3.1 will give a better overview. Data for this Figure are taken from literature [15]

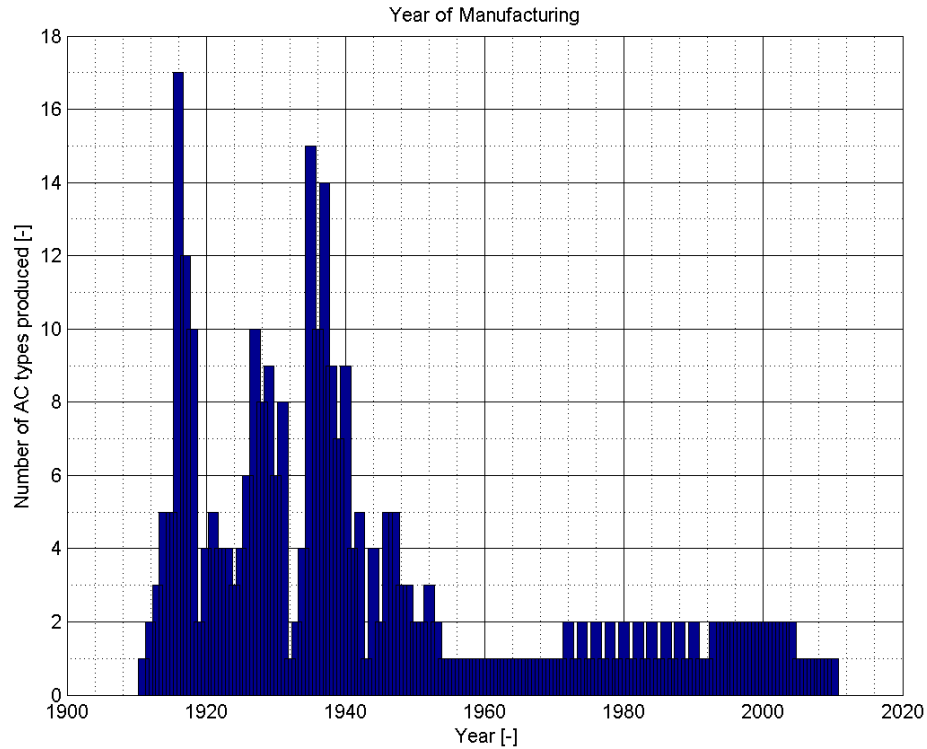


Fig. 3.1: Seaplane manufacturing timeline [15]

3.3 General requirements

Nowadays, there is effort to develop new type of seaplane that would correspond to present requirements. However, the requirements are very often contradictory. It means there always needs to be done compromise to satisfy huge amount of customers and meet all the necessary requirements.

The main requirement of the seaplane is to float on the water. Everything else has to be submitted to this requirement. Customers require a large range, huge horizontal speed and long endurance. They also want low operating cost and low-cost maintenance, long lifetime, high reliability. Very important is environment friendly factor. Most of the mentioned requirements above are unfortunately inversely proportional to the weight.

4 GENERAL TECHNICAL DESCRIPTION OF EV-55 AEROPLANE

4.1 Overview

EV-55 Outback is a turbo twin turboprop aeroplane powered by two PT6A-21 engines with four blade constant speed propeller. It is unpressurised all-metal high wing aircraft able to operate from paved and unpaved airfields. It is nine passenger aeroplane built up in according to European CS 23 regulations. Currently, two prototypes have been built¹. One flying prototype, the latter is for strength testing. Aeroplane can be built as passenger, cargo or combi version and there are ambulance and air-drop modifications available. From this point of view, the EV-55 aeroplane has a wide scope of use.

4.2 Wing

EV-55 is high wing configuration aeroplane - mounted on the upper side of fuselage. The wing is single-piece cantilever wing with two main spars. There are four pins connect the wing to the fuselage. The span is 16.10 meters and surface area of the wing is 25.187 square metres. It has trapezoidal shape of the wing and single - slotted Fowler flaps. There are also fuel tanks within the wing box.

4.3 Fuselage

Fuselage is typically for nine passengers and two pilots. Other modifications allow to carry three palettes or at least two configuration combine passengers and cargo. The pilot cabin is partly separated from passenger cabin. Pilots have their own doors. The doors for passengers are consist of two parts. The second one is used mainly for luggage. There is an emergency exit on the right side, as well.

4.4 Landing gear

Aeroplane has main landing gear attached to the two spars going through the fuselage. Steerable nose landing gear is attached to the bulkhead number three. Position of bulkhead number three is shown in Figure 9.1. This bulkhead will be used as a connection place for struts during seaplane modification.

¹Information from May, 2014

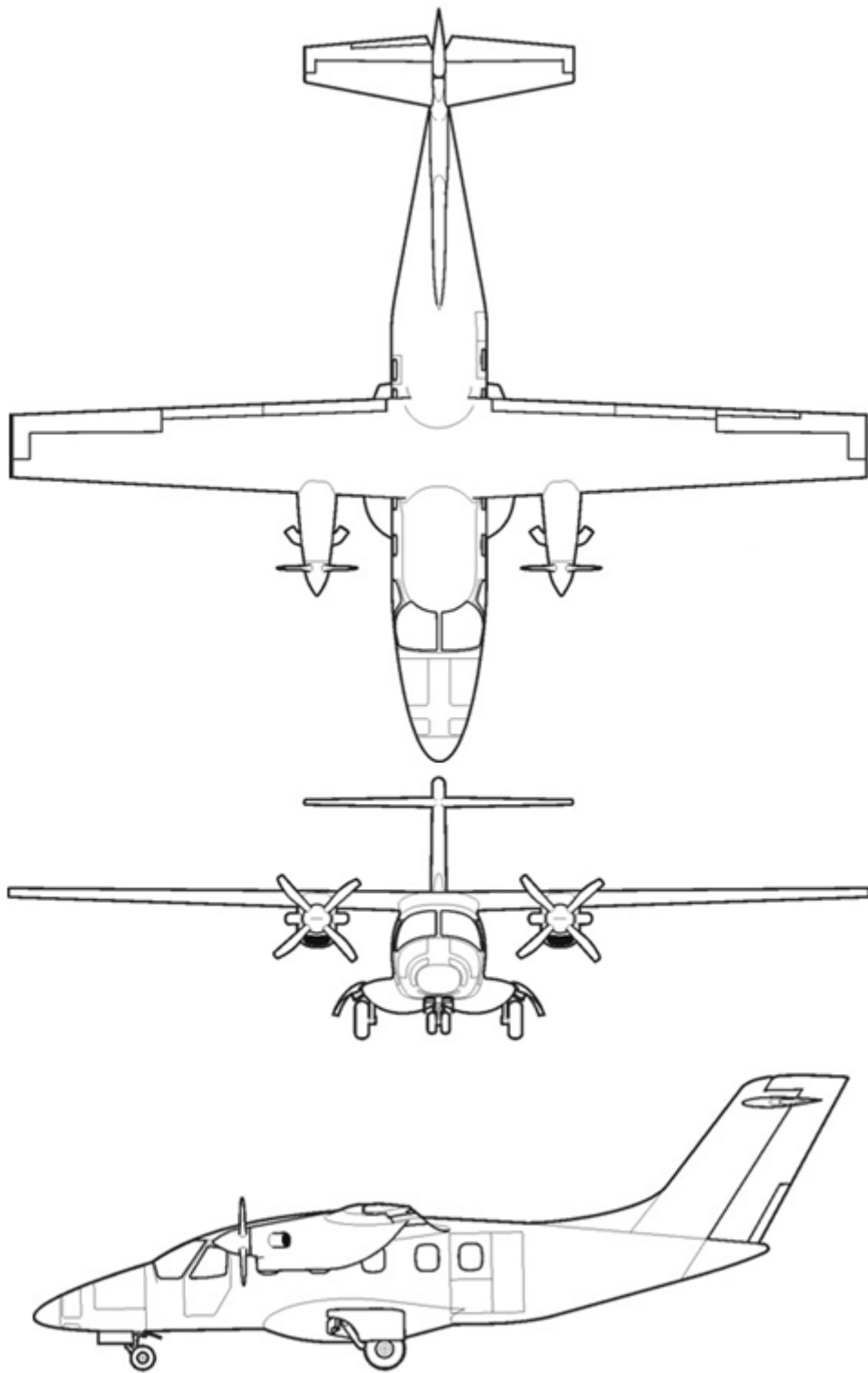


Fig. 4.1: Three-view drawing of the EV-55 Outback

4.5 Flight performance

Flight performance are listed below. All data are taken from corporate documents.

Tab. 4.1: Flight performance of EV-55

Speeds				
Max. speed of horizontal flight	220	KTAS	408	km/h TAS
Stall speed, 0° flaps	77	KEAS	143	km/h EAS
Stall speed, 38° flaps	64	KEAS	118	km/h EAS
Climb performance				
Both engines operative	1673	fpm	8.5	m/s
One engine in operative	453	fpm	2.3	m/s
Take-off performance (m_{MTOW})				
Ground run ISA, H = 0 ft	1122	ft	340	m
Total distance over 50 ft obstacle ISA, H = 0 ft (SL)	1378	ft	420	m
Total distance over 50 ft obstacle ISA, H = 0 ft (SL), STOL procedures	1224	ft	373	m
Ground run ISA +20 °C, H = 6,562 ft	1624	ft	495	m
Total distance over 50 ft obstacle ISA +20 °C, H = 6,562 ft	2001	ft	610	m
Landing performance (m_{MLW})				
Total distance over 50 ft obstacle ISA, H = 0 ft (SL)	1014	ft	309	m
Total distance over 50 ft obstacle ISA, H = 0 ft (SL), STOL procedures	1673	ft	510	m
Ground run ISA +20 °C, H = 6,562 ft	1391	ft	424	m
Total distance over 50 ft obstacle ISA +20 °C, H = 6,562 ft	1394	ft	425	m

5 THEORETICAL BACKGROUND

Before starting to solve specific problems and finding solutions, it is appropriate to introduce some basic terms used during seaplane design.

5.1 Basic terms

A seaplane is the aeroplane that is able to take-off and land only from the water level. This term is possible to use also for the seaplanes able to land also on the ground. A hydroplane is the same meaning as a seaplane.

A flying boat is a seaplane with a hull designed for floating. It has floating features of a boat and flying features of an aeroplane. Flying boat cannot land on the ground.

An amphibia is umbrella title for the seaplanes and the flying boats that are able to land on both the water level and the ground.¹

A float is a floating body which holds an seaplane above the water under the action of hydrostatic forces. If the float is moving forwards, hydrodynamic forces are formed.

5.2 Basic parts of a float

The float, shown in Figure 5.1, can be divided into two main parts: the fore-body and the after-body. The boundary of these parts is called step. The main rib is usually situated at the step position. The float can be equipped by rudder but it is not necessary for twin engine aeroplanes. There is a bumper at the bow of the float. Keel, deck and chine are other important terms.

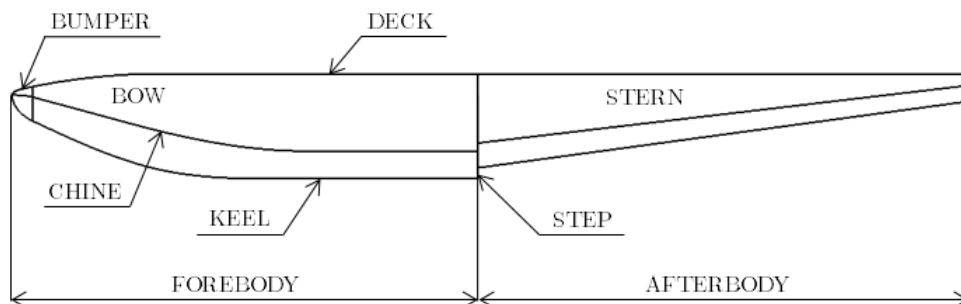


Fig. 5.1: Basic parts of the float

¹There will be used general expression 'seaplane' in this master's thesis.

5.3 Hydrodynamic characteristics of a float²

5.3.1 Boat hull

Buoyancy force is created by hydrostatic force. If the boat starts to move forward, the hydrodynamic drag grows proportionally to the square of the speed. It is not possible to use this boat shape for the floats or hull of the seaplane. The drag would be so great that the seaplane would never take-off. The dependence between hydrodynamic drag and forward speed is shown in the Figure 5.2.

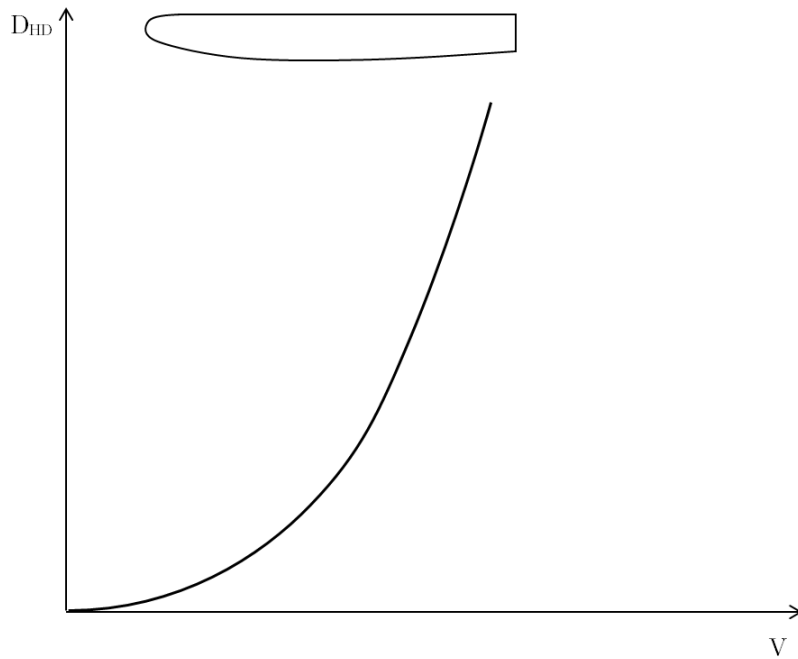


Fig. 5.2: Dependence between hydrodynamic drag D_{HD} and forward speed V [10]

5.3.2 Flying boat hull

Comparing to the boat hull, flying boat hull has a different shape of the hull. As it is shown in Figure 5.1, there is a step. This step helps much during take-off to decrease the hydrodynamic drag. The behaviour of the flying boat hull during slow speed is as same as it has been mentioned above at the subsection boat hull. During higher speed, the hydrodynamic buoyancy starts to lift up the hull out of the water. Then the hydrodynamic drag is almost constant. The main reason of decreasing the

²Figures in this section are originally taken from literature [10]. Unfortunately, the curves did not correspond to the assertion that the hydrodynamic drag grows proportionally to the square of the speed. Therefore Figures 5.2, 5.3 and 5.4 were corrected to meet previous assertion.

gradient of the hydrodynamic drag is decreasing of the spread area of the hull. The dependence between hydrodynamic drag and forward speed is shown in Figure 5.3.

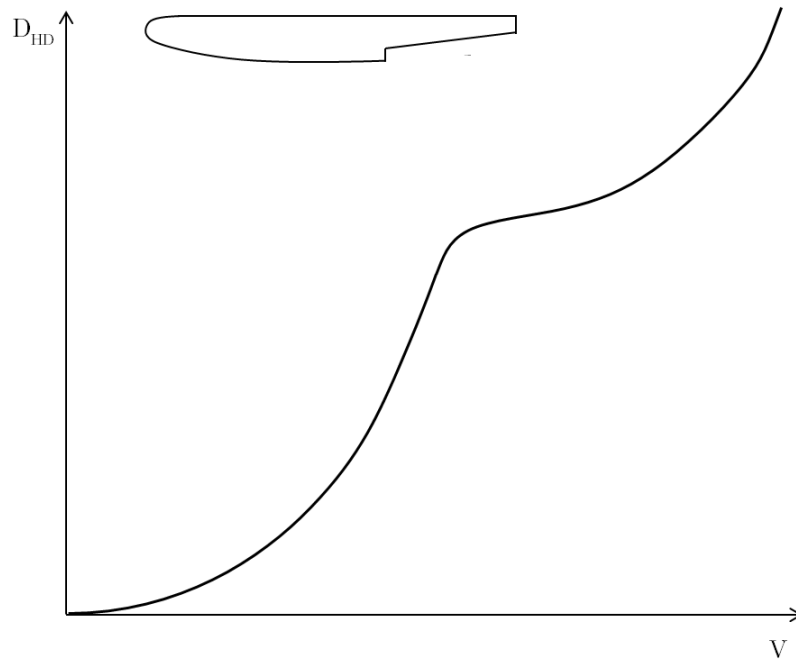


Fig. 5.3: Dependence between hydrodynamic drag D_{HD} and forward speed V [10]

5.3.3 Seaplane Float

Seaplane float has very similar shape as the flying boat hull. Only the position of the step is at different place. It is moved forward but still little bit behind the seaplane centre of gravity. Also, the process of the acceleration is as same as in previous version. However, when the float is getting out of the water, aerodynamic lift of the wing has larger and larger effect and hydrodynamic drag decreases. This aerodynamic force helps to get entire float out of the water. The weight equals the lift at V_{LOF} speed, hydrodynamic drag is nought and the seaplane, finally, lifts off. The dependence between hydrodynamic drag and forward speed is shown in Figure 5.4.

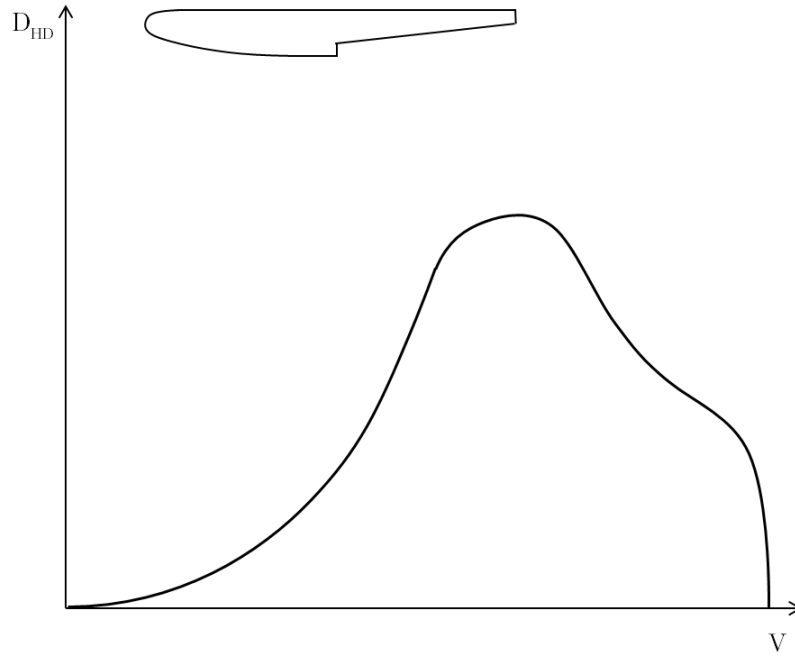


Fig. 5.4: Dependence between hydrodynamic drag D_{HD} and forward speed V [10]

Literature [10] mentions formula to determine critical speed V_{CR} and maximal hydrodynamic drag as follows:

$$D_{HD_{max}} = (0.15 \div 0.25) \cdot m_{TOW} \quad (5.1)$$

$$V_{CR} = (0.35 \div 0.45) \cdot V_{LOF} \quad (5.2)$$

where $D_{HD_{max}}$ is the maximal hydrodynamic drag, m_{TOW} is actual take-off weight, V_{LOF} is the lift-off speed and V_{CR} is the critical speed.

5.4 Hydrodynamic drag of the float

Hydrodynamic drag affects mainly the take-off distance of the seaplane. In general, the take-off distance should be as short as possible. Hydrodynamic drag consists of two components. Friction drag and form drag which depends on the shape of the float. The following applies:

$$D_{HD} = D_{FR} + D_F \quad (5.3)$$

where D_{HD} is the hydrodynamic drag, D_{FR} is the friction drag and D_F is the form drag.

6 MEETING THE REGULATIONS

To be able to certify seaplane, regulations has to be fulfilled. *CS 23* regulation is going to be fulfilled because EV-55 is developed in according to this regulation. Following paragraphs are taken from *CS 23* [5] regulation and there are comments describing how each paragraph is going to be fulfilled. These paragraphs has been also compared with Federal Aviation Regulations Part 23 [7]. There was not found any difference. Russian AP regulations have not been checked.

CS 23.231 Longitudinal stability and control

(b) A seaplane or amphibian may not have dangerous or uncontrollable porposing characteristics at any normal operating speed on the water.

For the first stage of development, longitudinal stability is checked and compared with recommended value in literature [14] and [16]. Some scaled tests in the tub has to be done in later stage of development.

CS 23.233 Directional stability and control

(a) A 90° cross-component of wind velocity, demonstrated to be safe for taxiing, take-off and landing must be established and must be not less than $0.2 \cdot V_{S0}$.

(d) Seaplanes must demonstrate satisfactory directional stability and control for water operations up to the maximum wind velocity specified in sub-paragraph (a).

Lateral stability is checked and compared with recommended value in literature [14] and [16]. Also, the Reed's diagram including wind influence is built. Demonstration of safe taxiing, take-off and landing is not part of this master's thesis and has to be done in later stage of development.

CS 23.237 Operation on water

Allowable water surface conditions and any necessary water handling procedures for seaplanes and amphibians must be established.

As stated previously, scaled tests in the tube has to be done in later stage of development.

CS 23.239 Spray characteristics

Spray may not dangerously obscure the vision of the pilots or damage the propellers or other parts of a seaplane or amphibian at any time during taxiing, take-off and landing.

Verified shape of the floats is used. It guarantees predictable spray characteristics and

it is sufficient for this development stage. It is necessary to test spray characteristics in later stage of development.

CS 23.301 Loads

(a) Strength requirements are specified in terms of limit loads (the maximum loads to be expected in service) and ultimate loads (limit loads multiplied by prescribed factors of safety). Unless otherwise provided, prescribed loads are limit loads.

The maximum possible loads are taken from load cases that are established in accordance with CS 23.521. The construction is dimensioned for this loads. Safety factor 1.5 is used.

(b) Unless otherwise provided, the air, ground and water loads must be placed in equilibrium with inertia forces, considering each item of mass in the aeroplane. These loads must be distributed to conservatively approximate or closely represent actual conditions. Methods used to determine load intensities and distribution on canard and tandem wing configurations must be validated by flight test measurement unless the methods used for determining those loading conditions are shown to be reliable or conservative on the configuration under consideration.

The main purpose is to design connection struts and not to determine load of the fuselage. Therefore the water loads are not placed in equilibrium with inertia forces but are placed in equilibrium with boundary conditions at specific single points.

CS 23.521 Water load conditions

(a) The structure of seaplanes and amphibians must be designed for water loads developed during take-off and landing with the seaplane in any attitude likely to occur in normal operation at appropriate forward and sinking velocities under the most severe sea conditions likely to be encountered.

(b) Unless a rational analysis of the water loads is made, CS 23.523 through CS 23.537 apply.

There is no rational analysis of the water loads in this master's thesis, thus paragraphs CS 23.523 through CS 23.537 are applied.

CS 23.523 Design weights and centre of gravity positions

(a) Design weights. The water load requirements must be met at each operating weight up to the design landing weight except that, for the take-off condition prescribed in CS 23.531, the design water take-off weight (the maximum weight for water taxi and take off run) must be used.

(b) Centre of gravity positions. The critical centres of gravity within the limits for

which certification is requested must be considered to reach maximum design loads for each part of the seaplane structure.

Extreme points of the weight envelope are used to meet requirements. There are included six, respectively five weight configurations.

CS 23.525 Application of loads

(a) Unless otherwise prescribed, the seaplane as a whole is assumed to be subjected to the loads corresponding to the load factors specified in CS 23.527.

(b) In applying the loads resulting from the load factors prescribed in CS 23.527, the loads may be distributed over the hull or main float bottom (in order to avoid excessive local shear loads and bending moments at the location of water load application) using pressures not less than those prescribed in CS 23.533 (b).

(c) For twin float seaplanes, each float must be treated as an equivalent hull on a fictitious seaplane with a weight equal to one-half the weight of the twin float seaplane.

(d) Except in the take-off condition of CS 23.531, the aerodynamic lift on the seaplane during the impact is assumed to be 2/3 of the weight of the seaplane. Load factors are computed in accordance with CS 23.527. It is assumed that each float carry one-half of the weight of the twin float seaplane.

CS 23.527 Hull and main float load factors

Load factors for landing conditions are computed in accordance with CS 23.527.

CS 23.529 Hull and main float landing conditions

Load factors from CS 23.527 are computed in accordance with landing conditions from CS 23.529.

CS 23.531 Hull and main float take-off condition

Load factors for take-off condition are computed in accordance with CS 23.531.

CS 23.533 Hull and main float bottom pressures

Bottom pressures are not computed in this master's thesis. These pressures are important to be able to design the float. This float is bought as a part from Wipaire Inc. company.

CS 23.535 Auxiliary float loads

There are not use any auxiliary floats.

CS 23.537 Sea wing loads

There are not use any auxiliary floats on the wing therefore the load factors determined from CS 23.527 and CS 23.531 can be used for this structure. This master's thesis does not deal with the wing inertia load.

CS 23.751 Main float buoyancy

(a) Each main float must have:

(1) A buoyancy of 80% in excess of the buoyancy required by that float to support its portion of the maximum weight of the seaplane or amphibian in fresh water; and

(2) Enough watertight compartments to provide reasonable assurance that the seaplane or amphibian will stay afloat without capsizing if any two compartments of any main float are flooded.

(b) Each main float must contain at least four watertight compartments approximately equal in volume.

Required volume for minimum buoyancy is increased by 80%. The density of the fresh water is used. Basic design of waterproof bulkheads is determined to provide flotation if two of them are flooded.

CS 23.753 Main float design

Each seaplane main float must meet the requirements of CS 23.521.

CS 23.755 Hulls

(a) The hull of a hull seaplane or amphibian of 680 kg (1 500 lb) or more maximum weight must have watertight compartments designed and arranged so that the hull, auxiliary floats and tyres (if used), will keep the aeroplane afloat without capsizing in fresh water when:

(1) For aeroplanes of 2 268 kg (5 000 lb) or more maximum weight, any two adjacent compartments are flooded;

It is calculated that even if two adjacent compartments are flooded, the seaplane will still float.

CS 23.757 Auxiliary floats

Auxiliary floats must be arranged so that when completely submerged in fresh water, they provide a righting movement of at least 1.5 times the upsetting moment caused by the seaplane or amphibian being tilted.

There are not use any auxiliary floats.

CS 23.925 Propeller clearance

(c) Water clearance. There must be a clearance of at least 46 cm (18 in) between each propeller and the water, unless compliance with CS 23.239 can be shown with a lesser clearance.

It is determined that the clearance between water level and blades of propeller is larger than 46 cm.

CS 23.1399 Riding light

(a) Each riding (anchor) light required for a seaplane or amphibian, must be installed so that it can:

(1) Show a white light for at least 3.2 km (2 miles) at night under clear atmospheric conditions; and

(2) Show the maximum unbroken light practicable when the aeroplane is moored or drifting on the water.

(b) Externally hung lights may be used.

Riding light is not goal of this master's thesis and can be solved in the last development stage.

7 CONCEPTUAL DESIGN

7.1 Introduction

As was already mentioned in Chapter 5, seaplanes can be divided into float seaplanes and flying boats. Both of them can be amphibian design or just a water-landing design. Mostly, amphibians are heavier than the latter. EV-55 is a terrestrial aeroplane and the conceptual design for both, a flying boat and a seaplane, is done. Additional landing gear attached to the floats weighs about 200 kg for the aeroplane, such as EV-55 is. Therefore, the modifications able to land only on the water level are going to be mentioned.

7.2 EV-55 as a flying boat

To make flying boats lateral stable on the water, there are two options how to do it. First way is to use auxiliary floats on the wing. This solution is shown in Figure 7.1. This Figure shows EV-55 as a flying boat with auxiliary floats at the tips of the wing. The same Figure also shows the similar conceptual design, however the floats are closer to the fuselage. This solution reduces the loading created by the auxiliary floats. The lateral stability is the best of all mentioned designs.

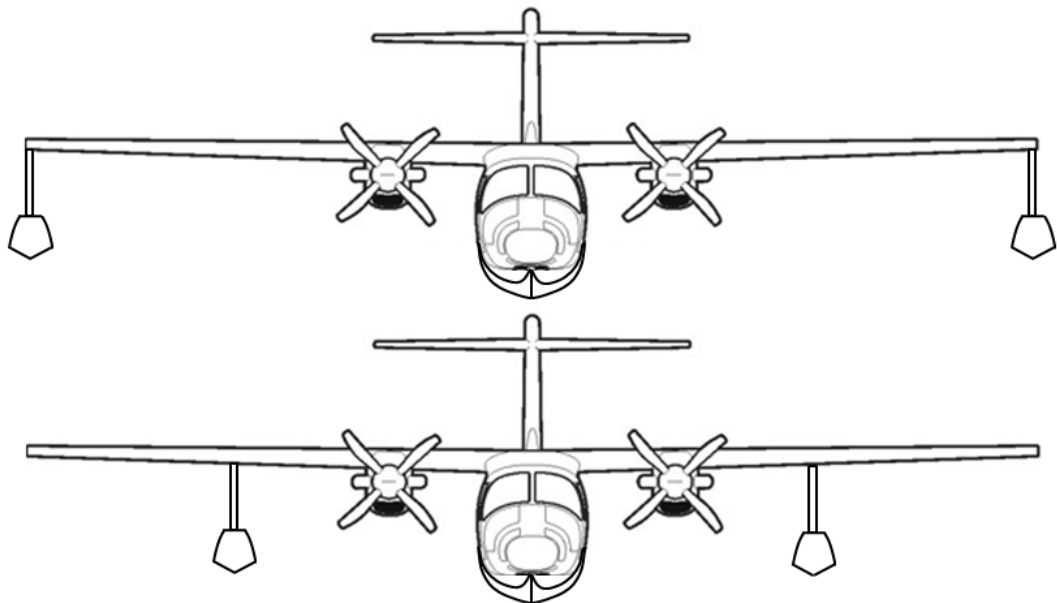


Fig. 7.1: EV-55 as a flying boat with auxiliary floats

In accordance with the fact that the wing is already designed, tips of the propellers are dangerously close to the water surface, the auxiliary floats create additional drag and need to be somehow attached, regardless how the load would increase the load of the wing, this design was denied.

The second way how to provide sufficient lateral stability is to widen the hull of a flying boat. Solution how this could be done is shown in Figure 7.2. This design compared to the previous one has several advantages:

- loading of the wing during landing is created only by its inertia
- additional drag is lower
- level of landing difficulty is lower
- fuselage can be placed directly to the jetty.

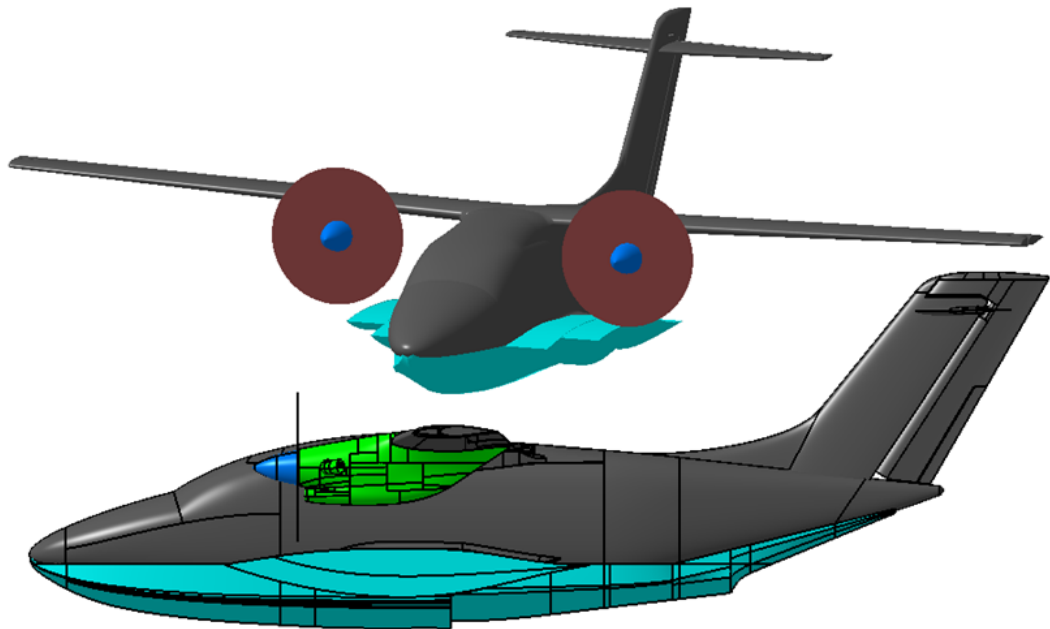


Fig. 7.2: EV-55 as a flying boat with widened fuselage

On the other hand, this design has also several disadvantages compared to the twin-float design:

- design does not meet paragraph CS 23.925 - minimum distance between water level and tips of the propeller blades. This is confirmed in Figure 7.3 for the most unfavourable weight and c.g. configuration. Minimum distance is fulfilled just when the flying boat has zero bank angle. Maximal bank angle can be about 14 degrees. This problem can be removed by using different position of the engines as is shown in Figure 7.4. Of course, this leads to redesign the wing
- passenger doors are too low and there is not any protection against water leakage into the fuselage

- connection of the hull to the existing fuselage seems to be unreal without serious intervention
- lateral stability, compared to the twin-float seaplane, is insufficient as is shown in Figure 7.6. The waves could turn the flying boat.

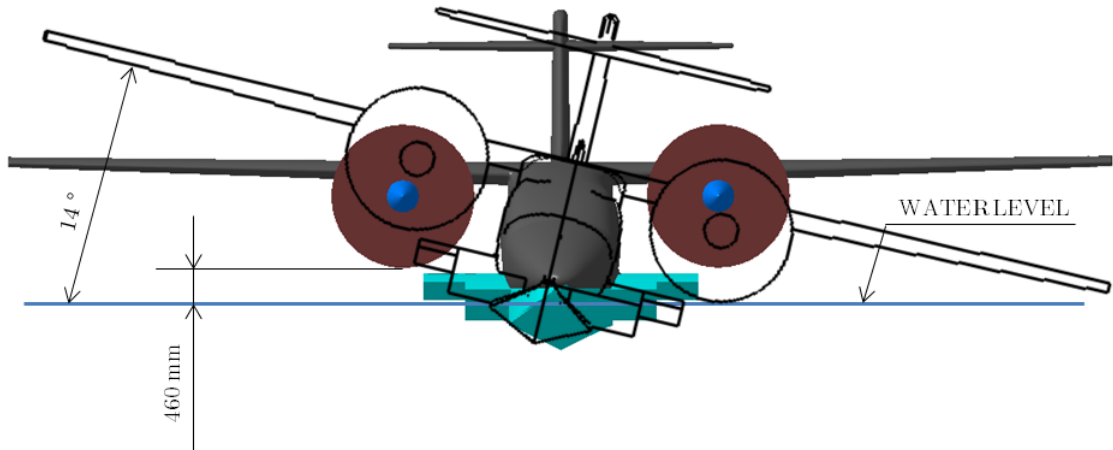


Fig. 7.3: EV-55 as a flying boat with widened fuselage - blade-strike

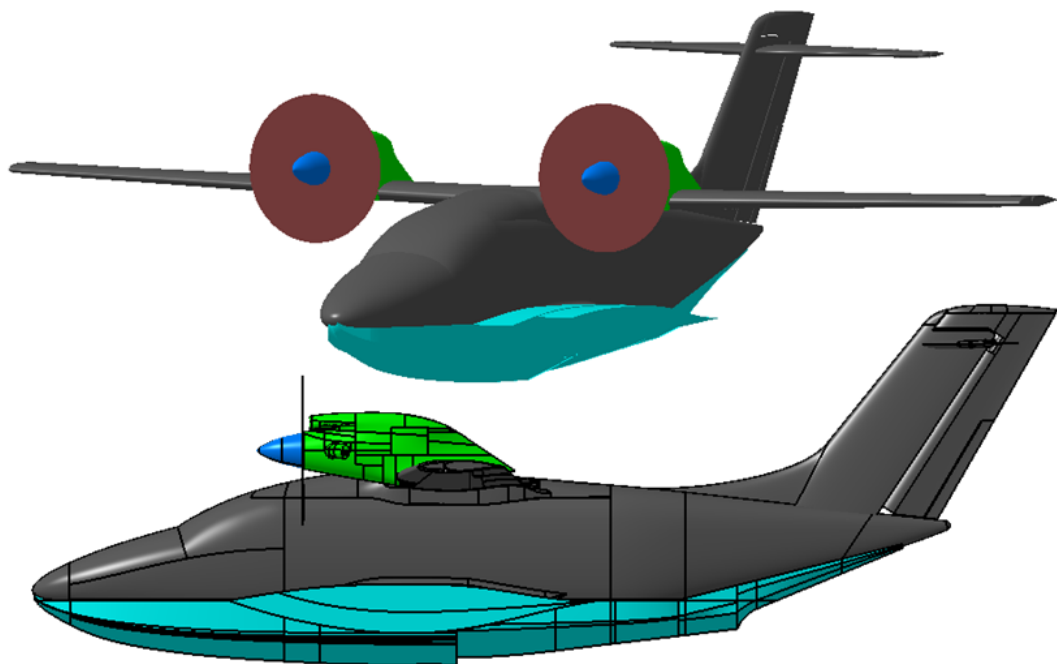


Fig. 7.4: EV-55 as a flying boat with widened fuselage and top-wing mounted engines

7.2.1 The pros and cons of a flying boat

Summary of the pros and cons is stated in Table 7.1.

Tab. 7.1: The pros and cons

Design	The pros \oplus	The cons \ominus
Flying boat - aux. floats at the end	Lateral stability	Additional drag Blades of propellers hazardously close to the water surface Higher load of the wing Attaching of the auxiliary floats
Flying boat - aux. floats in the middle	Lateral stability Lower load of the wing	Additional drag Blades of propellers hazardously close to the water surface Attaching of the auxiliary floats
Flying boat - widened fuselage	Lower load of the wing Lower additional drag Lower landing skills Mooring to the jetty	Blades of propellers hazardously close to the water surface Leakage into the fuselage through the passenger door Connection of the hull and existing fuselage Unsufficient lateral stability

7.3 EV-55 as a float seaplane

There are two conceptions which can be used for this design. Both of them are shown in Figure 7.5. From construction point of view this is the easiest way how to remake terrestrial version into seaplane. Single-float design was also denied due to required size of the float and it would be necessary to use auxiliary floats. Their disadvantages have been discussed. The advantages of twin-float seaplane are:

- floats can be bought from external company
- sufficient lateral stability
- existing attachment points for landing gear can be used
- twin-float seaplane can anchor directly next to the jetty
- there is possibility for easy change between terrestrial version and seaplane
- damaged floats can be easily changed
- sufficient distance between tips of the propellers and water level

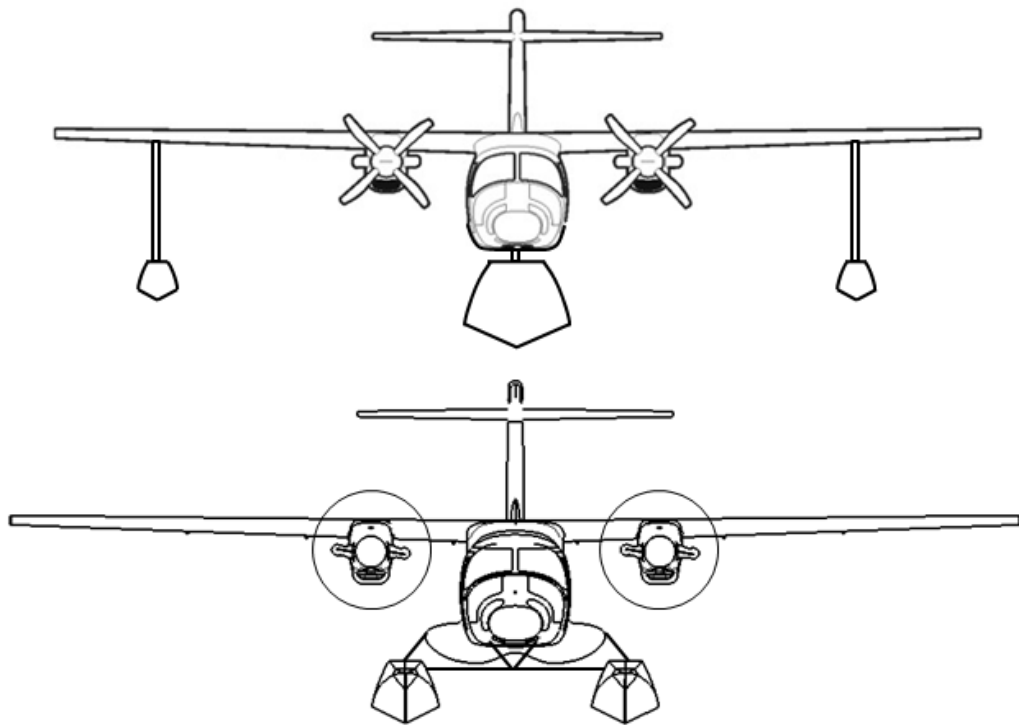


Fig. 7.5: Single/Twin-float design

Unfortunately, twin-float design has also disadvantages. Compared to the previous designs the worst includes:

- increasing of additional drag
- leakage of the water into the floats
- additional stress increase during unsymmetrical landing

- large amount of fasteners

7.3.1 The pros and cons of a float seaplane

Summary of the pros and cons is stated in Table 7.2.

Tab. 7.2: The pros and cons

Design	The pros	The cons
One-float seaplane - auxiliary floats	Lateral stability	Additional drag
	Purchase of the floats	Higher load of the wing
	Attachment points	Attaching of the auxiliary floats
	Changing between floats and landing gear	
	Sufficient distance between propellers and water surface	
Twin-float seaplane	Lateral stability	Additional drag
	Lower load of the wing	Leakage of the water
	Purchase of the floats	Unsymmetrical landing
	Mooring to the jetty	Fasteners
	Changing between floats and landing gear	
	Sufficient distance between propellers and water surface	

7.4 Conclusion

The lateral stability is checked in accordance with literature [14] and procedure is as same as is described later in Chapter 11. Reed's diagram for flying boat is shown

in Figure 7.6. Also, Reed's diagram of a twin-float seaplane is mentioned for better comparison.

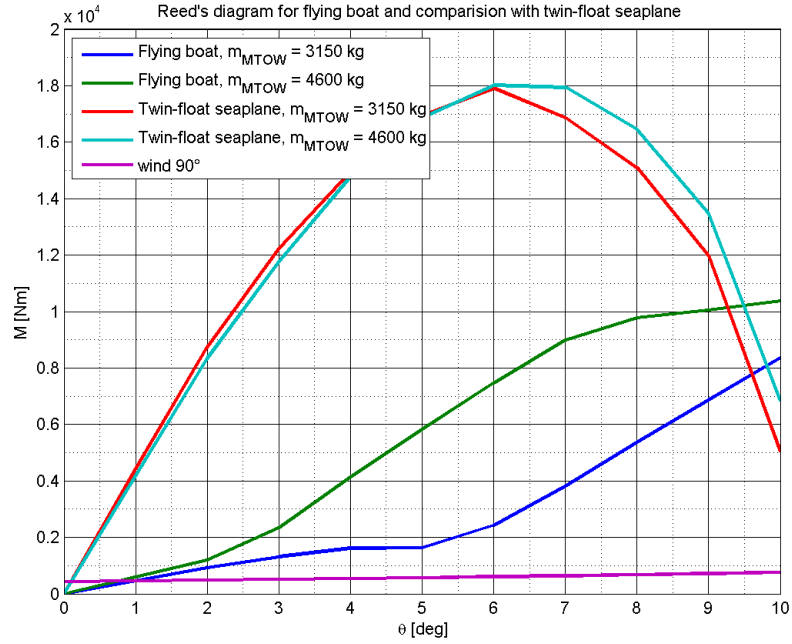


Fig. 7.6: Stability of EV-55 as a flying boat with widened fuselage

From previous Figure is seen that the gradient of reaction moment M as a product of buoyant force F_b for flying boat is lower than for twin-float seaplane. It means that the characteristic to get to neutral position is worse for flying boat than for twin-float seaplane. The worst situation comes up for empty seaplane. The flying boat can heel around longitudinal axis up to 5° and the reversible moment M is still almost same. It will take a lot of time than a seaplane is stabilized. Regardless, every wave or wind-gust will disturb this equilibrium position on the water.

Present fuselage has the passenger door only on the left side. This could be a problem during landing on the river when the jetty is on the right side. It is necessary to anchor the seaplane during docking on the river always up the river. Additional rudders on the floats are not used because EV-55 is twin-propeller aeroplane and turning can be done by using different thrust of each propeller. It will might be necessary to extend or add some vertical surfaces to increase the yaw stability. The floats, as well as fuselage adversely affect yaw stability.

Taking into account previous finding about construction, stability, drag, operational performance, maintenance, present stage of fuselage development and costs, suitable solution is to develop **twin-float seaplane**.

8 COMPETITIVE SEAPLANES

There are many types of seaplane in the World. Some of them are flying boats, the others are twin-floats seaplanes, a few of them are amphibious. In order to design a seaplane that will be competitive within the airline industry, it is imperative to first perform a competitor analysis of existing seaplanes in the market. From the design specification the seaplanes should have a design payload of 4 - 20 passengers. Thirteen seaplanes will be considered in the analysis [12]. The compiled data can be found in Appendix A. There will be final comparison with EV-55 seaplane in Chapter 18.

8.1 Graphs

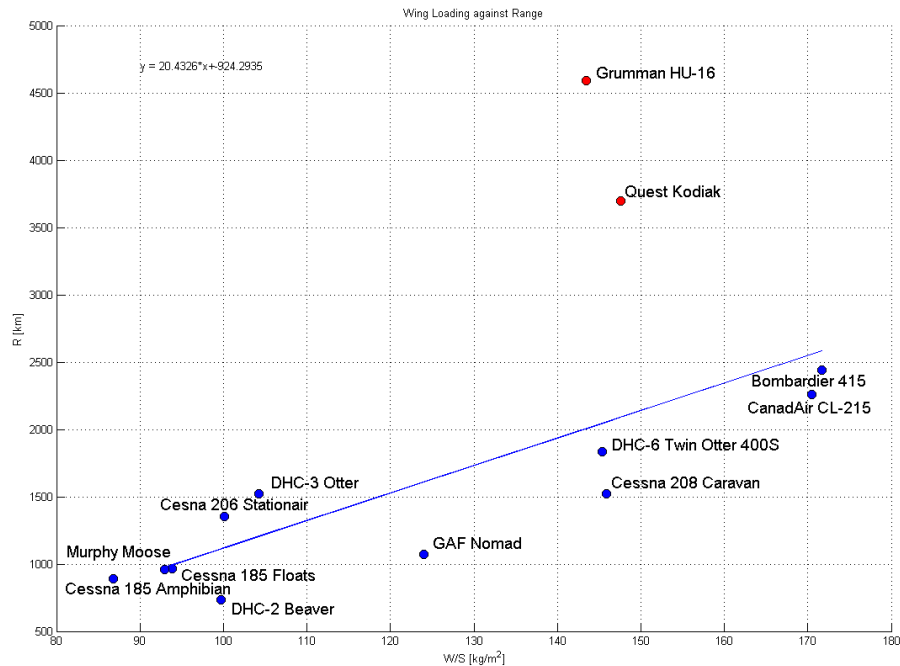


Fig. 8.1: Wing Loading against Range

Figure 8.1 shows Wing Loading - Range dependency. Red data are removed from linear regression.

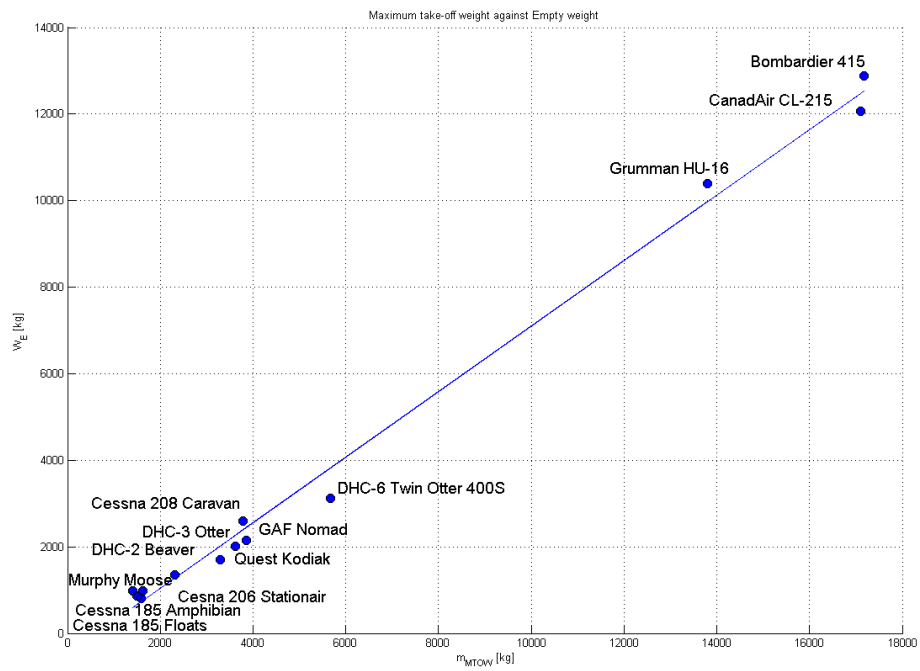


Fig. 8.2: Maximum take-off weight against Empty weight

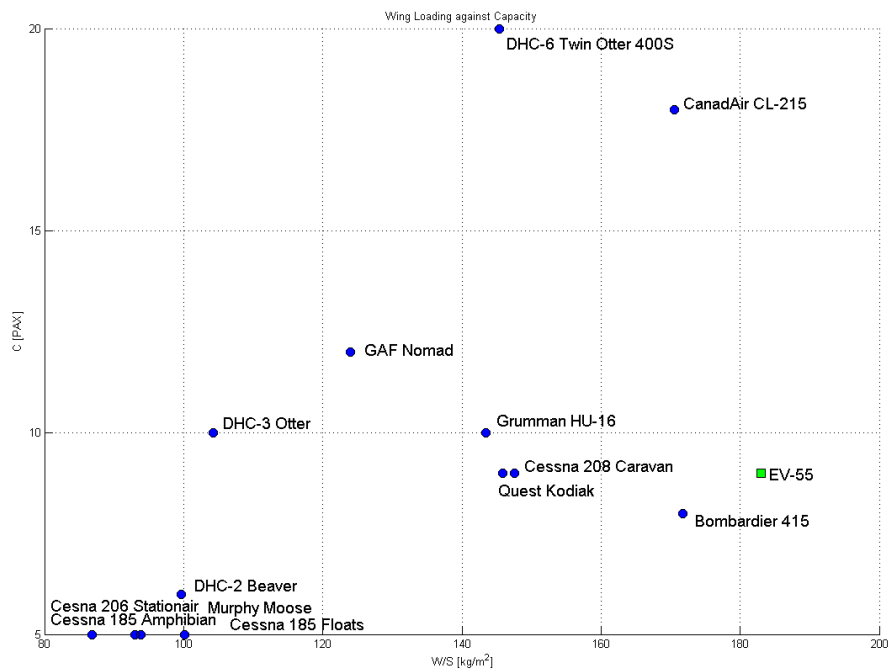


Fig. 8.3: Wing Loading against Capacity

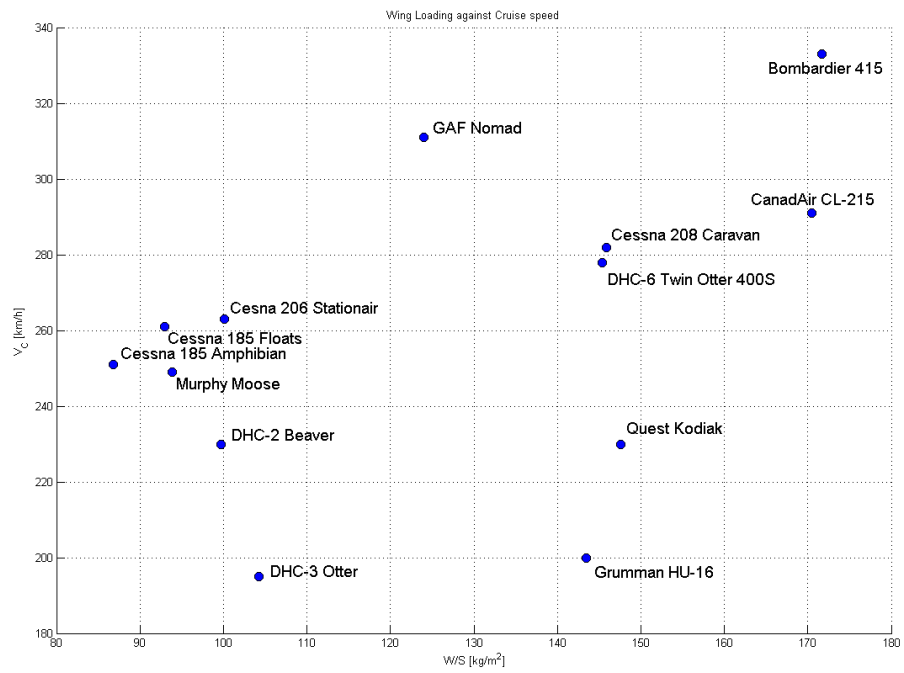


Fig. 8.4: Wing Loading against Cruise speed

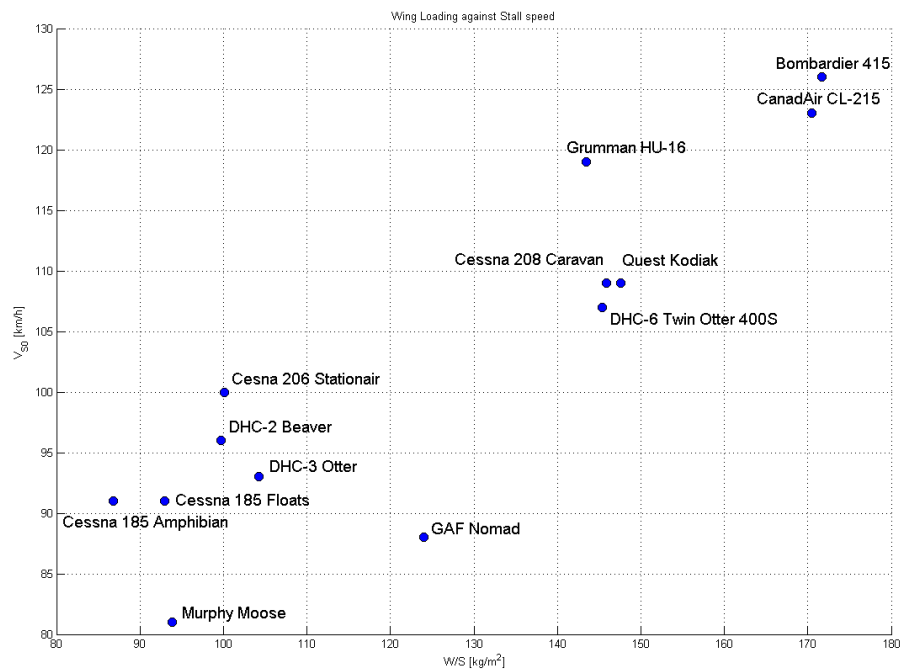


Fig. 8.5: Wing Loading against Stall speed

9 COORDINATION SYSTEM

There are used three main coordination systems in this master's thesis. The first one will be called 'The aeroplane coordination system', in short 'ACS', the second one will be called 'The float coordination system', in short 'FCS' and third one will be called 'The centre of gravity coordination system'.

9.1 The aeroplane coordination system

This coordination system is the basic system used in Evektor for EV-55 aeroplane. The origin of the ACS is situated 2800 mm in front of the third bulkhead, within the symmetry plane and basic plane of the fuselage. See Figures 9.1 and 9.2. The x-axis points from the origin backwards, y-axis points upwards and z-axis points to the left wing.

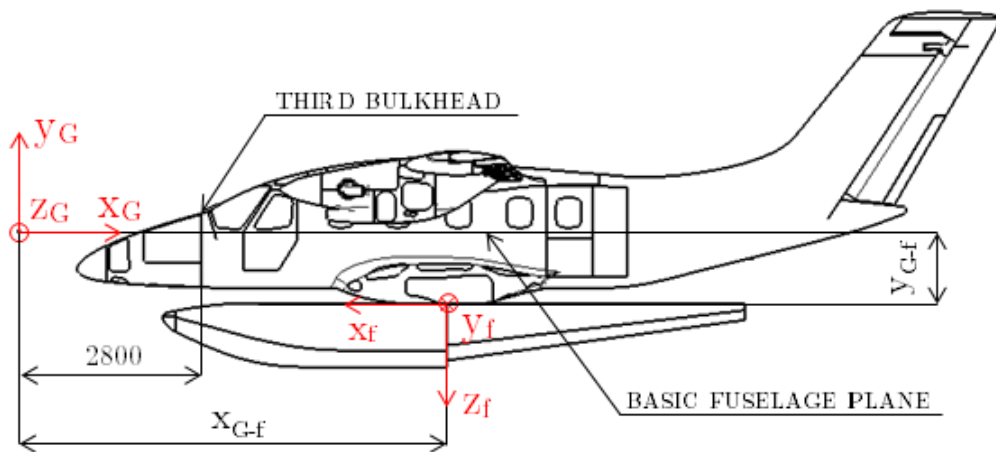


Fig. 9.1: Aeroplane and float coordination system - side view

9.2 The float coordination system

This system is used only for calculations linked with float. The x-axis points forward, y-axis points to the right wing and z-axis points downwards. See Figures 9.1 and 9.2.

9.3 Mutual position of ACS and FCS

The ACS is used as a global coordination system in this master's thesis therefore the labels have 'G' subscript. The FCS is used as a local coordination system. The

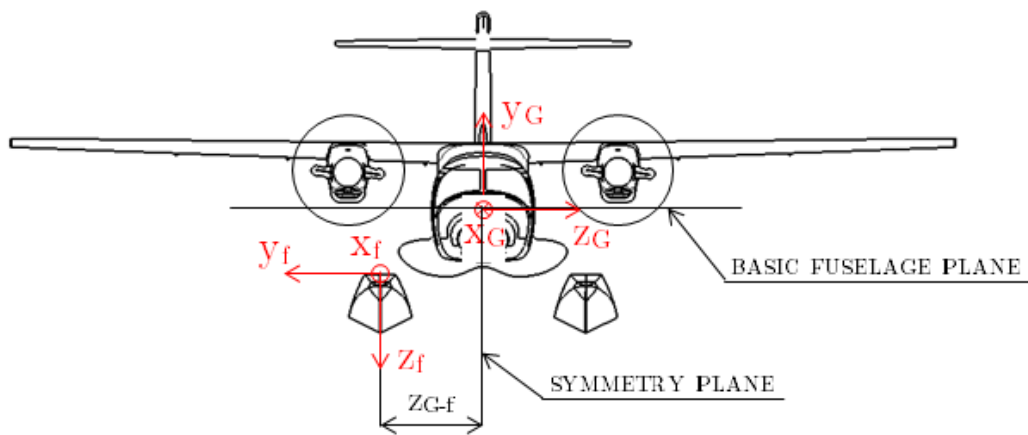


Fig. 9.2: Aeroplane and float coordination system - front view

labels have 'f' subscript. The position of the float coordination system is set by three coordinates: x_{G-f} , y_{G-f} and z_{G-f} (see Figures 9.1 and 9.2). The numerical values of these coordinates are set later on.

9.4 The centre of gravity coordination system

There is used centre of gravity coordination system for the moment of inertia characteristics. This system is oriented as same as the aeroplane coordination system but the origin is transferred. The origin of the centre of gravity coordination system is at the actual c.g. of the aeroplane. The labels have 'c.g.' subscript. See Figure 9.3 for details. There are used other local coordination systems, especially in the

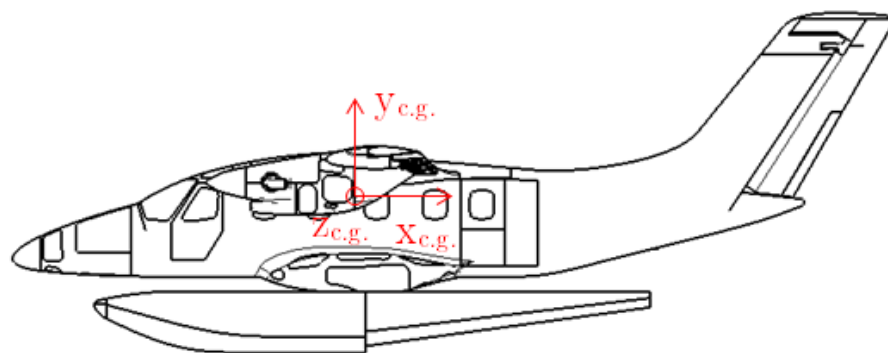


Fig. 9.3: Centre of gravity coordination system - side view

chapter deals with stress analysis. This coordination systems are described in the appropriate chapter.

10 SHAPE OF THE FLOAT

10.1 Determination of the float shape

To determine proper shape of a float, water tests needs to be done. Therefore Wipaire, Inc. company from United States was addressed. This company provided modified floats 'Wipline 8750'. These floats are originally used for Cessna Caravan. However the volume of these floats was not sufficient for EV-55. Thus, the floats were scaled up to fulfill CS 23 regulation, more specifically CS 23.751.

10.2 Important angles

During load factor determination it will be necessary to know angles α_f and α_a . These angles are shown in Figures 14.3 and 14.5. The angles are measured in accordance with CS 23.529. Position of measuring and values of the angles are stated in Figure 10.1. These angles were measured in CATIA. 3D model provided by Wipaire, Inc. was used.

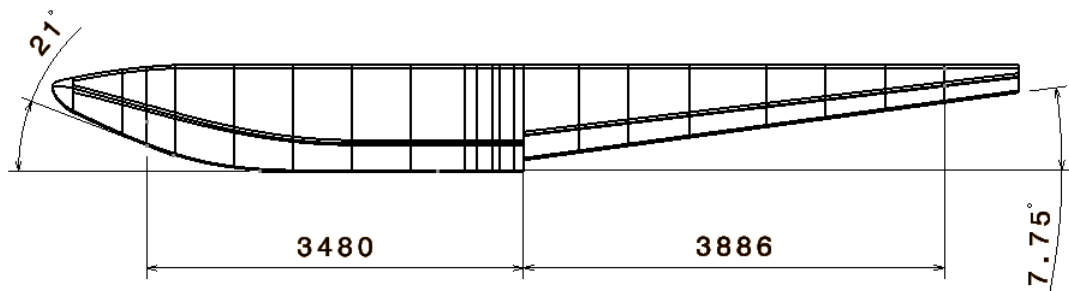


Fig. 10.1: Front and aft attachment points

It is necessary to mention that the position of measuring depends on front and aft length of the float. Details are stated in CS 23.529, paragraph (1), (2) and (3).

11 HYDROSTATIC CALCULATIONS

11.1 A Volume

A Volume of the floats needs to be determined. From the main buoyant condition and Archimedes' principle (see Figure 11.1) can be written:

$$W = F_b \quad (11.1)$$

$$m_{TOW} \cdot g = V_f \rho g \quad (11.2)$$

$$V_f = \frac{m_{TOW}}{\rho} \quad (11.3)$$

where W is the weight of the seaplane, F_b is the buoyant force, m_{TOW} is the take-off weight of the seaplane, V_f is the volume of the floats, ρ is the density of the water and g is the gravitational acceleration.

Taking into account the worst conditions, it is necessary to use density of the fresh water and maximum take-off weight m_{MTOW} . In accordance with CS 23.751 regulation, the volume of each main float must have a buoyancy of 80% in excess of the buoyancy required by that float to support its portion of the maximum weight of the seaplane or amphibian in fresh water. Thus, necessary volume of the floats is computed as follows:

$$V_f = \frac{m_{MTOW}}{\rho} \cdot 1.8 = \frac{4600}{998} \cdot 1.8 = 8.297 \text{ m}^3. \quad (11.4)$$

Thus, one float has to have volume of 4.149 m^3 .

11.2 Stability

Stability of the seaplane on the water is very important. The stability can be split on the lateral and longitudinal stability. Set the lateral stability is usually bigger problem than setting of longitudinal stability. The latter mentioned is generally given by the length of the floats and is usually sufficient. Following formulas are determined for lateral stability, however are valid also for longitudinal stability.

11.2.1 Conditions of equilibrium

The centre of buoyancy (c.b.) has to lie directly below the centre of gravity (c.g.), which is the point where all the gravity forces are assumed. The c.b. is the centre of the buoyant force. If the object is floating freely, the force of gravity has to equal the force of buoyancy (see Figure 11.1).

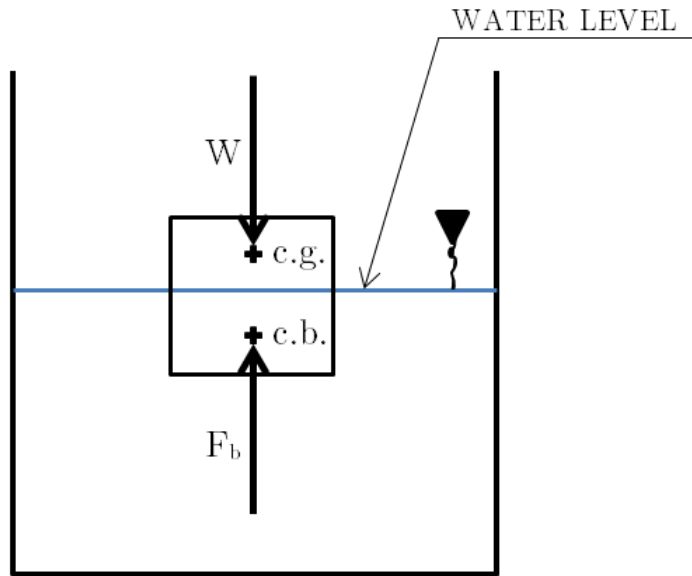


Fig. 11.1: Basic buoyancy condition

11.2.2 Stable condition

The floats are floating upright at waterline W-L, the force of gravity is acting downwards at the centre of gravity and buoyant force is acting at the centre of buoyancy against the force of gravity. Both of the forces have the same magnitude and lie on the centreline of the seaplane (see Figure 11.2).

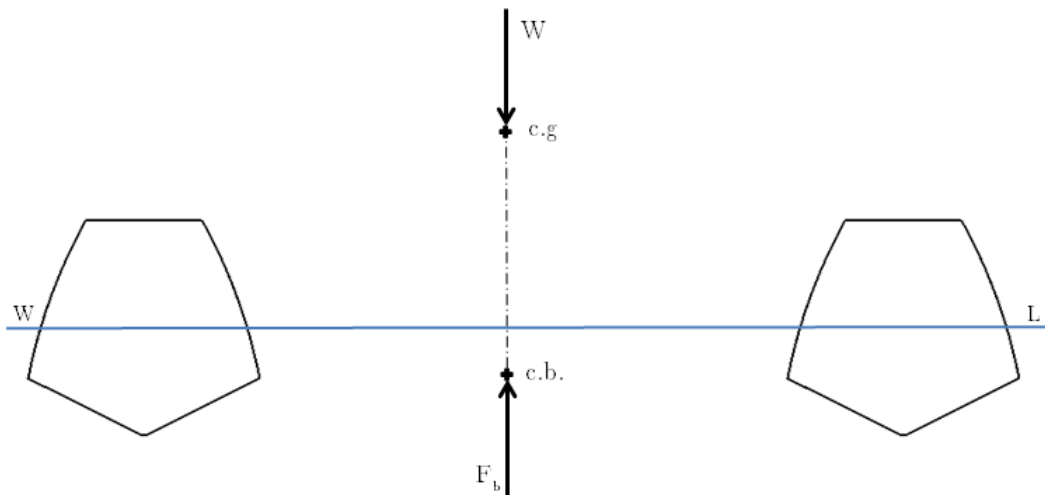


Fig. 11.2: Stable buoyant condition

Imagine a situation when the seaplane is heeled by an external force. The seaplane is rotated around its *c.g.* and waterline $W - L$ has been changed to waterline $W1 - L1$. The *c.b.* (point B in Figure 11.3) has moved to the new position, that corresponds to the geometric centre of underwater part of the floats and has new label: B_1 . Original *c.b.* moved along circle to the position B . The magnitude of the acting forces has not been changed but the position of buoyant force has. Now, the force is acting at B_1 . The following idea considers only small angles of heeling. The literature [9] recommends maximum heeling angle up to 10 degrees. Whereas the maximum possible angle before the wing touches the water level is 15 degrees and maximum angle between water level and blades of propeller is 12 degrees, this simplification is fully sufficient. This simplification has to be done, allowed us to use linear displacement of the points B , B_1 and G , Z . Immediately after heeling, there is developed moment that returns the seaplane to original position. This moment is developed by couple of forces W and F_b and their mutual distance \overline{GZ} . It can be seen that the buoyant line of heeled seaplane meets the buoyant line of the upright seaplane at the point M . This point is called metacentre and the distance \overline{GM} is called metacentric height. If the point M is above point G , it is positive metacentric height and the seaplane is automatically stable.

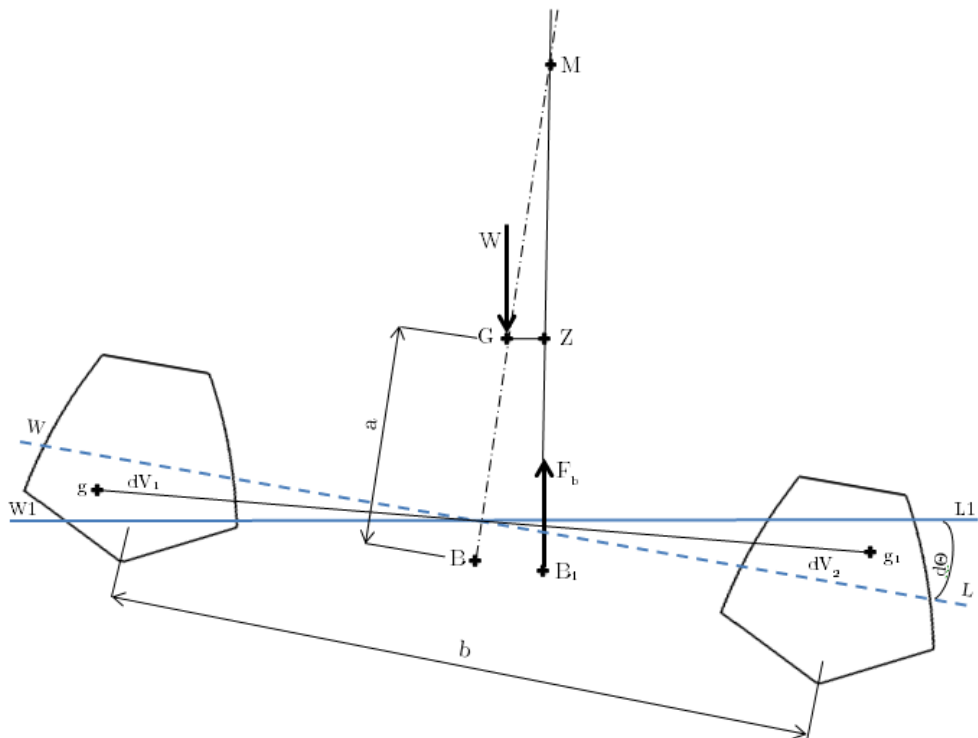


Fig. 11.3: Stable buoyant condition - floats

There were considered two conditions in the previous paragraph:

- The external acting moment does not lead to change the displacement of the seaplane
- The heel is up to 10 degrees

By using condition one, volume dV_1 has to equal dV_2 :

$$dV_1 = \frac{1}{2} \int_{-l/2}^{l/2} y_1 dA dx = \frac{d\theta}{2} \int_{-l/2}^{l/2} y_1^2 dx = \frac{1}{2} \int_{-l/2}^{l/2} y_1^2 dx = \frac{1}{2} \int_{-l/2}^{l/2} y_2^2 dx. \quad (11.5)$$

When the seaplane starts to heel, emerge volume dV_1 with its own c.g. g moves to new position dV_2 with c.g. g_1 . Consequently, c.b. (point B) moves to new position B_1 . Therefore:

$$\overline{BB_1} = \frac{dV}{V} \cdot \overline{gg_1}. \quad (11.6)$$

If $\overline{gg_1}$ is expressed like:

$$\overline{gg_1} = 2 \cdot \frac{2}{3}y, \quad (11.7)$$

and inserted volume dV_1 from equation 11.5 back to the equation 11.6, following can be written:

$$\overline{BB_1} = \frac{\frac{2}{3} \int_{-l/2}^{l/2} y^3 dx}{V} d\theta. \quad (11.8)$$

Expression in numerator is moment of inertia I_x of floatation water plane to the x-axis. Distance $\overline{BB_1}$ can be also written as:

$$\overline{BB_1} = \overline{BM} \cdot d\theta. \quad (11.9)$$

If metacentric radius \overline{BM} is expressed from equation 11.9 and instead of $\overline{BB_1}$ the equation 11.8 is inserted, the formula for metacentric radius is received:

$$\overline{BM} = \frac{I_x}{V}. \quad (11.10)$$

Finally, the metacentric height can be determined, as follows:

$$\overline{GM} = \frac{I_x}{V} - a \quad (11.11)$$

where I_x is moment of inertia of floatation waterplane to the x-axis, V is the immersed volume of the floats and a is the distance among c.b. and c.g.

11.3 Lateral and vertical position of the floats

As was mentioned in previous subsection, the metacentric height depends on moment of inertia I_x of floatation waterplane to the x_f axis, immersed volume V , c.g. and

c.b. distance, see Equation 11.11. Moment of inertia I_x is function of the track of the floats and can be simply written as follows:

$$I_x = 2 \cdot \left(I_{x_0} + \left(\frac{b}{2} \right)^2 \cdot A_{wp} \right) \quad (11.12)$$

where I_{x_0} is the moment of inertia of the floatation waterplane to its x_f axis, b is the track of the floats and A_{wp} is the area of the floatation waterplane.

For the constant weight, I_x depends on one parameter - track of the floats b . Metacentric height depends also on parameter a - vertical position of the floats. Totally, Equation 11.11 can be solved with two independent variables: track of the floats b and vertical position of the floats a . The equation looks as follows:

$$\overline{GM} = \frac{2 \cdot \left(I_{x_0} + \left(\frac{b}{2} \right)^2 \cdot A_{wp} \right)}{V} - a. \quad (11.13)$$

Solving this equation in MATLAB, 3D plot can be displayed:

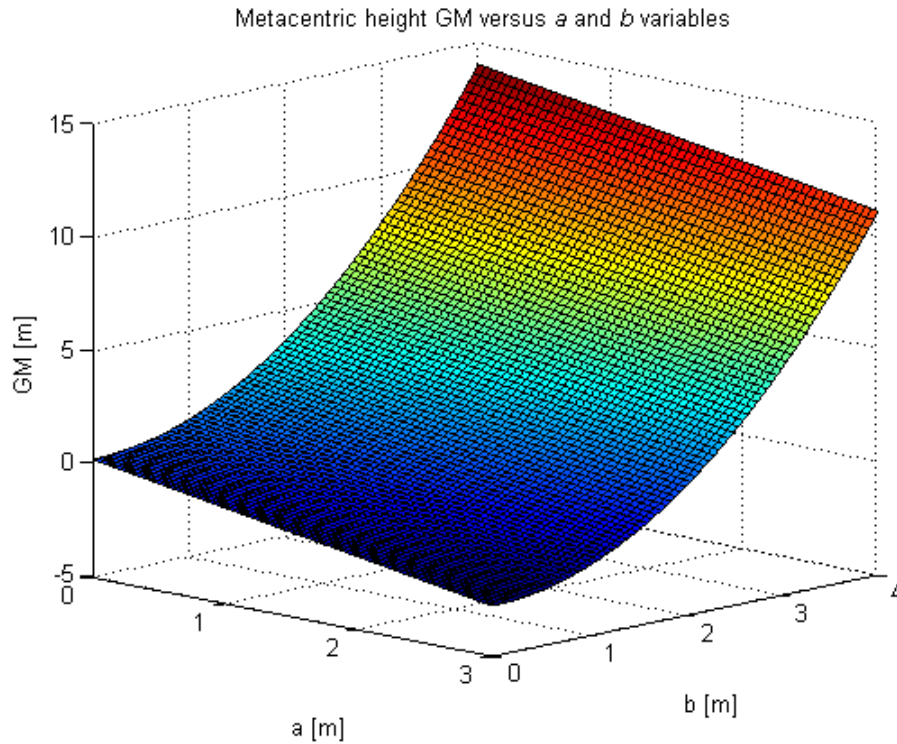


Fig. 11.4: Metacentric height \overline{GM} versus a and b variables

By plotting contour lines of metacentric height \overline{GM} from Figure 11.4, the Figure 11.5 is obtained.

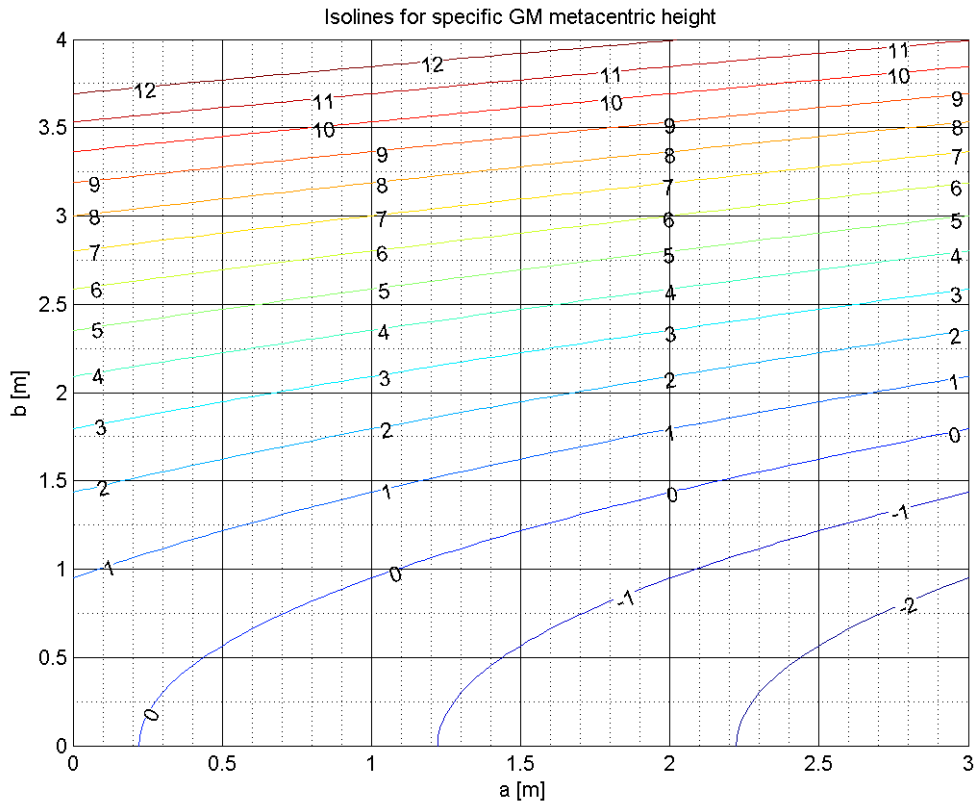


Fig. 11.5: Contour lines of metacentric height \overline{GM}

Literature [14] suggests sufficient metacentric height for lateral stability 9 metres. This value is given by following formula:

$$\overline{GM} = K \cdot \sqrt[3]{W} \quad (11.14)$$

where K is the constant for the type of seaplane and for twin-float seaplane it is 1.4. W is the weight of the seaplane in pounds.

For appropriate contour lines following variables a and b were chosen:

Tab. 11.1: Chosen variables a and b

Variable	value	unit
a	1800	mm
b	3500	mm

11.4 Longitudinal position of the floats

Longitudinal position of the floats is given by position of the c.g. of the aeroplane. This problem is mentioned in Chapter 12. The longitudinal stability needs to be checked. Same equations as in previous section are used. Moment of inertia to y_f axis is simply given by following formula:

$$I_y = 2 \cdot \frac{1}{12} b \cdot (l_f + l_a)^3 \quad (11.15)$$

where I_y is moment of inertia of floatation waterplane to the y_f axis, b is the mean width of the float, l_f and l_a are the front and aft length of the float, respectively. Metacentric height for longitudinal stability is:

$$\overline{GM} = \frac{I_y}{V} - a. \quad (11.16)$$

Literature [14] suggests sufficient metacentric height for longitudinal stability as same as for lateral stability. Using Equation 11.16 longitudinal metacentric height 9.5 m is received. This is approximately same as the lateral metacentric height. The seaplane is longitudinal stable.

11.5 Waterline position

Waterline position was determined for three weight configuration and six static margin values. Everything in accordance with weight envelope shown in Figure 12.5. CATIA was used to set c.b. position and values H_f , H_a , ϕ and b were measured. See Figure 11.6 for details.

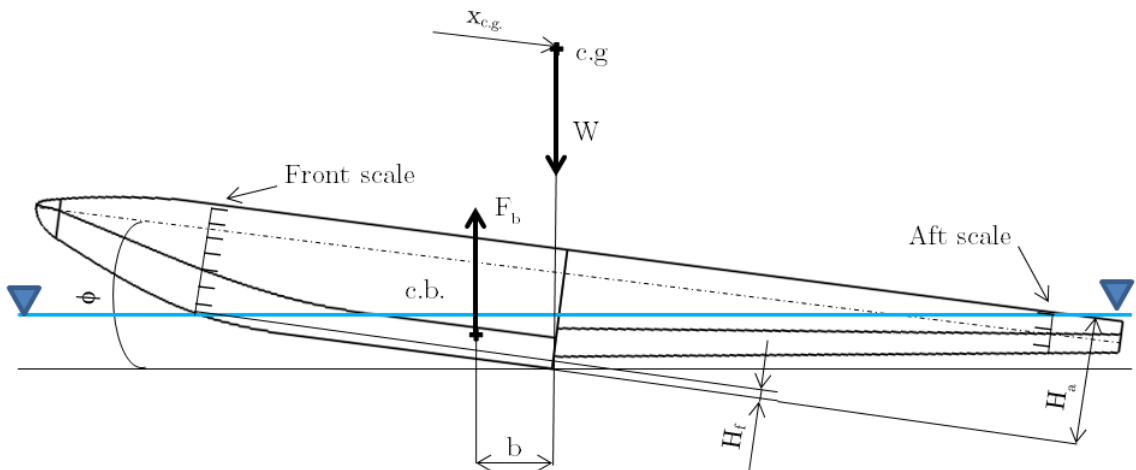


Fig. 11.6: Geometric data measured in CATIA V5

Following procedure was used to determined waterline for different weight and c.g. position:

Using Catia model of the float, the immersed volume for angles $\phi = -3^\circ, 0^\circ, 3^\circ, 6^\circ$ was determined. This was done for every weight configuration and c.g. position. The values H_f and H_a was measured. From known c.b. and c.g. position the distance b was measured, as well. Previous procedure is in accordance with literature [10].

The stabilizing moment can be computed as follows:

$$M = W \cdot \frac{b}{1000} = m_{MTOW} \cdot g \cdot \frac{b}{1000} \quad (11.17)$$

where M is the stabilizing moment, g is the gravitational acceleration and b is the righting arm. Values H_f and H_a shows the position measured vertically from the step. H_f is the scale at the front part of the float, precisely speaking 3000 mm from the step and H_a is the scale at the aft part of the float, precisely speaking 3500 mm from the step.

Figures 11.7, 11.8 and 11.9 show dependency between longitudinal heel angle ϕ and righting moment M and also position of waterline on the front and aft scale on the floats. Points of righting moment are approximated by second order polynomial function.

Tab. 11.2: Data for Figure 11.7

$m_{TOW} = 3150 \text{ kg}$						
Static margin			8.0%		21.5%	
ϕ	H_f	H_a	b	M	b	M
[°]	[mm]	[mm]	[mm]	[Nm]	[mm]	[Nm]
-3	613.6	0	1127	34826	1338	41346
0	522	0	676.5	20905	887	27410
3	382.5	749	45.2	1397	165.9	5127
6	203.5	939	-1032	-31890	-821.7	-25392

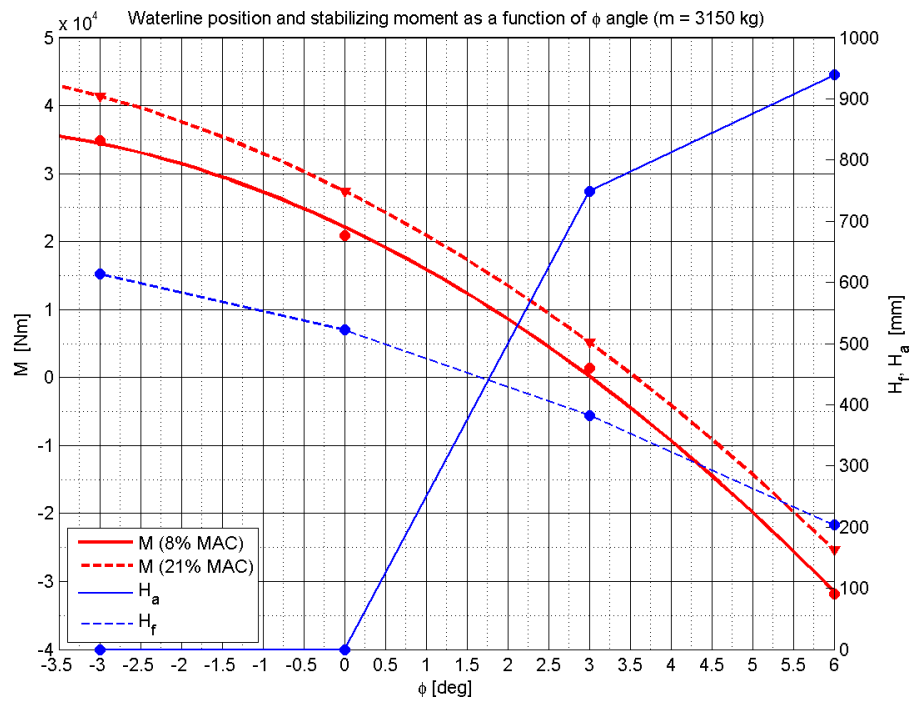


Fig. 11.7: Waterline position and stabilizing moment ($m_{TOW} = 3150 \text{ kg}$)

Tab. 11.3: Data for Figure 11.8

$m_{TOW} = 3777 \text{ kg}$						
Static margin			12.0%		30.6%	
ϕ	H_f	H_a	b	M	b	M
[°]	[mm]	[mm]	[mm]	[Nm]	[mm]	[Nm]
-3	691.7	0	1125	41684	1423.5	43988
0	578	0	665.5	24658	963	29758
3	430	797	-78.5	-2909	219	6767
6	256.9	984.2	-914	-33866	-616.4	-19048

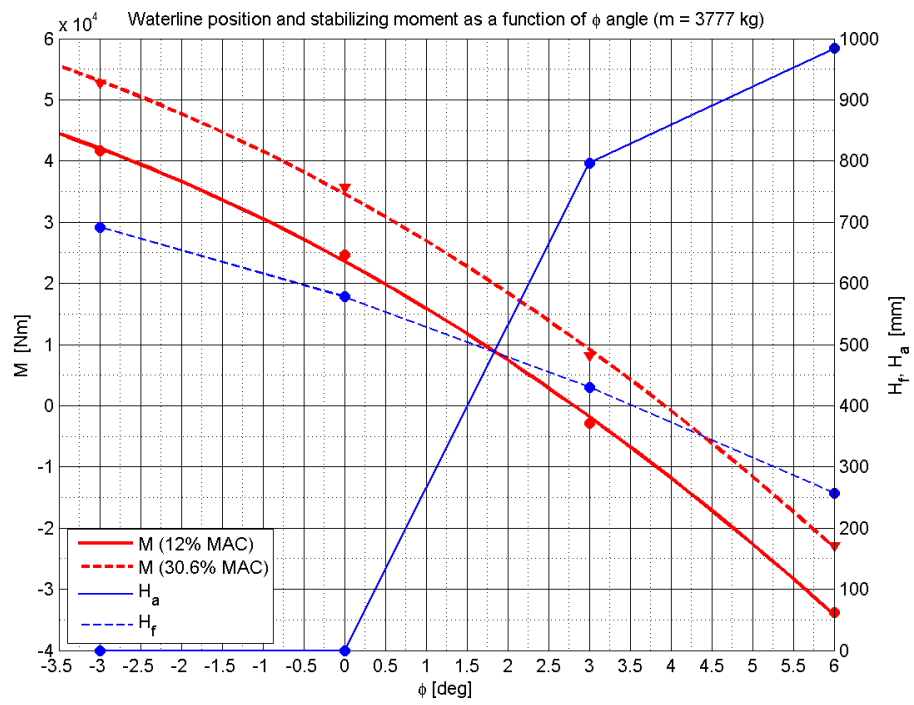


Fig. 11.8: Waterline position and stabilizing moment ($m_{TOW} = 3777 \text{ kg}$)

Tab. 11.4: Data for Figure 11.9

$m_{TOW} = 4600 \text{ kg}$						
Static margin			17.4%		31.4%	
ϕ	H_f	H_a	b	M	b	M
[°]	[mm]	[mm]	[mm]	[Nm]	[mm]	[Nm]
-3	774.5	0	1112	41202	1335.5	41269
0	648.3	648.3	654.5	24251	877.3	27110
3	492	492	-85.5	18230	136.9	4230
6	331	331	-716	-26529	-492.3	-15213

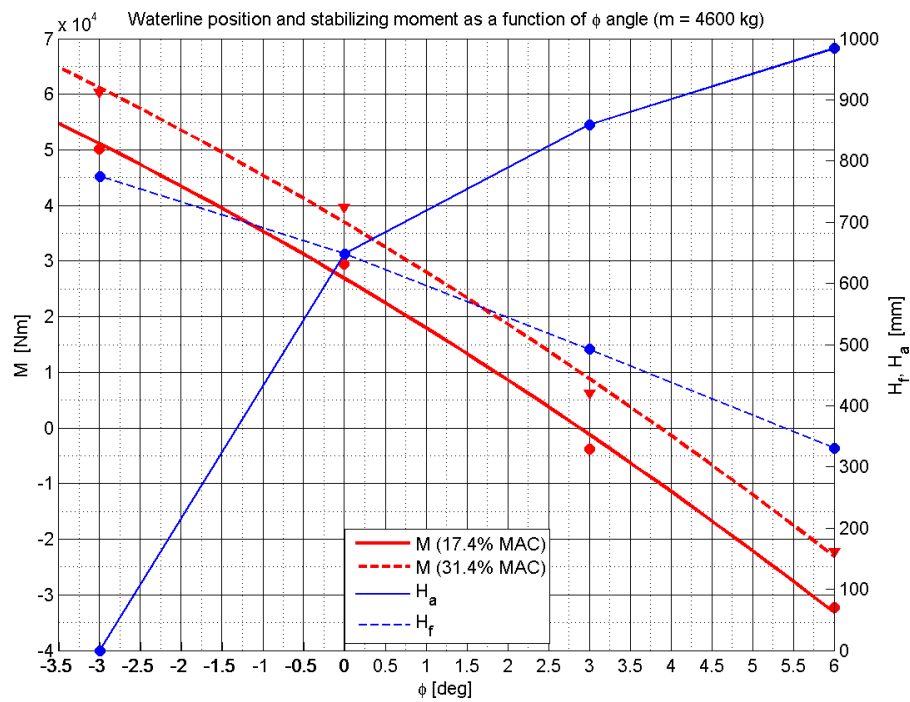


Fig. 11.9: Waterline position and stabilizing moment ($m_{MTOW} = 4600kg$)

From previous figures can be seen that the neutral righting moment is in range from 2.8 to 4 degrees. It means, if the seaplane will stay on calm water, the angle between water level and longitudinal axis will be different compared to terrestrial version. This is not a problem if the seaplane does not move.

11.6 Waterline position when using full thrust

Full thrust is usually used for take-off. Especially at the beginning of take-off, the elevator is not effective because of small speed and pilot cannot affect the position of the float using pitching moment of elevator. The propellers create available thrust T_{ava} and the floats create the hydrostatic drag D_{HS} . Both of the forces create moments. Visually it is shown in Figure 11.10

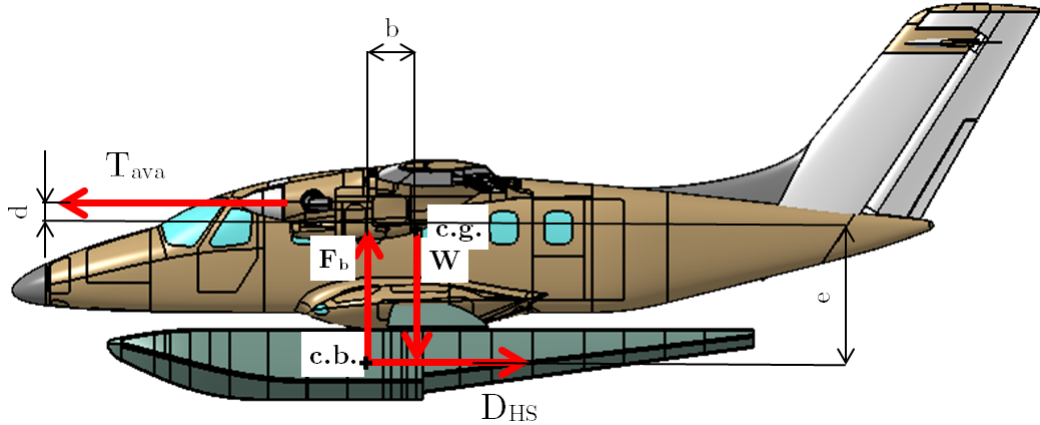


Fig. 11.10: Forces acting during take-off

Previous Figure 11.10 is possible to describe mathematically. Maximal hydrostatic force in accordance with literature [14] is following:

$$D_{HS} = 0.1 \cdot m_{MTOW} \cdot g \quad (11.18)$$

where m_{MTOW} is the maximum take-off weight of the seaplane and D_{HS} is the hydrostatic drag at the beginning of acceleration and g is the gravitational acceleration. The equilibrium still has to be valid during take-off. In according to Figure 11.10:

$$D_{HS} \cdot e + T_{ava} \cdot d = F_b \cdot b \quad (11.19)$$

where d is the distance between point of the thrust force and c.g., F_b is the buoyant force, b is the horizontal distance between c.g. and c.b. determined in section 11.5 and e is the distance between c.g. and acting point of hydrodynamic force. The product $W \cdot b$ from Figure 11.10 is righting moment also stated in section 11.5. The moment created by thrust is:

$$M_T = T_{ava} \cdot d = 19362.4 \cdot 0.665 = 12876 \text{ Nm}. \quad (11.20)$$

Thrust available T_{ava} was obtained for maximal thrust available for zero altitude, zero speed and temperature 15°C from performance deck for PT6 engines. Moment M_T corresponds to following angles from Figures 11.7, 11.8 and 11.9:

Tab. 11.5: Change of waterline angle ϕ with a full thrust

	$m_{TOW} = 3150 \text{ kg}$		$m_{TOW} = 3777 \text{ kg}$		$m_{MTOW} = 4600 \text{ kg}$	
Static margin	8%	21%	12%	30.6%	17.4%	31.4%
ϕ_{thrust}	1.60°	2.30°	1.25°	2.55°	1.60°	2.75°

From table 11.5 is seen that full thrust causes the negative moment which corresponds for change of angles from 1.6 to 2.75 degrees. When the seaplane is floating freely on the water there is angle from 2.8 to 4 degrees between longitudinal axis and water level (Read Figures 11.7, 11.8 and 11.9 for $M = 0$) . When the full thrust is used, these angles are changed:

$$\phi_{total} = \phi - \phi_{thrust} \quad (11.21)$$

where ϕ is angle between longitudinal axis of the seaplane and water level during free flotation read from Figures 11.7, 11.8 and 11.9 for $M = 0$ and ϕ_{thrust} is the angle by which changes the initial angle ϕ .

Final angles ϕ_{total} for extreme static margins and take-off weights are stated in Table 11.6.

Tab. 11.6: Final angle ϕ_{total} between longitudinal axis and water level

		$m_{TOW} = 3150 \text{ kg}$		$m_{TOW} = 3777 \text{ kg}$		$m_{MTOW} = 4600 \text{ kg}$	
Static margin	[%]	8	21	12	30.6	17.4	31.4
ϕ	[°]	3.0	3.5	2.8	4.0	2.9	3.9
ϕ_{thrust}	[°]	1.6	2.3	1.25	2.55	1.6	2.75
ϕ_{total}	[°]	1.4	1.2	1.6	1.5	1.3	1.2

To keep as same angle of attack as during take-off from runway, floats has to be set about 1.5° to positive value. This change is insignificant and therefore will be neglected during next computations.

11.7 Reed's diagram

As was already mentioned, external moment can caused stabilizing or destabilizing effect. This depends on mutual position of metacentre and c.g. position. There was also said that the magnitude of the stabilizing moment depends on the distance \overline{GZ} . Let us recall this in Figure 11.11.

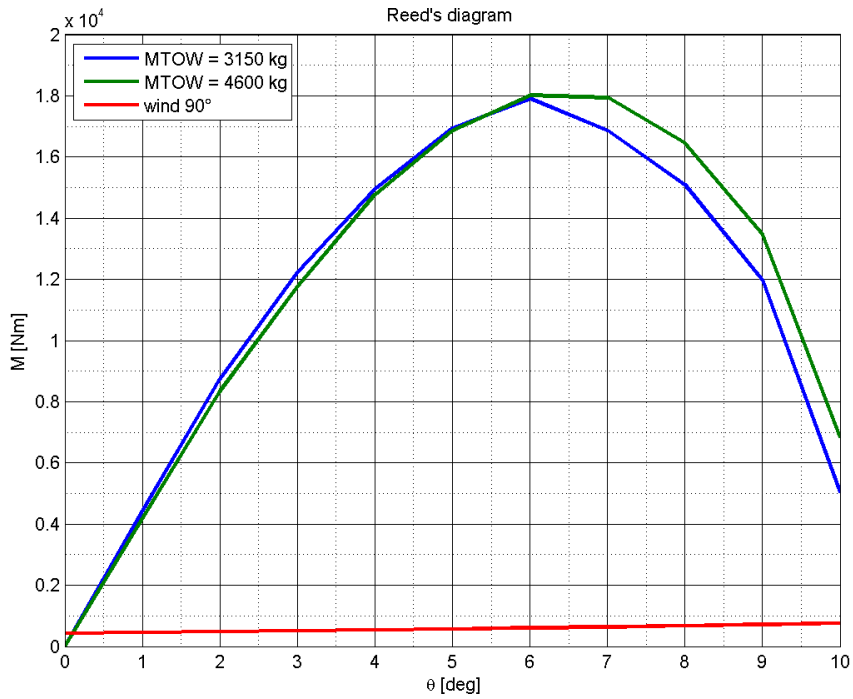


Fig. 11.11: Reed's diagram

The $M - \theta$ curve is called Reed's diagram and shows the dependence of the righting moment of stability M on the heeling angle θ . There are two curves in Figure 11.11. The blue one shows the righting moment of stability in accordance with Equation 11.22 and is done for take-off weight 3150 kg. This equation is referring to Figure 11.11 and can be written as follows:

$$\overline{GZ} = \overline{BM} \cdot \sin \theta - a \cdot \sin \theta. \quad (11.22)$$

The second curve - green one is for maximum take-off weight 4600 kg. It can be seen that the seaplane is stable let us say to 12 degrees, approximately. It is enough, taking into account that maximum angle before the propellers touch the water level is about 12 degrees, as well. There is also red curve in Figure 11.11. This curve shows influence of the wind and lateral heeling angle. At the beginning, the wind causes acting moment on the seaplane around x-axis. This results in immersing of the float and increasing the righting moment caused by buoyant force. When the both moments are in equilibrium, this is maximal heeling angle caused by wind gust. The wind gust acting moment is determined in accordance with literature [14]. There is Figure 11.12 showing dependency between wind-gust direction θ_{gust} and coefficient c .

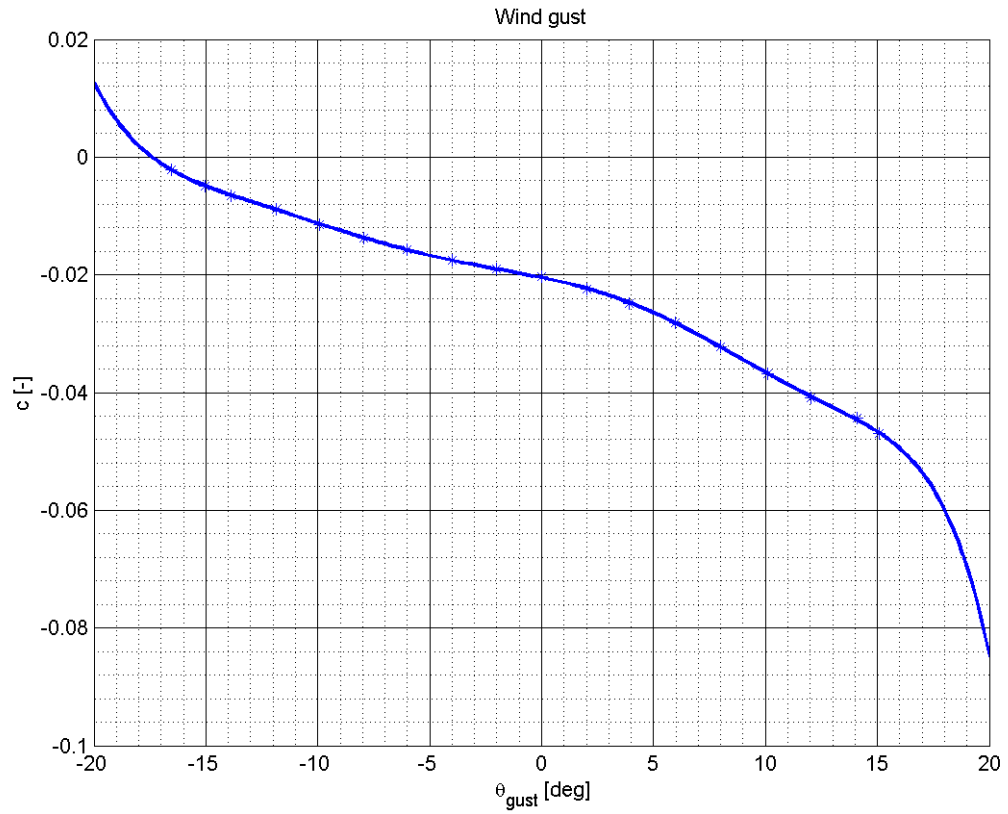


Fig. 11.12: Wind gust

Data are approximated by fourth order polynomial function:

$$c = 6.48e^{-8} \cdot \theta^4 - 1.5e^{-6} \cdot \theta^3 - 3.8e^{-5} \cdot \theta^2 - 1.0e^{-3} \cdot \theta - 2e^{-2}. \quad (11.23)$$

The wind gust acting moment can be computing as follows:

$$M_{wind} = c \cdot b \cdot \rho \cdot S \cdot u^2 \quad (11.24)$$

where c is coefficient determined previously, b_f is the length of the fuselage, ρ is the density of the air, S is the wing area and u is the speed of the wind.

12 WEIGHT BREAKDOWN

Weight breakdown of EV-55 is done within EV55004-04-W_G document [21]. Because the floats will be attached instead of landing gear, removing the landing gear items and hydraulic items was priority. Complete itemization of landing gear items and hydraulic items is stated in Appendix D. The following Table 12.1 shows the total weight of each group and moments of inertia linked to the Aeroplane Coordination System.

Tab. 12.1: Mass, c.g. and inertia characteristic for each group

Group	m	x_G	y_G	z_G	I_{x_G}	I_{y_G}	I_{z_G}
[–]	[kg]	[mm]	[mm]	[mm]	[kg · m ²]	[kg · m ²]	[kg · m ²]
Landing gear	179.47	5817	-800	0	6604.4	117.1	115.0
Anti-lock braking system	1.00	5300	-780	-390	28.1	0.6	0.2
Hydraulic cylinders	16.80	5119	-833	0	470.3	11.7	6.3
Hydraulic items	49.42	2379	-421	177	362.0	13.3	4.5

It was decided, that landing gear, anti-lock braking system and hydraulic cylinders will be removed when conversion to seaplane should be done. Hydraulics items represent about 50 kg of weight and if these items will be kept in the aeroplane, it is possible to change modifications between seaplane and terrestrial version.

Groups that will be removed (in accordance with weight breakdown table in Appendix D):

- Landing gear
- Anti-lock braking system
- Hydraulic cylinders

12.1 Weight of the floats

The weight of the floats was determined in accordance with L.W. Rosenthal - The Weight of Seaplanes Floats [18]. There is mentioned relation between the weight of the floats and their volume:

$$W_f = 0.134 \cdot V_f^{0.8812} \quad (12.1)$$

where W_f is the weight of the floats and V_f is the volume of the floats in decimetres cubic. The equation mentioned above is shown in Figure 12.1. Estimated weight of the floats is about 380 kg if $V_f = 8297 \text{ dm}^3$ is considered. However, this is only the weight of the floats. Further accessories has to be considered. Using available data on Wipaire Inc. web pages, the weight of the further accessories was set to 120 kg . Especially, the data from DHC-6 and Cessna Caravan 208 were used. Floats, struts and accessories for Cessna Caravan 208 has 452 kg . From Figure 12.1 and known maximum take-off weight of Cessna Caravan 208, the weight of struts and accessories can be computed as follows:

$$m_{acc+struts} = 452 - 0.134 \cdot \left(\frac{m_{MTOW}}{998} \cdot 1.8 \cdot 1000 \right)^{0.8812} \quad (12.2a)$$

$$m_{acc+struts} = 452 - 0.134 \cdot \left(\frac{3969}{998} \cdot 1.8 \cdot 1000 \right)^{0.8812} = 118 \text{ kg} \quad (12.2b)$$

where $m_{acc+struts}$ is the weight of struts and accessories, m_{MTOW} is the maximum take-off weight of Cessna Caravan 208 and 452 kg is the weight of the float assembly, that was got from company web pages. Together, the estimated weight of the floats with accessories was set to 500 kg .

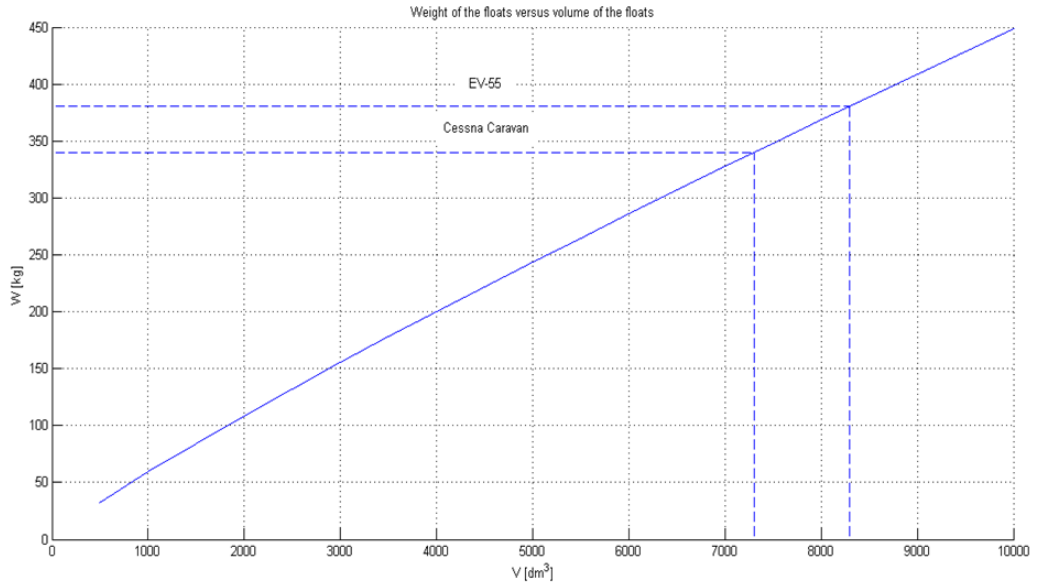


Fig. 12.1: Weight of the floats versus volume of the floats

12.2 Terrestrial version of EV-55

Weight envelope for terrestrial version was taken from EV55004-04-W_G document [21], as well. Figure 12.2 represents this weight envelope. It is seen that there are six weight configuration with different static margin. Red dashed line shows restriction from lower side of weight envelope due to adding the floats. Details will be mentioned in the following section.

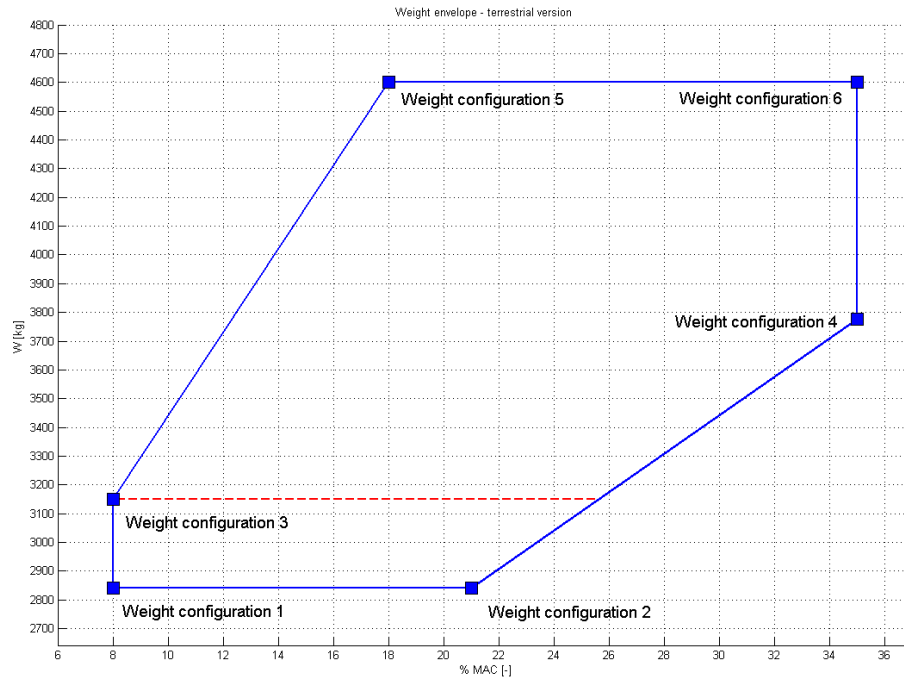


Fig. 12.2: Weight envelope of the terrestrial version

12.2.1 Moment of inertia

Moment of inertia was taken from SAVLE program (System of automatic aeroplane computations). Configurations corresponding to the weight envelope were chosen. The list of the moments of inertia for these configurations is in Table 12.2. Moments of inertia are related to the coordination system corresponding to the relevant c.g. position.

Tab. 12.2: c.g. position and moment of inertia from SAVLE

Weight	SAVLE	x_G	y_G	z_G	$I_{x_{c.g.}}$	$I_{y_{c.g.}}$	$I_{z_{c.g.}}$
config.	config.	[mm]	[mm]	[mm]	[kg · m ²]	[kg · m ²]	[kg · m ²]
1	2101	6124.0	310.0	4.0	11709.9	24630.5	16848.8
2	2203	6331.9	346.9	1.2	12074.4	24.672.3	16809.7
3	404	6124.1	327.5	9.3	12415.3	26486.7	18220.1
4	2011	6555.3	224.1	25.0	12733.0	28754.2	20489.4
5	509	6283.7	393.3	12.0	20041.4	34539.7	19490.7
6	1812	6555.5	110.5	1.1	13204.7	26726.2	18811.0

12.3 Seaplane version of EV-55

The seaplane version has, comparing to the terrestrial version, two floats and no wheel landing gear. The weight of the floats was determined within previous section. By adding the floats, the centre of gravity moves downwards and minimum weight increases. Previously was mentioned that by increasing the weight the minimum weight of flight envelope moves upwards. The difference between terrestrial version and a seaplane in empty weight is 300 kg. Also, because the c.g. of the floats is in front of the c.g. of the aeroplane, resulting c.g. will move forward. This envelope, called Seaplane weight envelope is in Figure 12.3. This envelope has only five weight configurations. Unfortunately, this weight envelope is out of the original envelope.

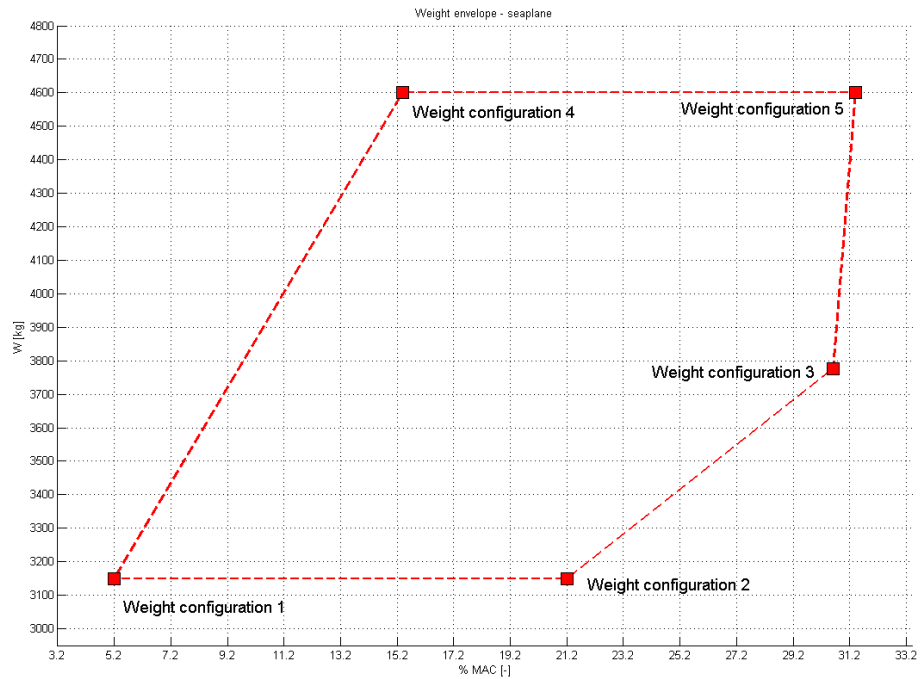


Fig. 12.3: Weight envelope of the seaplane version

To keep static margin in its original state or within the original state, weight layout has to be changed. Therefore 43 kg of luggage from front storage space in the nose of the seaplane was removed. The weight envelope for this configuration is called Seaplane - modified weight envelope and is shown in Figure 12.4. These five configurations will be used during next development, especially during determination of the water loads.

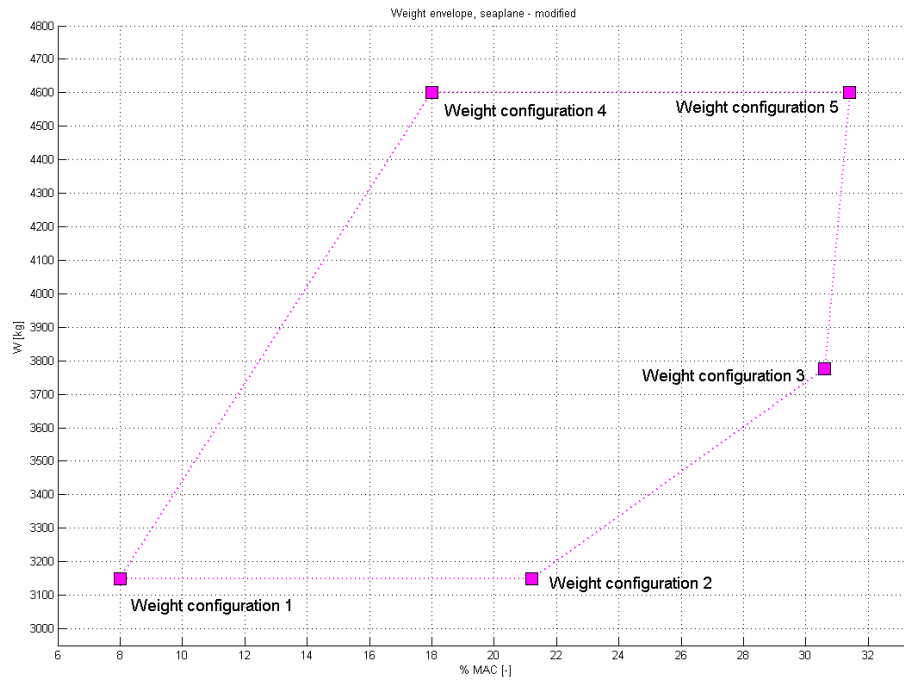


Fig. 12.4: Weight envelope of seaplane version - modified

For illustration, all of the weight envelopes together are shown in Figure 12.5. The range of the configurations was decreased. Minimum take-off weight is 3150 kg and static margin has lower range.

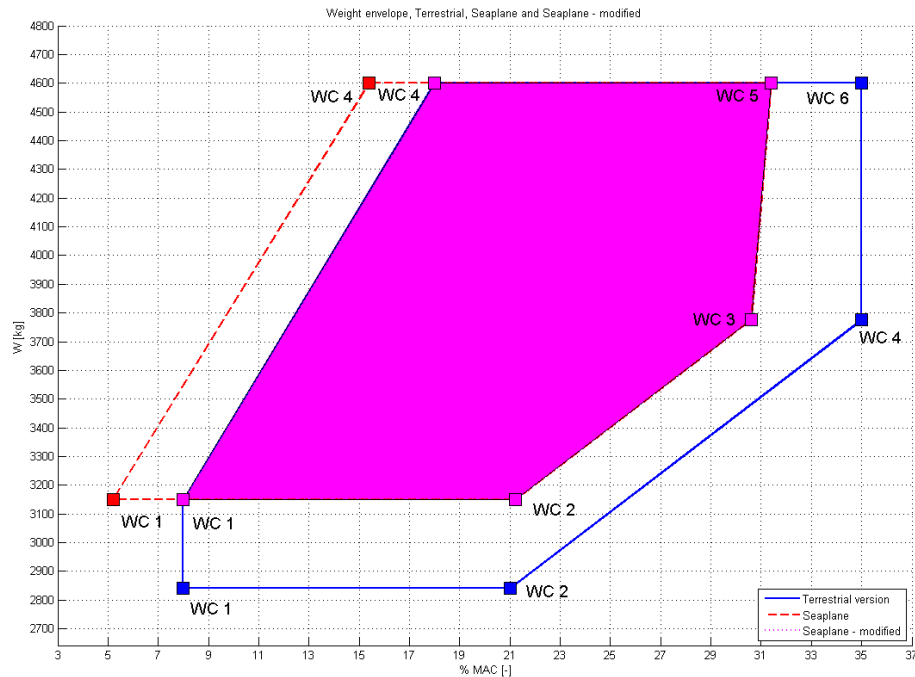


Fig. 12.5: Weight envelope of the terrestrial version, the seaplane version, and the seaplane - modified

The summary of the weight configurations mentioned in the modified seaplane envelope - Figure 12.4 is stated in Table 12.3.

Tab. 12.3: Summary of the weight configurations

Weight configuration	weight	unit	% MAC
1	3150	kg	8
2	3150	kg	21.2
3	3777	kg	30.6
4	4600	kg	18
5	4600	kg	31.4

12.3.1 Moment of inertia

Because the weight of the floats is not insignificant, moments of inertia from SAVLE need to be converted. The conversion will be done by using following considerations. Moment of inertia of the entire aeroplane around the axis of rotation is the sum

of particular moments of inertia of each component relative to the axis mentioned before¹. See Equations 12.3a, 12.3b and 12.3c.

$$I_{x_G} = \sum_{i=1}^n I_{x_{G_i}} = I_{x_{G_1}} + I_{x_{G_2}} + I_{x_{G_3}} + \dots + I_{x_{G_n}} \quad (12.3a)$$

$$I_{y_G} = \sum_{i=1}^n I_{y_{G_i}} = I_{y_{G_1}} + I_{y_{G_2}} + I_{y_{G_3}} + \dots + I_{y_{G_n}} \quad (12.3b)$$

$$I_{z_G} = \sum_{i=1}^n I_{z_{G_i}} = I_{z_{G_1}} + I_{z_{G_2}} + I_{z_{G_3}} + \dots + I_{z_{G_n}} \quad (12.3c)$$

where I_{x_G} is the moment of inertia of entire aeroplane and $I_{x_{G_i}}$ is the moment of inertia of each part. In order to simplify the determination of the moment of inertia, the following will be considered:

- As mentioned before - own moments of inertia will be neglected - except floats.
- Instead of parts, the groups used in Table 12.1 will be considered.
- Centre of gravity position of each groups will be taken into account.
- The weight of the each group will be taken into account, as well.

Moment of inertia for each group can be computed as follows:

$$I_{x_{G_i}} = m_i \cdot \sqrt{y_{G_i}^2 + z_{G_i}^2}^2 \quad (12.4a)$$

$$I_{y_{G_i}} = m_i \cdot \sqrt{x_{G_i}^2 + z_{G_i}^2}^2 \quad (12.4b)$$

$$I_{z_{G_i}} = m_i \cdot \sqrt{x_{G_i}^2 + y_{G_i}^2}^2 \quad (12.4c)$$

where x_{G_i} , y_{G_i} and z_{G_i} are the coordinates of c.g., m_i is the mass of each group.

Combining Equations 12.3a - 12.4a, 12.3b - 12.4b and 12.3c - 12.4c, removed groups can be excluded, while the floats and struts can be added.

The computations was done in Excel. Important results are stated in Table 12.4. Entire table is shown in Appendix E.

¹The own moments of inertia were due to their size neglected - except floats.

Tab. 12.4: c.g. position and moment of inertia for seaplane

Weight config.	SAVLE config.	$x_{c.g.-G}$ [mm]	$y_{c.g.-G}$ [mm]	$z_{c.g.-G}$ [mm]	I_{x_G} [kg · m ²]	I_{y_G} [kg · m ²]	I_{z_G} [kg · m ²]
1	404	6123.5	121.3	7.4	14781.5	28031.3	20142.5
2	1753	6334.4	82.0	23.4	14527.4	27716.6	20331.7
3	2011	6485.6	26.9	32.1	14869.9	30499.0	22460.5
4	509	6274.7	181.3	16.5	22476.0	36153.7	28469.8
5	1812	6497.5	-76.7	32.1	15186.1	28469.8	20614.7

12.4 Ratio of distance

Ratio of distance r_x is necessary to determine because this value is used in paragraph CS 23.527. It is used in Chapter 14, Equation 14.3 and Equation 14.4. Ratio of distance is value measured parallel to hull reference axis, from the centre of gravity of the seaplane to the hull longitudinal station at which the load factor is being computed to the radius of gyration in pitch of the seaplane, the hull reference axis being a straight line, in the plane of symmetry, tangential to the keel at main step [5].

$$r_{x_b} = \frac{\frac{a_f}{1000}}{\frac{I_{z_G}}{m_{MLW}}} \quad (12.5)$$

$$r_{x_s} = \frac{\frac{b_f}{1000}}{\frac{I_{z_G}}{m_{MLW}}} \quad (12.6)$$

where r_{x_b} is ratio of distance for bow landing case, r_{x_s} is ratio of distance for stern landing case, a_f and b_f are distances between c.g. and longitudinal stations at which the load factors are being computed in millimetres, I_{z_G} is radius of gyration in pitch of the seaplane and m_{MLW} is the maximum landing weight.

13 SPEED CORRECTIONS

Stall speed V_{S0} in landing configuration and stall speed V_{S1} in any other configuration depend on maximal lift coefficient C_{Lmax} , maximum take-off weight m_{MTOW} and position of c.g. Let us discuss these factors in more detail.

13.1 Lift curve correction

Because the floats were added, drag coefficient C_D increased. Also the lift coefficient C_L for specific angle of attack α has been changed. In other words, the lift curve could have been changed. The floats have destabilize pitching moment, thus the higher negative lift at horizontal tail has to be produced. Total lift has to be kept, that means the higher lift at the wing has to be created. Previous can be reached by higher angle of attack. If the angle of attack is increased, the floats will create lift, as well. Using previous consideration, following can be claimed: By adding the floats, lift curve is not changed too much and stall speed remains as same as for terrestrial version. It should be noted that previous is applied only for lift curve correction. In order to include change of lift curve in the calculation, it is necessary to know $C_L - \alpha$ dependence.

13.2 Weight correction

The stall speed of terrestrial version has been determined for specific points in weight envelope - Figure 12.2. It is also necessary to know stalling speed at different points in weight envelope - different weight See Figure 12.4. One way is to do flight tests, more acceptable is to use some conversion formulas in this stage of development. The latter mentioned will be discussed in the next sections. The formulas are taken from literature [13]. Once the aeroplane weight has been determined, the calibrated stalling speed determined at each data point is corrected for weight using the following equation from literature [13]:

$$V_{S0_{weight}} = V_{ST} \sqrt{\frac{W_S}{W_T}} \quad (13.1)$$

where $V_{S0_{weight}}$ is the weight corrected calibrated stalling speed, V_{ST} is the stalling speed corrected for instrument and position error, W_T is the aeroplane weight at the stall and finally W_S is the standard weight, or the weight to which certification is sought; normally the maximum take-off weight. Speed V_{ST} was taken from internal document [1]. The results are stated in Table 13.1.

Tab. 13.1: Weight corrected calibrated stalling speed

Weight configuration	W_S [kg]	W_T [kg]	V_{ST} [km/h]	$V_{S0_{weight}}$ [km/h]
1	3150	3150	98.8	98.8
2	3150	3150	98.8	98.8
3	3777	3800	107.9	107.6
4	4600	4600	118.0	118.0
5	4600	4600	118.0	118.0

It is seen that there is difference in weights only for weight configuration number three. The weights corresponds in other points of weight envelope and weight correction gives, of course, same values. Also, the difference between stall speeds in weight configuration number three is insignificant.

13.3 Centre of gravity correction

To accomplish centre of gravity correction, one must first correct the weight corrected stalling speed to a value of lift coefficient using the following equation:

$$C_{L_{comp}} = \frac{2 \cdot m_{MTOW} \cdot g}{\rho \cdot S \cdot (V_{S0_{weight}})^2} \quad (13.2)$$

where $C_{L_{comp}}$ is the maximum lift coefficient at the computed c.g., m_{MTOW} is the maximum landing weight, g is the gravitational acceleration, ρ is the density of the air, S is the area of the wing and $V_{S0_{weight}}$ is the weight corrected calibrated stalling speed.

One then corrects this, lift coefficient can be computed, as follows [13]:

$$C_{L_{ref}} = C_{L_{comp}} \left[1 + \frac{MAC}{l_t} \cdot \left(\frac{c \cdot g_{ref} - c \cdot g_{comp}}{100} \right) \right] \quad (13.3)$$

where $C_{L_{ref}}$ is the maximum lift coefficient at the desired c.g., $C_{L_{comp}}$ is the maximum lift coefficient at the computed c.g., MAC is the mean aerodynamic chord and l_t is the length of the tail (assumed to be from 1/4 chord of the wing to 1/4 chord of the horizontal tail).

The new $C_{L_{ref}}$ is converted back to stalling speed:

$$V_{S0} = \sqrt{\frac{2 \cdot m_{MLW} \cdot g}{\rho \cdot A \cdot C_{L_{ref}}}} \quad (13.4)$$

Tab. 13.2: Centre of gravity correction

Weight configuration	m_{MTOW} [kg]	$V_{S0_{weight}}$ [km/h]	$C_{L_{comp}}$ [1]	$C_{L_{ref}}$ [1]	$c.g.comp$ [%]	$c.g.ref$ [%]	V_{S0} [km/h]
1	3150	98.8	2.6575	2.6575	8	8	98.8
2	3150	98.8	2.6575	2.7344	8	21.2	97.4
3	3777	107.6	2.6880	2.7581	18	30.6	106.2
4	4600	118.0	2.7207	2.7159	18	17.4	118.1
5	4600	118.0	2.7207	2.7196	18	31.4	116.5

The same adjustment can be done for stall speed V_{S1} for flaps 20° configuration. This configuration was chosen in accordance with CS 23.531 paragraph where following is written: V_{S1} seaplane stalling speed (knots) at the design water take-off weight with flaps extended in the appropriate take-off position [5].

$$V_{S1_{weight}} = V_{ST} \sqrt{\frac{W_S}{W_T}}, \quad (13.5)$$

$$C_{L_{comp}} = \frac{2 \cdot m_{MLW} \cdot g}{\rho \cdot A \cdot (V_{S0_{weight}})^2}, \quad (13.6)$$

$$C_{L_{ref}} = C_{L_{comp}} \left[1 + \frac{MAC}{l_t} \cdot \left(\frac{c.g.ref - c.g.comp}{100} \right) \right], \quad (13.7)$$

$$V_{S1} = \sqrt{\frac{2 \cdot m_{MLW} \cdot g}{\rho \cdot A \cdot C_{L_{ref}}}}. \quad (13.8)$$

The results are stated in following Table 13.3:

Tab. 13.3: Centre of gravity correction

Weight configuration	m_{MTOW} [kg]	$V_{S1_{weight}}$ [km/h]	$C_{L_{comp}}$ [1]	$C_{L_{ref}}$ [1]	$c.g.comp$ [%]	$c.g.ref$ [%]	V_{S1} [km/h]
1	3150	119.4	1.8196	1.8196	8	8	119.4
2	3150	119.4	1.8196	1.8723	8	21.2	117.7
3	3777	130.1	1.8376	1.8855	18	30.6	128.4
4	4600	142.7	1.8603	1.8571	18	17.4	142.8
5	4600	142.7	1.8603	1.9089	18	31.4	142.9

From previous tables is evident, that the change in stalling speed is very low and could be neglected. However, all the computations are programmed in MATLAB, thus corrected speeds are used in this master's thesis.

14 WATER LOADS

Water loads are determined in accordance with CS 23.527, CS 23.529 and CS 23.531 paragraphs. It is solved for every weight configuration stated in Chapter 12. The weight configurations are listed in Table 11.1. The forces and load factors are limit loads. Reaction forces are computed for both floats together. To get reaction force acting on one floats, results needs to be divided by two.

14.1 Symmetrical step landing case

Quantities used for symmetrical step landing are marked by subscript *A*. Symmetrical step landing case is defined in CS 23.529 as a landing, when the resultant water load must be applied at the keel, through the centre of gravity, and must be directed perpendicularly to the keel line. See Figure 14.1.

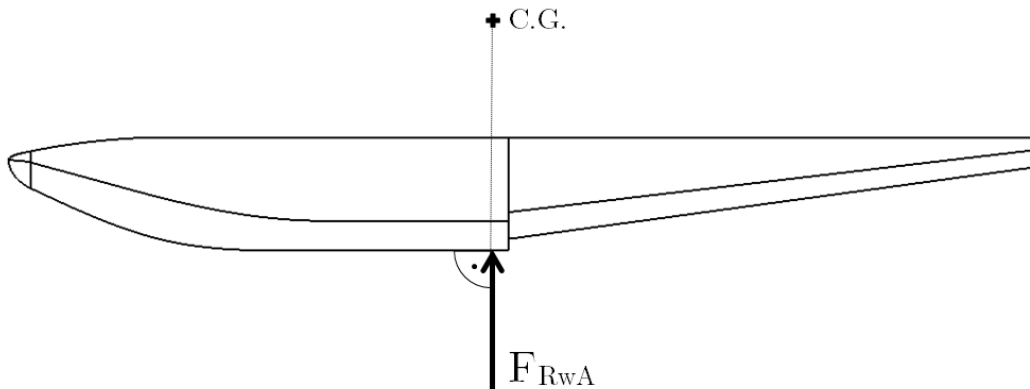


Fig. 14.1: Position of applied resultant water load for step landing

In accordance with CS 23.527, water reaction factor n_{w_A} must be computed in the following manner:

$$n_{w_A} = \frac{C_1 \cdot V_{S0}^2}{\left(\tan^{\frac{2}{3}} \beta\right) \cdot (m_{LW})^{\frac{1}{3}}} \quad (14.1)$$

where n_{w_A} is the water reaction load factor, C_1 is the empirical seaplane operations factor equal to 0.012 [5] (except that this factor may not be less than that necessary to obtain the minimum value of step load factor of 2.33), V_{S0} is the seaplane stalling speed in knots with flaps extended in the appropriate landing position - determined in Table 13.2 and with no slipstream effect, β is the angle of dead rise at the longitudinal station at which the load factor is being determined in accordance with Figures 14.1 and 14.2, m_{LW} is the seaplane design landing weight in pounds. Using

corrected speeds that have been set in Chapter 13, appropriate weight configuration and dead rise angles measured in CATIA, following load factors are get:

Tab. 14.1: Load factors n_{w_A} for step landings

Weight configuration	V_{S0}	m_{LW}	β	n_{w_A}
[-]	[kn]	[lb]	[°]	[1]
1	53.3	6945	26.3	2.86
2	52.5	6945	26.7	2.74
3	57.3	8327	26.7	3.07
4	63.6	10141	26.7	3.56
5	62.8	10141	26.7	3.46

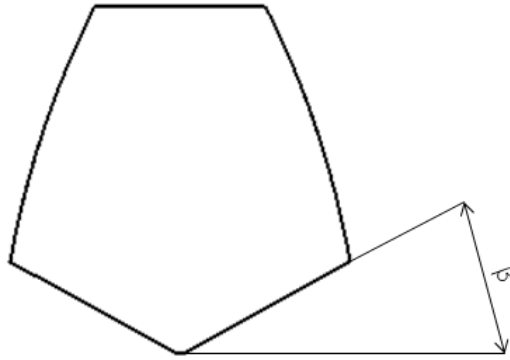


Fig. 14.2: Dead rise angle position

Taking into account Newton's second law, following can be written:

$$F_{Rw_A} = m_{LW} \cdot g \cdot \left(n_{w_A} + \frac{2}{3} \right) \quad (14.2)$$

where n_{w_A} is water reaction load factor for symmetrical step landing, m_{LW} is the seaplane design landing weight and g is the gravitational acceleration. Except in the take-off condition of CS 23.531, the aerodynamic lift on the seaplane during the impact is assumed to be 2/3 of the weight of the seaplane [5]. For known weight configurations following reaction forces F_{Rw_A} oriented in according to Figure 14.1 are received:

Tab. 14.2: Reaction forces F_{Rw_A} for symmetrical step landings

Weight configuration	F_{Rw_A}	x_f
[-]	[N]	[mm]
1	108881.7	374.1
2	105338.6	163.1
3	138395.6	11.9
4	190452.5	222.8
5	186099.4	0.0

Because reaction forces F_{Rw_A} have different points of action x_f , the worst case in terms of the stress of the struts is determined in the Chapter 16. Table 14.2, inter alia, contains x_f coordinates in the FCS, where the forces act.

14.2 Symmetrical bow landing case

Quantities used for symmetrical step landing are marked by subscript B . Symmetrical bow landing case is defined in CS 23.529 as a landing where the resultant water load must be applied at the keel, one-fifth of the longitudinal distance from the bow to the step, and must be directed perpendicularly to the keel line. See Figure 14.3.

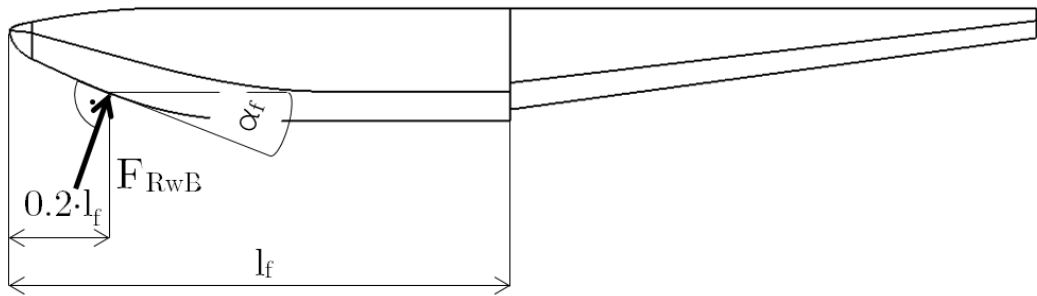


Fig. 14.3: Position of applied resultant water load for bow landing

Load factor for bow landing is given in CS 23.527 by the following equation:

$$n_{wB} = \frac{C_1 \cdot V_{S0}^2}{\left(\tan^{\frac{2}{3}} \beta\right) \cdot (m_{LW})^{\frac{1}{3}}} \cdot \frac{K_1}{(1 + r_{x_b}^2)^{\frac{2}{3}}} \quad (14.3)$$

where n_{wB} is the water reaction load factor for bow landing, C_1 is the empirical seaplane operations factor equal 0.012 (except that this factor may not be less than that necessary to obtain the minimum value of step load factor of 2.33), V_{S0} is the seaplane stalling speed in knots with flaps extended in the appropriate landing position - determined in Table 13.2 and with no slipstream effect. β is the angle of dead rise at the longitudinal station at which the load factor is being determined in accordance with Figure 14.3. m_{LW} is the seaplane design landing weight in pounds, K_1 is the empirical hull station weighing factor in accordance with Figures B.1, B.2, B.3, B.4 and B.5, r_{x_b} is the ratio of distance that has been determined in Chapter 12, measured parallel to hull reference axis, from the centre of gravity of the seaplane to the hull longitudinal station at which the load factor is being computed to the radius of gyration in pitch of the seaplane, the hull reference axis being a straight line, in the plane of symmetry, tangential to the keel at the main step.

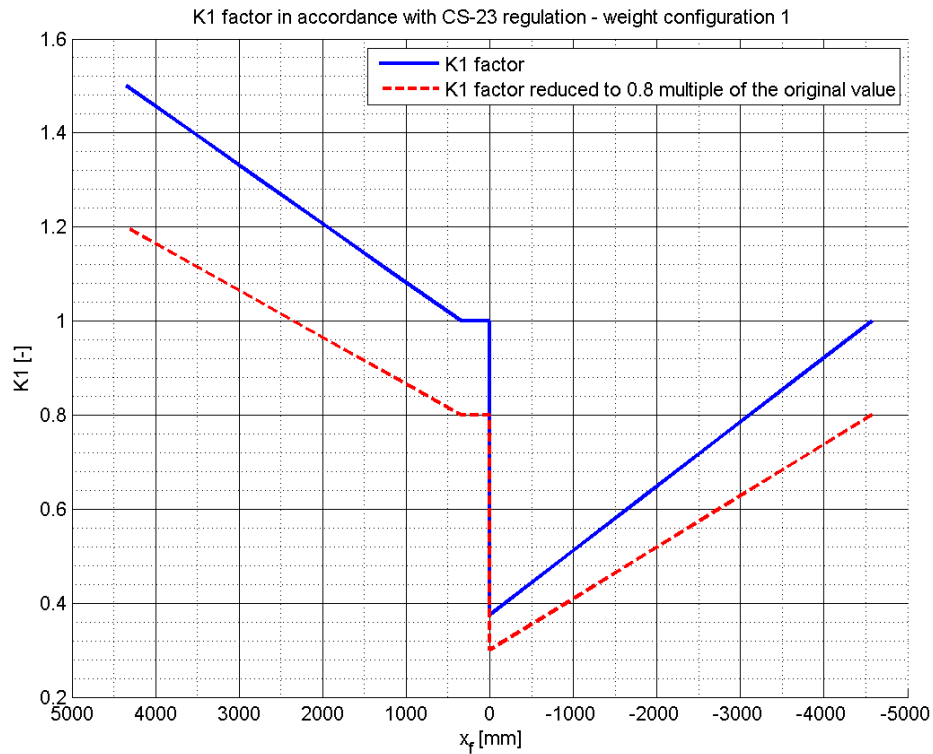


Fig. 14.4: K_1 factor against x_f coordinate - weight configuration 1

For a twin float seaplane, because of the effect of flexibility of the attachment of the floats to the seaplane, the factor K_1 may be reduced at the bow and stern to 0.8 of the original value. Figure 14.4 shows two curves: blue solid line shows standard K_1 factor. Red dashed line shows decreased K_1 factor using rule from paragraph

CS 23.527. This reduction could be applied only to the design of the carry through and seaplane structure. Graphs for the other weight configurations are stated in Appendix B.

For all the five weight configurations, K_1 factors for bow landings are computed in following Table 14.3 in according to position x_f of reaction force F_{RwB} from Table 14.5.

Tab. 14.3: K_1 factor for different weight configuration

Weight configurations	K_1 factor
[-]	[-]
1	1.110
2	1.115
3	1.120
4	1.115
5	1.120

In accordance with Table 14.3, Equation 14.3 and using corrected speeds V_{S0} from Chapter 13 and ratio of distance r_{x_b} from Chapter 12, and dead rise angle β set in Chapter 10, the load factor n_{w_B} is computed. The results are mentioned in Table 14.4.

Tab. 14.4: Load factors n_{w_B} for bow landings

Weight configuration	V_{S0}	m_{LW}	β	n_{w_B}
[-]	[kn]	[lb]	[°]	[1]
1	53.3	6945	40.2	1.08
2	52.5	6945	40.2	1.07
3	57.3	8327	40.2	1.16
4	63.6	10141	40.2	1.20
5	62.8	10141	40.2	1.14

By using Equation 14.2, the same one like in section 14.1, reaction forces F_{RwB} and their appropriate positions are:

Tab. 14.5: Reaction forces F_{RwB} for symmetrical bow landings

Weight configuration	F_{RwB}	x_f
[-]	[N]	[mm]
1	53983.2	3480
2	53621.7	3480
3	67632.3	3480
4	84069.8	3480
5	81706.1	3480

14.3 Symmetrical stern landing case

Quantities used for symmetrical step landing are marked by subscript C . Symmetrical stern landing case is defined in CS 23.529 as a landing where the resultant water load must be applied at the keel, at a point 85% of the longitudinal distance from the step to the stern post, and must be directed perpendicularly to the keel line. See Figure 14.5.

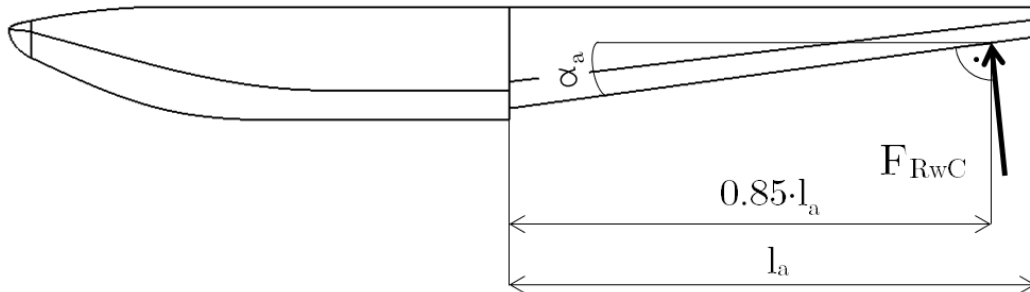


Fig. 14.5: Position of applied resultant water load for stern landing

Load factor for stern landing is given by the following equation:

$$n_{wC} = \frac{C_1 \cdot V_{S0}^2}{\left(\tan^{\frac{2}{3}} \beta\right) \cdot (m_{LW})^{\frac{1}{3}}} \cdot \frac{K_1}{(1 + r_{x_s}^2)^{\frac{2}{3}}} \quad (14.4)$$

Description of the variables in Equation 14.4 is same like in Equation 14.3 and therefore will not be explained again. For all five weight configuration K_1 factors for bow landings are computed in following Table 14.6 in according to position x_f of reaction force F_{RwC} from Table 14.8.

Tab. 14.6: K_1 factor for different weight configuration

Weight configurations	K_1 factor
[-]	[-]
1	0.720
2	0.720
3	0.720
4	0.720
5	0.720

Again, n_{wC} load factor can be computed using the equation 14.4. Results are in Table 14.7.

Tab. 14.7: Load factors n_{wC} for stern landings

Weight configuration	V_{S0}	m_{LW}	β	n_{wC}
[-]	[kn]	[lb]	[°]	[-]
1	53.3	6945	25.1	0.95
2	52.5	6945	25.1	0.93
3	57.3	8327	25.1	0.99
4	63.6	10141	25.1	1.03
5	62.8	10141	25.1	0.98

Finally, the result forces, determined by using equation 14.2 are stated in Table 14.8:

Tab. 14.8: Reaction forces F_{Rw} for symmetrical bow landings

Weight configuration	F_{RwC}	x_f
[-]	[N]	[mm]
1	49952.0	-3886.2
2	49253.8	-3886.2
3	61687.5	-3886.2
4	76477.8	-3886.2
5	74190.7	-3886.2

14.4 Unsymmetrical landing case

Quantities used for symmetrical step landing are marked by subscript D . The unsymmetrical loadings consists of an upward load at the step of each float of 0.75 and a side load of $0.25 \cdot \tan \beta$ at one float times the step landing load reached under CS 23.527. The side load is directed inboard, perpendicularly to the plane of symmetry midway between the keel and chine lines of the float, at the same longitudinal station as the upwards load. See Figure 14.6 and following Equations¹.

$$F_{RwD,y} = 0.75 \cdot F_{RwA} \quad (14.5a)$$

$$F_{RwD,z} = 0.25 \cdot \tan \beta \cdot F_{RwA} \quad (14.5b)$$

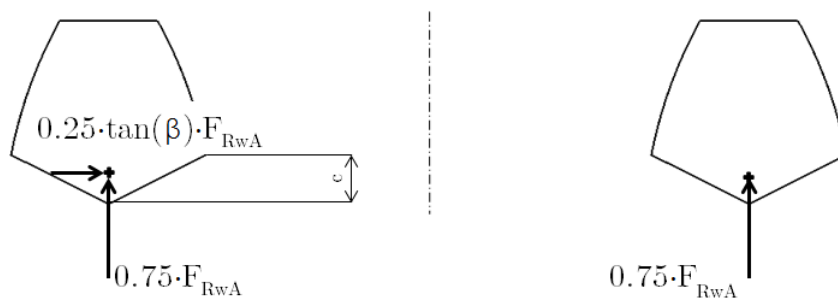


Fig. 14.6: Position of applied resultant water load for unsymmetrical landing case

Taking into account data that have been gotten in section 14.1 and previous paragraph, following table 14.9 is built:

¹It is necessary to use original version of CS 23 regulation. There is a mistake in Czech translation. Instead of 0.75 there is written $0.75 \cdot \tan \beta$

Tab. 14.9: Reaction forces $F_{Rw_D,y}$ and $F_{Rw_D,z}$ for unsymmetrical step landings

Weight configuration	x_f	y_f	z_f	F_{Rw_A}	$F_{Rw_D,y}$	$F_{Rw_D,z}$
[-]	[mm]	[mm]	[mm]	[N]	[N]	[N]
1	374.1	126.5	1750	108881.7	61246.0	13276.3
2	163.1	126.5	1750	105338.6	59253.0	19266.4
3	11.9	126.5	1750	138395.6	77847.5	25312.5
4	222.8	126.5	1750	190452.5	107129.5	34833.7
5	0.0	126.5	1750	186099.4	104680.9	34037.5

There was used reaction force acting only on one float in Table 14.9. The reason is that forces act

14.5 Take-off case

Quantities used for symmetrical step landing are marked by subscript E . In accordance with paragraph CS 23.531, the aerodynamic wing lift is assumed to be zero for the wing and its attachment to the hull or a main float and downward inertia load, corresponding to a load factor computed from the following formula, must be applied [5]:

$$n_{w_E} = \frac{C_{TO} \cdot V_{S1}^2}{\left(\tan^{\frac{2}{3}} \beta\right) \cdot (m_{TOW})^{\frac{1}{3}}} \quad (14.6)$$

where n_{w_E} is the inertia load factor, C_{TO} is the empirical seaplane operations factor equal 0.004, V_{S1} is the seaplane stalling speed in knots at the design take-off weight with the flaps extended in the appropriate take-off position. Flap position was set to 20° . β is the angle of dead rise at the main step (in degrees) in accordance with Figures 14.1 and 14.2. m_{TOW} is the design water take-off weight in pounds.

Using same method as many times above, loading factor n_{w_E} is determined:

Tab. 14.10: Load factors n_{w_E} for take-off

Weight configuration	V_{S1}	m_{TOW}	β	n_{w_E}
[-]	[kn]	[lb]	[°]	[-]
1	64.4	6945	26.3	1.39
2	63.4	6945	26.7	1.34
3	69.2	8327	26.7	1.50
4	77.0	10141	26.7	1.73
5	75.9	10141	26.7	1.69

Newton's law expressed by Equation 14.2 gives the result forces:

Tab. 14.11: Reaction forces F_{Rw} for take-off

Weight configuration	F_{Rw_E}	x_f
[-]	[N]	[mm]
1	42996.4	374.1
2	41272.1	163.1
3	55460.0	11.9
4	78212.4	222.8
5	76087.0	0.0

14.6 Hydrostatic drag

In accordance with literature [14], hydrostatic drag can be expressed as:

$$D_{HS} = 0.1 \cdot W \quad (14.7)$$

where W is the weight. The hydrostatic drag acts at the centre of buoyancy. Hydrodynamic drag, in accordance with literature [14] is expressed as follows:

$$D_{HD} = (0.15 \div 0.25) \cdot m_{TOW} \quad (14.8)$$

The results of the previous formulas summarizes following table:

Tab. 14.12: Hydrostatic drag D_{HS} and hydrodynamic drag D_{HD}

Weight configuration	D_{HS}	D_{HD}
[-]	[N]	[N]
1	3090	7726
2	3090	7726
3	3706	9263
4	4513	11282
5	4513	11282

14.7 Summary

Load factors n_{w_A} , n_{w_B} , n_{w_C} , n_{w_D} , n_{w_E} have been determined for five weight configurations. These load factors are related to the symmetrical landing cases - step landing, bow landing and stern landing, take-off and unsymmetrical landing case. Further, reaction forces F_{Rw_A} , F_{Rw_B} , F_{Rw_C} , F_{Rw_D} , F_{Rw_E} , $F_{Rw_D,y}$, $F_{Rw_D,z}$ were determined for previous cases, as well. Finally, there are forces caused by hydrostatic and hydrodynamic drag - D_{HS} and D_{HD} . Acting point of hydrostatic and hydrodynamic force is at c.b. All these forces mentioned in this paragraph are stated in Table C.1 in Appendix C.

Maximal load factor computed in accordance with [5] is $n_{w_A} = 3.56$. Paragraph CS 23.525 is applied, thus the maximum load factor is:

$$n_{w_{max,LL}} = n_{w_A} + \frac{2}{3} = 3.56 + 0.66 = 4.22 \quad (14.9)$$

Safety of margin 1.5 is used:

$$n_{w_{max,UL}} = n_{w_{max,LL}} \cdot 1.5 = 6.33 \quad (14.10)$$

This ultimate load factor was gained for weight configuration 4 and symmetrical step landing case. This value is compared with load factors for landing cases for terrestrial version from SAVLE for terrestrial version. The highest load factor at c.g. for terrestrial version during ground load is for weight configuration 2610. This configuration is for maximum take-off weight $m_{MTOW} = 4600 \text{ kg}$ and minimum static margin 18%. This ultimate load is $n = 5.58$ in y-direction (ACS).

It is seen that maximum ultimate load factor for seaplane is 11.8% greater than for ground version. This means that parts like fuselage, wing, horizontal tail and

nacelles will be loaded by higher inertia forces. Applied ultimate loads at landing gear spars needs to be checked and compared with ultimate loads from water level landing. This is solved in Chapter 16. Previous needs to be done also for other parts mentioned earlier.

15 ATTACHMENT POINTS

For the easiest modification between terrestrial and seaplane version, there is effort to use existing attachment points for landing gear. Existing joints are shown in Figure 15.1.

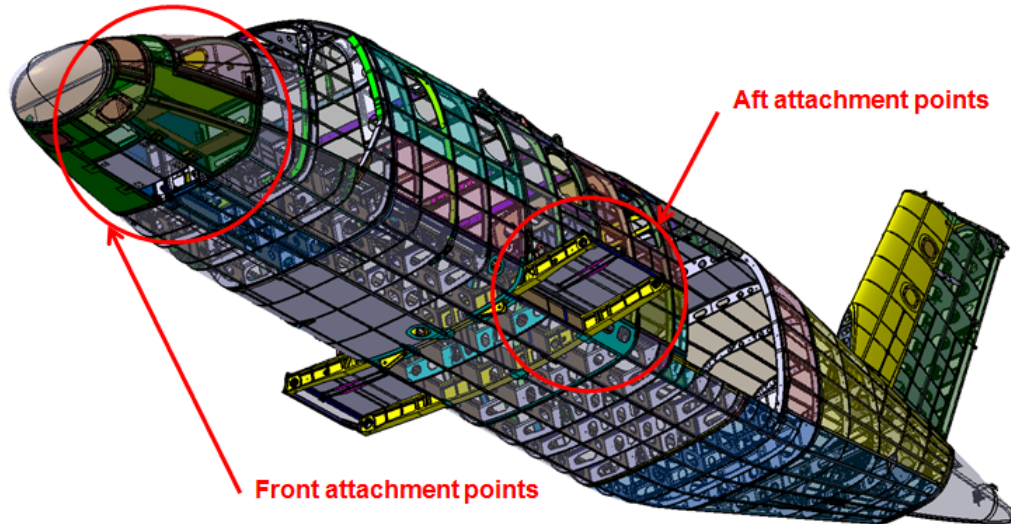


Fig. 15.1: Front and aft attachment points

15.1 Front attachment points

Existing landing gear is attached to the lugs which are connected to the longitudinal spars and via stringers to the bulkhead number three. It is shown in Figure 15.2. There will be mentioned later that lugs for front struts are not suitable because the stress in rods increases rapidly due to frame geometry. Thus, these connection points will be used as an auxiliary joints. The main connection point has to be higher. One of possible solution is shown in Figure 15.3. Blue dashed line represents horizontal stringer that has to be added to transfer horizontal part of loading from the strut to the bulkhead.

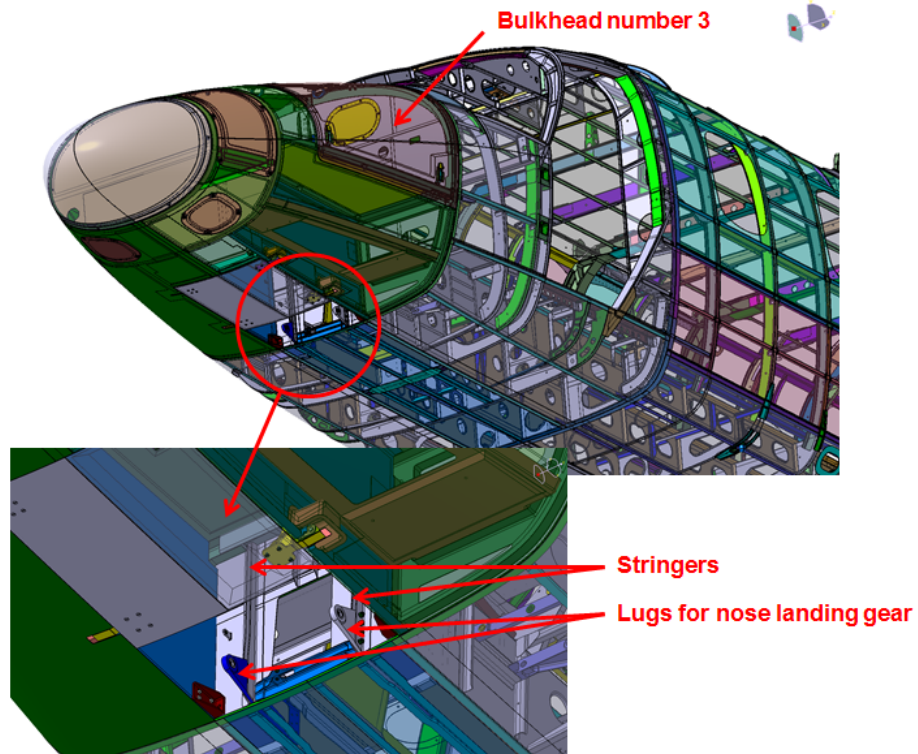


Fig. 15.2: Front attachment points

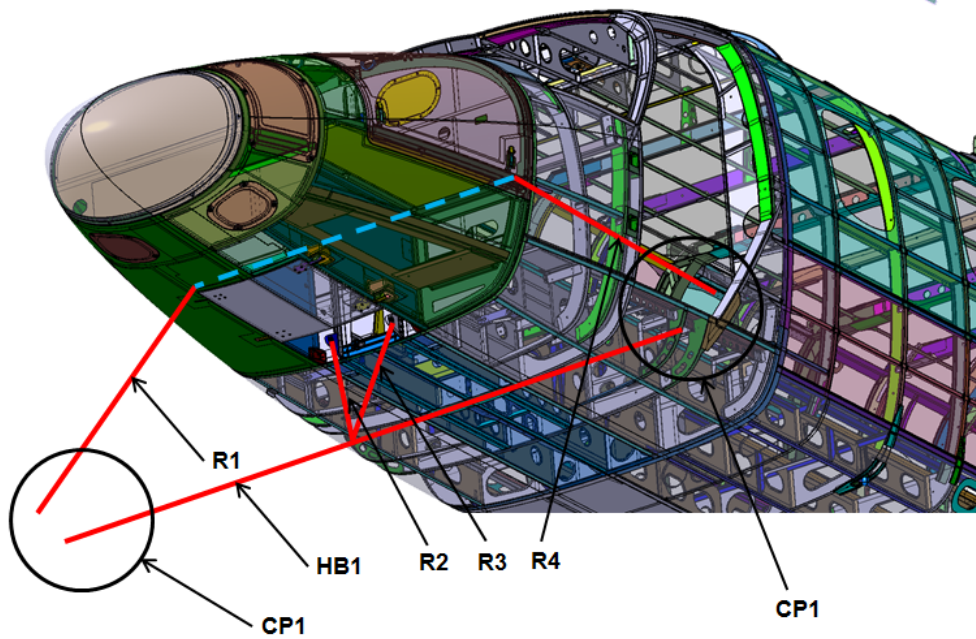


Fig. 15.3: Front attachment points - solution

15.2 Aft attachment points

Aft attachment points are shown in Figure 15.4. This solution assumes that the main legs ML(1) to ML(4) are connected to the longitudinal rotational axis. Thus, the loading is transferred via this axis to the front and aft landing gear spars.

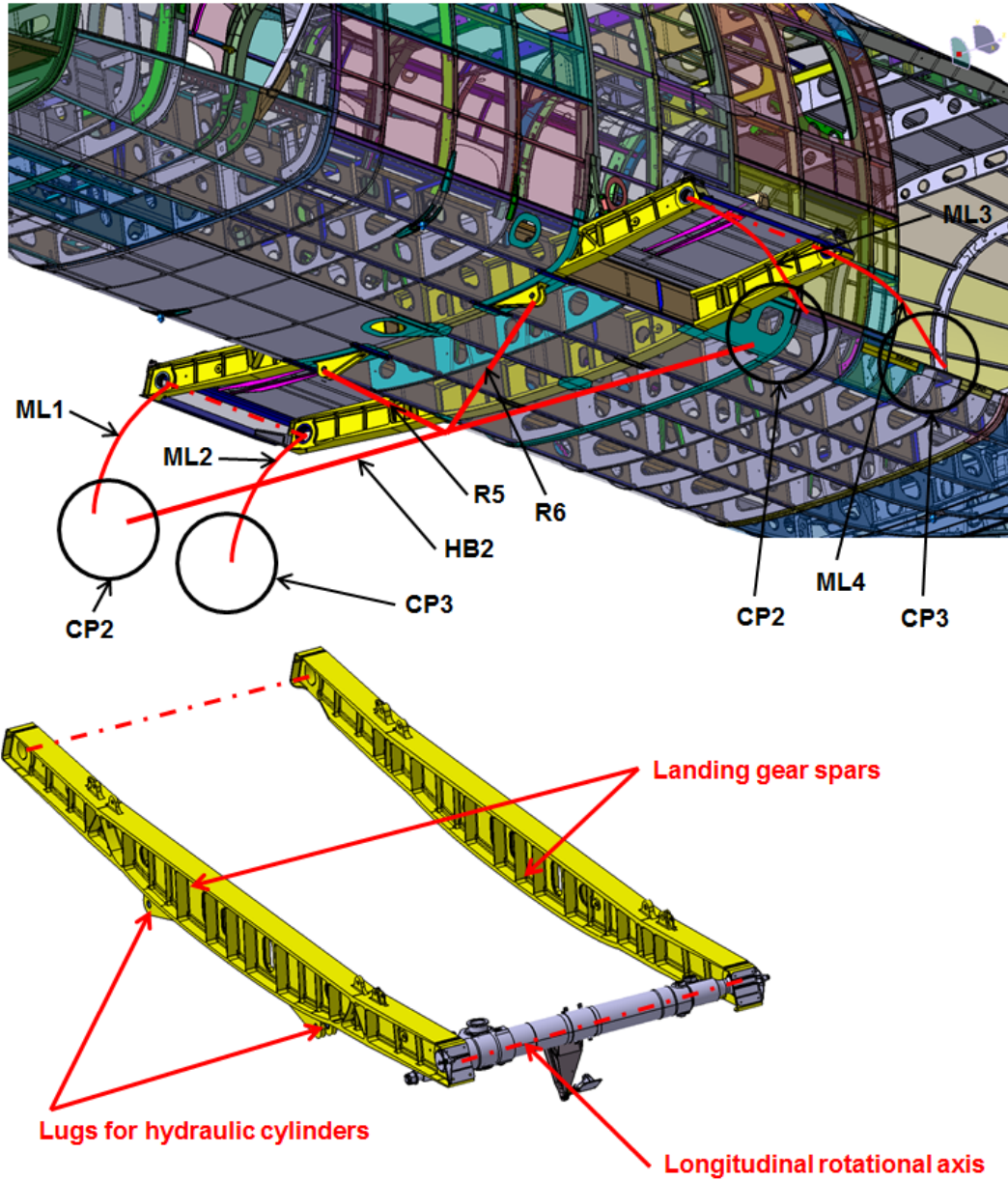


Fig. 15.4: Aft attachment points

16 STRESS ANALYSIS

This chapter is dealing with stress calculation for design chosen during development. The strength calculation were done for about 5 modifications which are not mentioned in the master's thesis due to page restriction. The solution that fulfils both the construction requirements and the strength requirements was chosen for deeper analysis.

16.1 Ultimate load

The ultimate load is the limit load that is multiplied by prescribed factors of safety. The limit load is the maximum load to be expected in service and was determined in chapter 14. Factor of safety is set to 1.5 in accordance with literature [5]. Following tables show conversion of limit load to ultimate load for different loading cases. Aeroplane coordination system is used. Forces are taken from Chapter 14. Also, the forces are distributed to the directions corresponding to ACS. Appropriate angles α_f and α_a from Figures 14.3 and 14.5 are set in Chapter 10. From here further only ultimate load will be used. If the special factor of safety is used, it is going to be mentioned in appropriate part of the master's thesis.

Tab. 16.1: Limit and Ultimate reaction forces for step landing

Step landing				
Limit load				
Load case	F_{Rw_A}	$F_{Rw_A,x}$	$F_{Rw_A,y}$	$F_{Rw_A,z}$
[-]	[N]	[N]	[N]	[N]
LC 1	108881.7	0	108881.7	0
LC 2	105338.6	0	105338.6	0
LC 3	138395.6	0	138395.6	0
LC 4	190452.5	0	190452.5	0
LC 5	186099.4	0	186099.4	0
Ultimate load				
Load case	F_{Rw_A}	$F_{Rw_A,x}$	$F_{Rw_A,y}$	$F_{Rw_A,z}$
[-]	[N]	[N]	[N]	[N]
LC 1	163322.6	0	163322.6	0
LC 2	158007.9	0	158007.9	0
LC 3	207593.4	0	207593.4	0
LC 4	285678.8	0	285678.8	0
LC 5	279149.1	0	279149.1	0

Tab. 16.2: Limit and Ultimate reaction forces for bow landing

Bow landing				
Limit load				
Load case	F_{Rw_B}	$F_{Rw_B,x}$	$F_{Rw_B,y}$	$F_{Rw_B,z}$
[-]	[N]	[N]	[N]	[N]
LC 6	53983.2	19345.8	50397.7	0
LC 7	53621.7	19216.3	50060.2	0
LC 8	67632.3	24237.2	63140.2	0
LC 9	84069.8	30127.9	78485.9	0
LC 10	81706.1	29280.8	76279.2	0
Ultimate load				
Load case	F_{Rw_B}	$F_{Rw_B,x}$	$F_{Rw_B,y}$	$F_{Rw_B,z}$
[-]	[N]	[N]	[N]	[N]
LC 6	80974.8	29018.8	75596.5	0
LC 7	80432.6	28824.4	75090.3	0
LC 8	101448.5	36355.9	94710.3	0
LC 9	126104.7	45191.9	117728.9	0
LC 10	122559.2	43921.3	114418.8	0

Tab. 16.3: Limit and Ultimate reaction forces for stern landing

Stern landing				
Limit load				
Load case	F_{Rw_C}	$F_{Rw_C,x}$	$F_{Rw_C,y}$	$F_{Rw_C,z}$
[-]	[N]	[N]	[N]	[N]
LC 11	49952.0	6736.1	49495.7	0
LC 12	49253.8	6641.9	48803.9	0
LC 13	61687.5	8318.6	61124.0	0
LC 14	76477.8	10313.1	75779.2	0
LC 15	74190.7	10004.7	73513.0	0
Ultimate load				
Load case	F_{Rw_C}	$F_{Rw_C,x}$	$F_{Rw_C,y}$	$F_{Rw_C,z}$
[-]	[N]	[N]	[N]	[N]
LC 11	74928.0	10104.1	74243.6	0
LC 12	73880.7	9962.9	73205.9	0
LC 13	92531.3	12477.9	91686.1	0
LC 14	114716.7	15469.7	113668.9	0
LC 15	111286.1	15007.0	110269.6	0

Tab. 16.4: Limit and Ultimate reaction forces for unsymmetrical landing

Unsymmetrical landing				
Limit load				
Load case	F_{Rw_D}	$F_{Rw_D,x}$	$F_{Rw_D,y}$	$F_{Rw_D,z}$
[-]	[N]	[N]	[N]	[N]
LC 16	108881.7	0	81661.3	13276.3
LC 17	105338.6	0	79004.0	12844.3
LC 18	138395.6	0	103796.7	16875.0
LC 19	190452.5	0	142839.4	23222.5
LC 20	186099.4	0	139574.6	22691.7
Ultimate load				
Load case	F_{Rw_D}	$F_{Rw_D,x}$	$F_{Rw_D,y}$	$F_{Rw_D,z}$
[-]	[N]	[N]	[N]	[N]
LC 16	163322.6	0	122491.9	19914.4
LC 17	158007.9	0	118505.9	19266.4
LC 18	207593.4	0	155695.1	25312.5
LC 19	285678.8	0	214259.1	34833.7
LC 20	279149.1	0	209361.8	34037.5

16.2 General description

The floats are attached to the fuselage using two struts (R1) and (R4) at the bulkhead number three, four main beams (ML1), (ML2), (ML3) and (ML4) between front and rear landing gear spars. There are also horizontal beams (HB1) and (HB2) connecting floats together. These horizontal beams are supported by struts (R2), (R3), (R5) and (R6). The vertical loads are transferred by elements (R1), (R2), (R3), (R4), (ML1), (ML2), (ML3) and (ML4). The horizontal longitudinal loads are transferred by shear wall between beams (ML1), (ML3) and (ML2), (ML4) and then by these beams to the landing gear spars. The side loads are transferred by front frame made from elements (R1), (R2), (R3), (R4), (HB1) and also aft frame

made from elements (ML1), (ML3), (HB2), (R5) and (R6). The torsional moment is transferred by elements (ML1), (ML2), (ML3) and (ML4). See Figure 16.1.

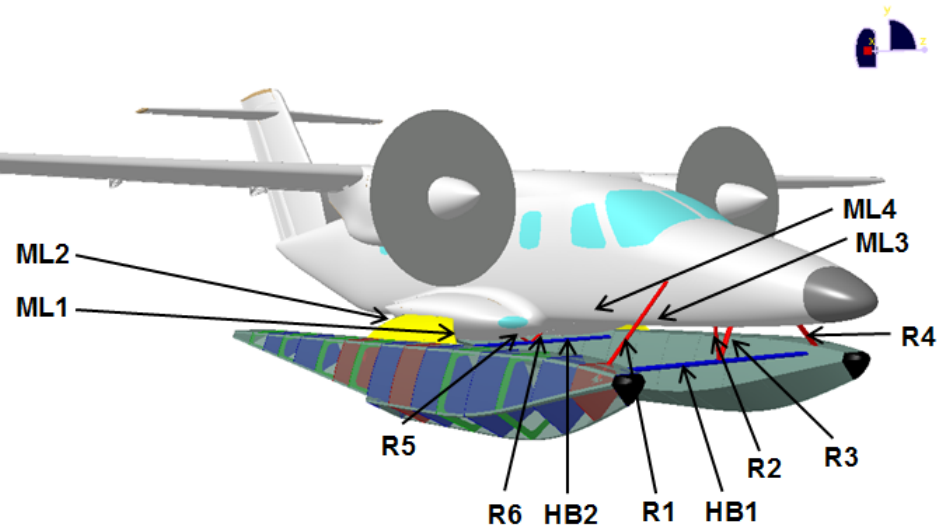


Fig. 16.1: General description of loaded elements

16.3 Finite Element Method - description

To determine stress on the elements, FEM model of the EV-55 is used. There is used EV55_v7_00_03 version of FEM model in this master's thesis (Figure 16.2).

0:EV55_v7_00_03_original.nas : ORIGINAL STATE



Fig. 16.2: EV55-v7-00-03 version of FEM model

Because only the stress analysis of the attachment elements is going to be determined, some simplification of the FEM model is done. First of all, the landing gear is removed. All of the mass concentration points CONM2 and their rigid body elements RBE3 are removed and entire wing is removed, as well. The clean FEM model of fuselage is shown in Figure 16.3.

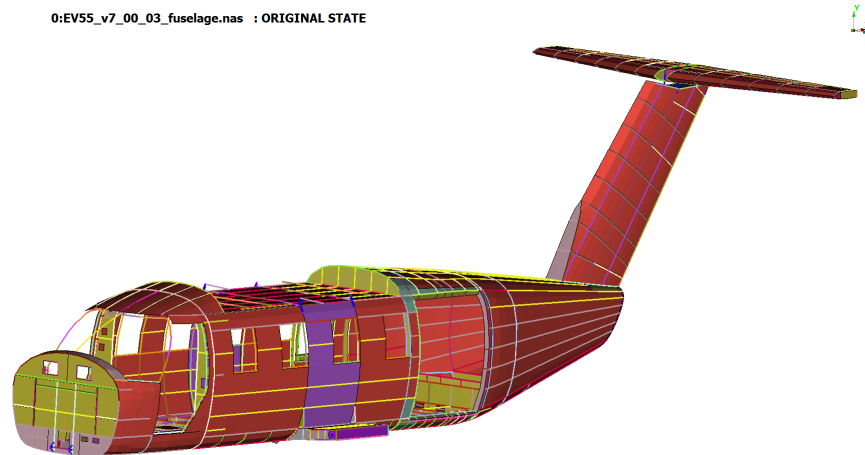


Fig. 16.3: Clean model of the fuselage

After cleaning the original FEM model, the new elements are added. Beam elements of the floats, rod elements of the struts, beam elements of the horizontal struts, rigid body elements connecting the struts, shear walls, boundary conditions and forces.

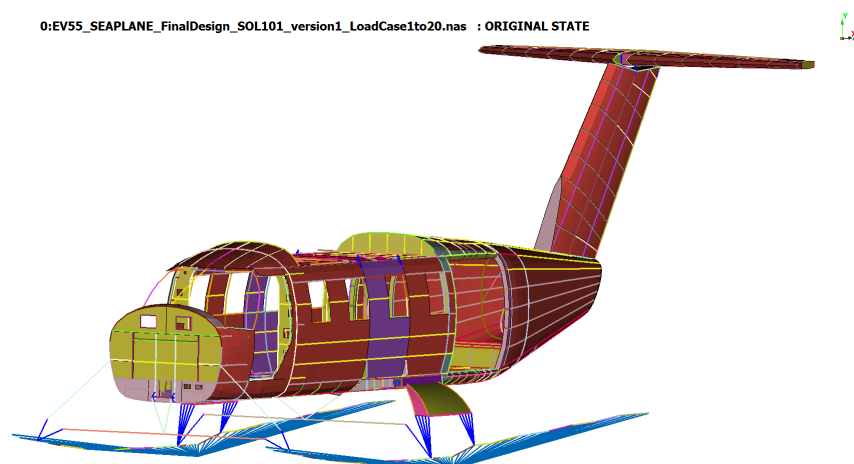


Fig. 16.4: FEM model of the EV-55 Seaplane

16.3.1 FEM model of the floats

3D model of the floats was simplified to 1D beam elements. These elements have 22 properties depending on their position. These input data are listed in Appendix F. Top and side view of the float elements are in Figure 16.6 and 16.5.

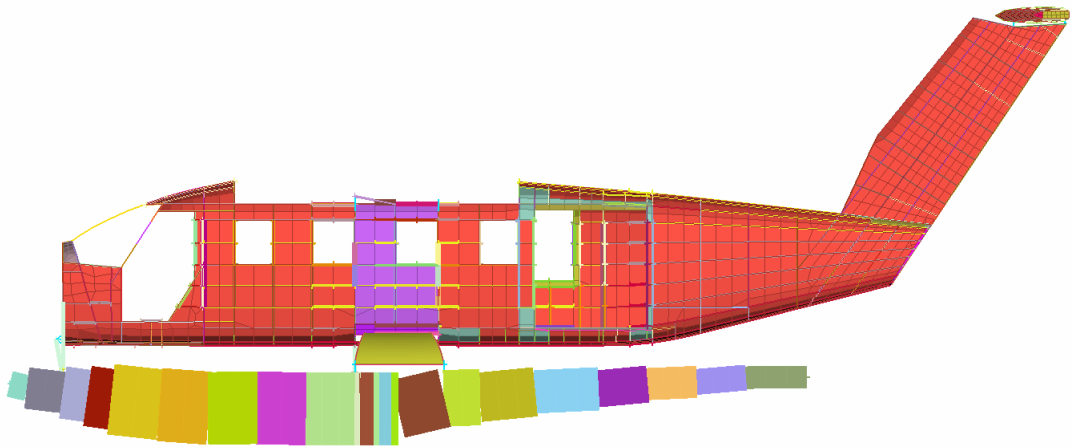


Fig. 16.5: FEM model of the floats - side view

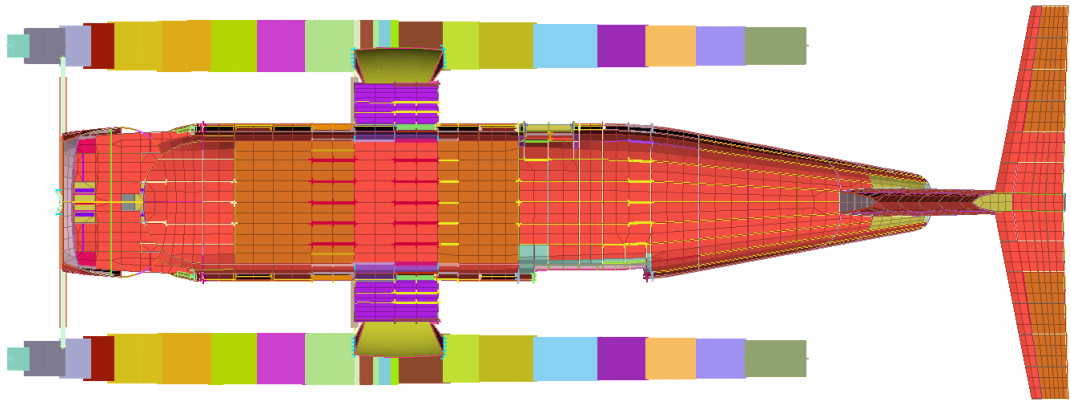


Fig. 16.6: FEM model of the floats - top view

16.3.2 FEM model of the struts

The struts, described in Figure 16.7, are based on CROD elements. This 1D element is able to transfer only tension, pressure and torsional loads. Because this model does not assume any bending loads at these elements, rod elements are sufficient enough. Input data are listed in Appendix G.

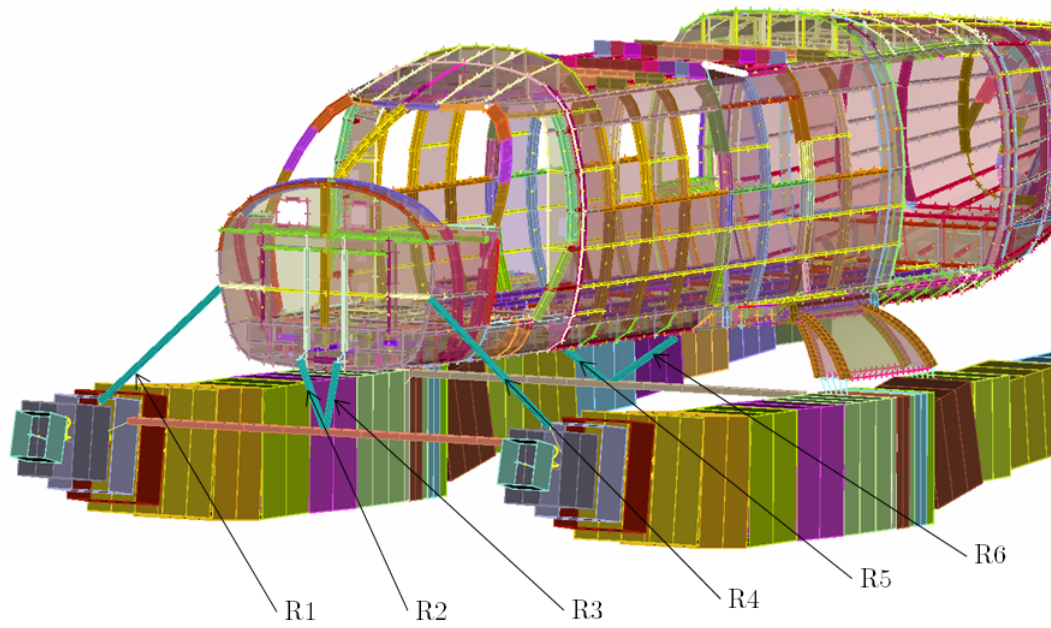


Fig. 16.7: FEM model of the rods

16.3.3 FEM model of the horizontal beams

Horizontal beams have a light green colour in Figure 16.8 and are labelled HB1 and HB2. The purpose of these beams is to keep constant track of the floats. The horizontal beams are bended due to water loads and rod supports in the middle. Input data are listed in Appendix G.

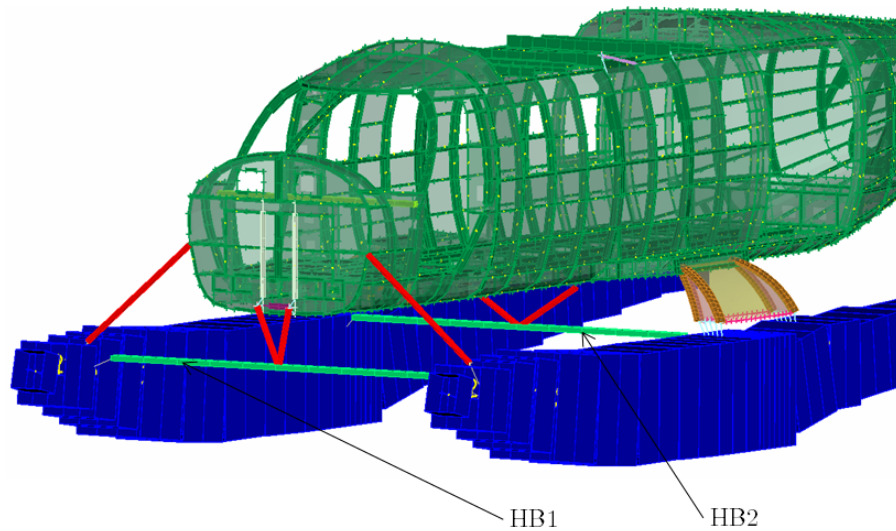


Fig. 16.8: FEM model of the horizontal beams

16.3.4 RBE2 and RBE3 elements

There are used RBE2 and RBE3 elements in this FEM model. Their marking is visible in Figure 16.9. Table 16.5 shows and describes which degrees of freedom are transferred and which kind of rigid body element it is.

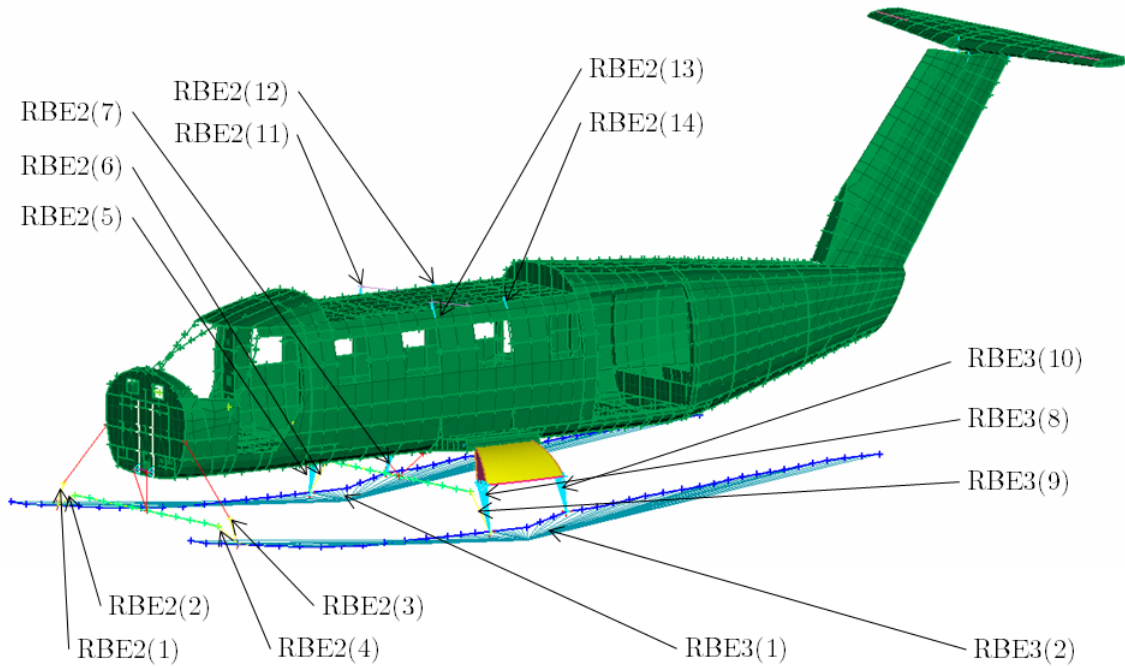


Fig. 16.9: FEM model of the RBE2 and RBE3 elements

16.3.5 Main leg beams and shear wall

Main loads are transferred to the fuselage via main leg beams, horizontal longitudinal axis and two landing gear spars. Longitudinal loads from hydrodynamic forces are transferred via floats to the shear wall and from this shear wall to the main leg beams and again via horizontal longitudinal axis to the landing gear spars.

Tab. 16.5: RBE2 and RBE3 elements

Name	Element	Transferred DOF
[-]	[-]	[-]
RBE2(1)	RBE2	1236
RBE2(2)	RBE2	123
RBE2(3)	RBE2	1236
RBE2(4)	RBE2	1236
RBE2(5)	RBE2	1234
RBE2(6)	RBE2	123
RBE2(7)	RBE2	1234
RBE2(8)	RBE2	1234
RBE2(9)	RBE2	1236
RBE2(10)	RBE2	1234
RBE2(11)	RBE2	123
RBE2(12)	RBE2	123
RBE2(13)	RBE2	123
RBE2(14)	RBE2	123
RBE3(1)	RBE3	123
RBE3(2)	RBE3	123

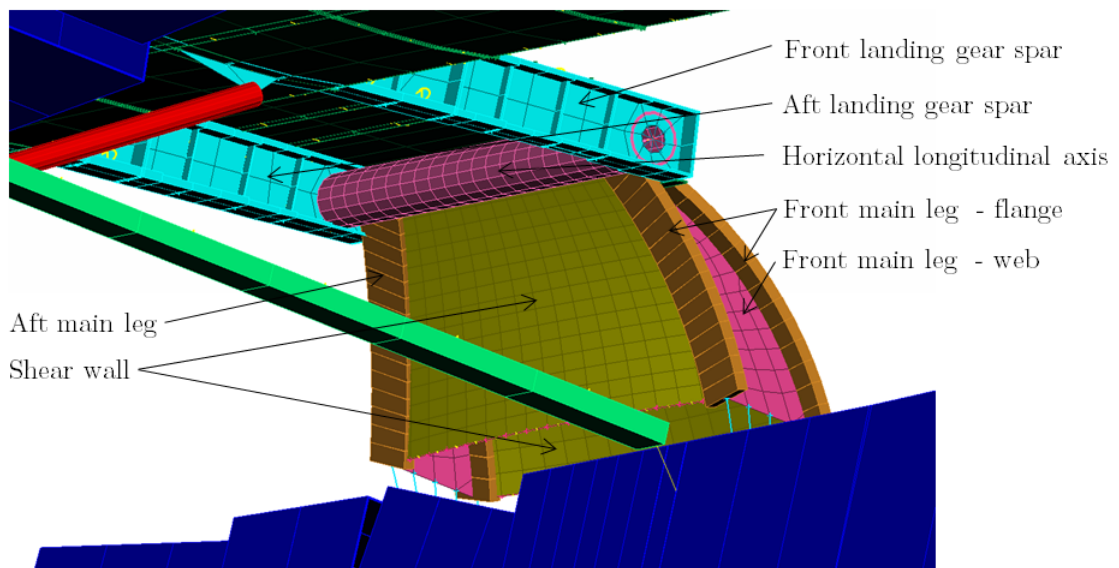
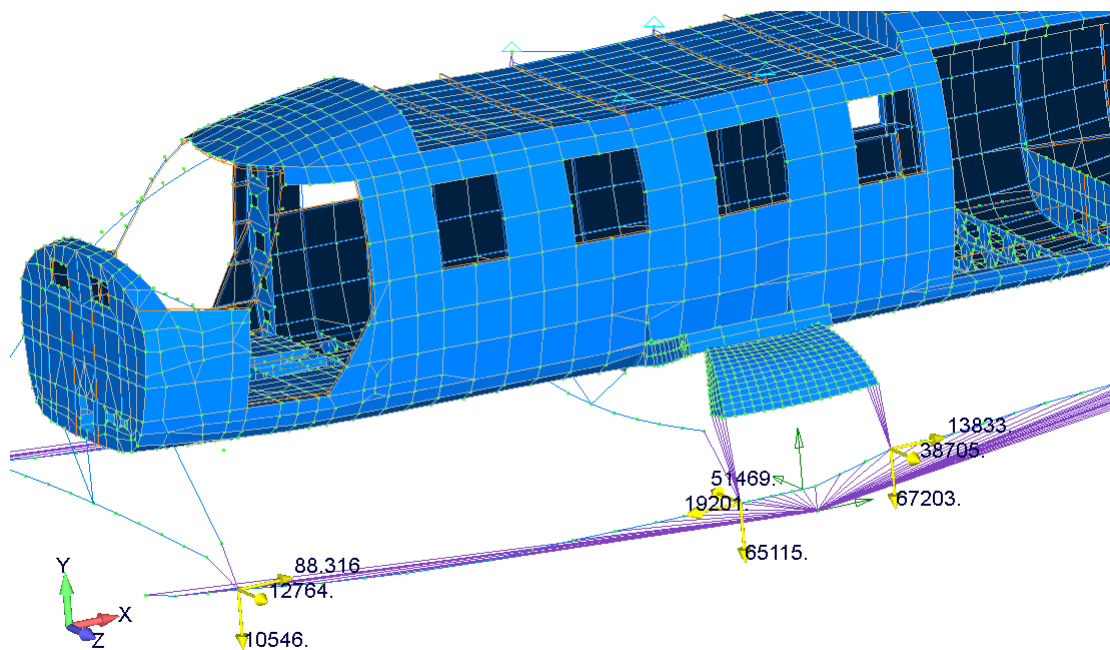


Fig. 16.10: FEM model of the main legs

16.4 Finite Element Method - results

16.4.1 Reaction forces - Connection Points CP1, CP2 and CP3

Reaction forces at connection points CP1, CP2 and CP3 have been determined from FEM model. The worst loading cases were chosen for every direction in appropriate coordination system. Also, they are spread into tension and compressive loads. These reaction forces will be used for next analysis, especially for main leg beams 1, 2, 3 and 4. There are stated reaction forces in Table 16.6 and Figures 16.11, 16.12 and 16.13. Forces and their components are stated in Aeroplane Coordination System.



Output Set: MSC/NASTRAN Case 3, Deformed(39.99): Total Translation, Freebody: Connection_Points_floats

Fig. 16.11: Action forces at connection point CP1, Load Case 3

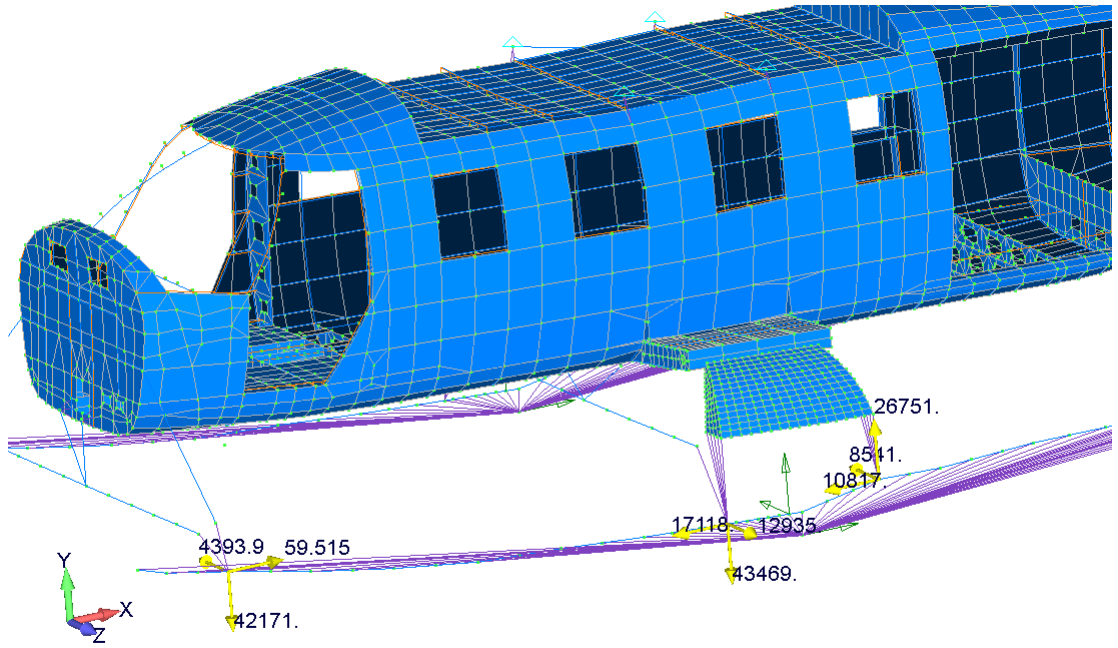


Fig. 16.12: Action forces at connection point CP2, Load Case 8

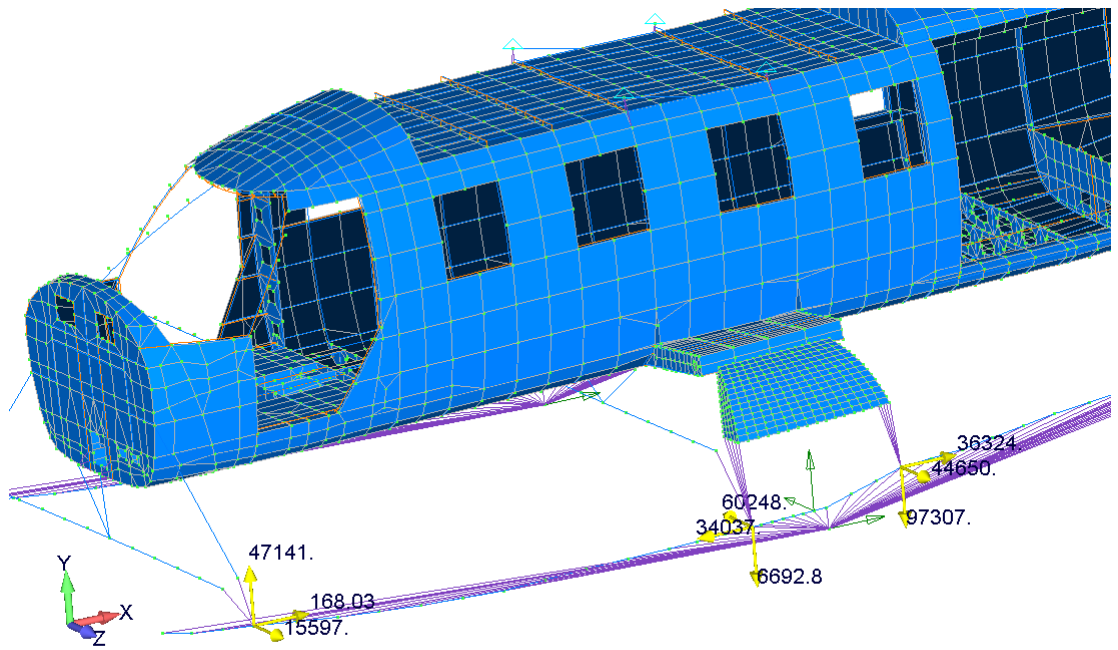


Fig. 16.13: Action forces at connection point CP3, Load Case 13

Tab. 16.6: Reaction forces at connection points CP1, CP2 and CP3

Connection point CP1			
Force component	F_x	F_y	F_z
Positive direction ¹	168 N	47 141 N	15597 N
	LC 13	LC 13	LC 13
Negative direction ²	-	42171 N	4394 N
	-	LC 8	LC 8
Connection point CP2			
Force component	F_x	F_y	F_z
Positive direction	34037 N	-	60248 N
	LC 13	-	LC 13
Negative direction	-	65115 N	12935 N
	-	LC 3	LC 8
Connection point CP3			
Force component	F_x	F_y	F_z
Positive direction	36324 N	26751 N	44650 N
	LC 13	LC 8	LC 13
Negative direction	10817 N	97307 N	8511 N
	LC 8	LC 13	LC 8

16.4.2 Front Frame

Front frame consists of horizontal beam 1 (HB1) and rods (R1), (R2), (R3), and (R4) as is shown in Figure 16.14. Each element has two lugs labelled as L_{R1} , L_{HB1} etc., also shown in Figure 16.14.

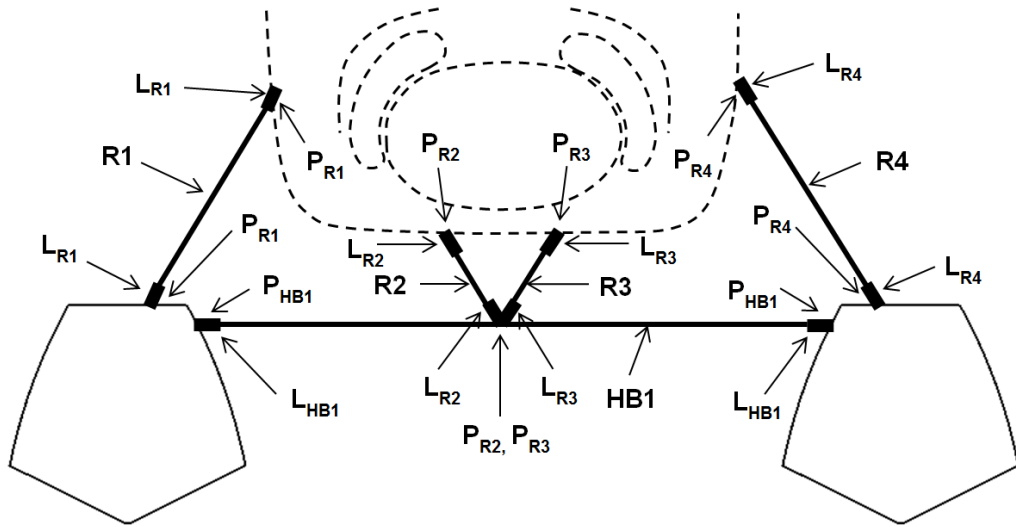


Fig. 16.14: Element description of Front frame

Geometrical and material properties

Cross-sections of the horizontal beam HB1 and Rods R1-R4 are shown in Figure 16.15. Geometrical properties are stated in Table 16.7 and material properties in Table 16.8 [23].

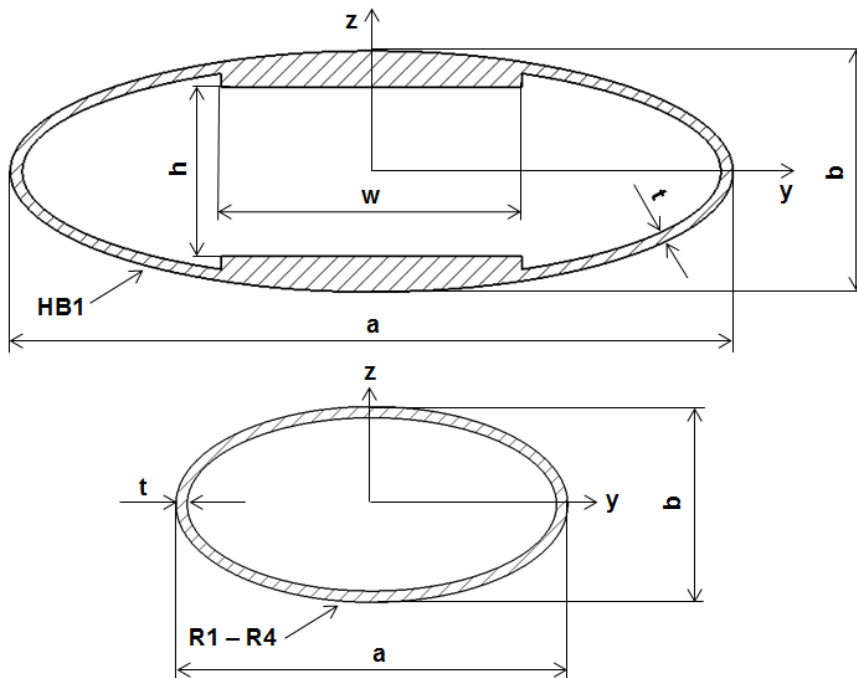


Fig. 16.15: Geometrical description of HB1, R1, R2, R3 and R4

Tab. 16.7: Geometrical properties of HB1, R1, R2, R3 and R4

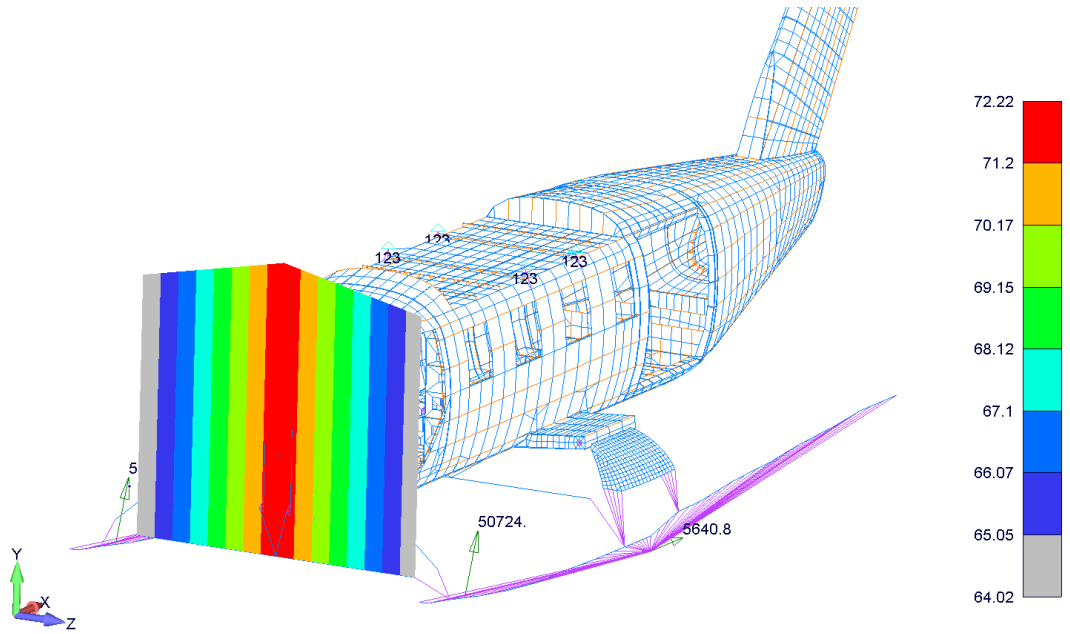
	Horizontal beam HB1	Rods 1 and 4	Rods 2 and 3	
Label	value	value	value	unit
<i>a</i>	180	100	30	<i>mm</i>
<i>b</i>	60	50	15	<i>mm</i>
<i>w</i>	80	-	-	<i>mm</i>
<i>h</i>	60	-	-	<i>mm</i>
<i>L</i>	2790	1132	465.5	<i>mm</i>
<i>t</i>	2.0	2	1.5	<i>mm</i>
<i>A</i>	1868	892.2	183.8	<i>mm</i> ²
<i>J_y</i>	1924965	154907	2680	<i>mm</i> ⁴
<i>J_z</i>	3038137	456618	8286	<i>mm</i> ⁴
<i>J</i>	2807613	449493	7855	<i>mm</i> ⁴

Tab. 16.8: Material properties of HB1, R1, R2, R3 and R4 [23]

	Horizontal beam HB1	Rods 1 and 4	Rods 2 and 3	
Label	value	value	value	unit
Material	2024 T3	2024 T3	2024 T3	-
<i>E</i>	72400	72400	72400	<i>MPa</i>
<i>G</i>	27846	27846	27846	<i>MPa</i>
<i>ρ</i>	2850	2850	2850	<i>kg · m</i> ⁻³
<i>R_m</i>	427	427	427	<i>MPa</i>
<i>R_{p0.2}</i>	310	310	310	<i>MPa</i>

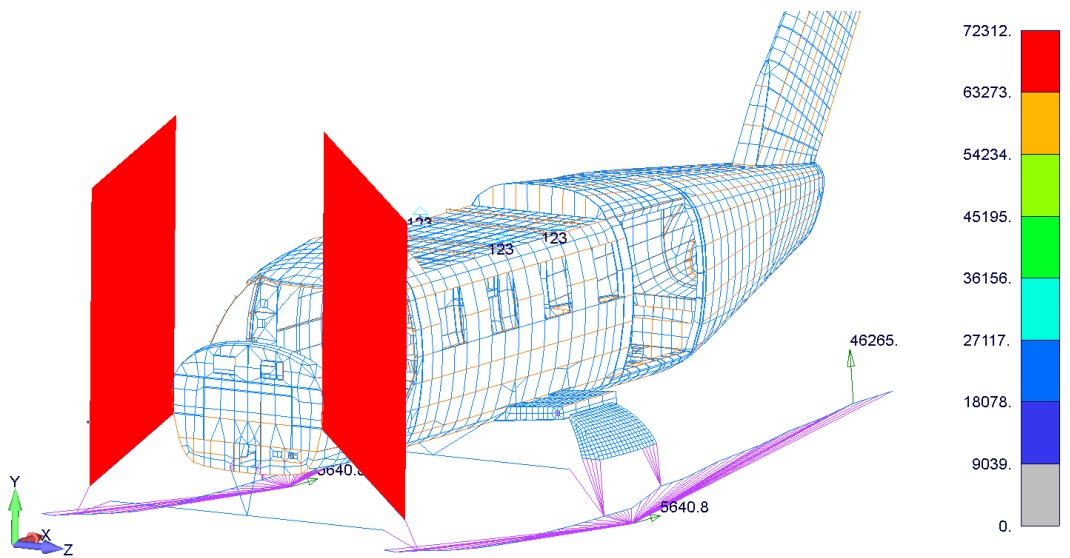
FEM results

Maximal combined stress at horizontal beam 1 is for load case 8 as is shown in Figure 16.16. Maximal tensile force at ROD 1 and 4 is for load case 13 and maximal compressive force for load case 8. See Figures 16.17 and 16.18. Same for ROD 2 and 3 is shown in Figure 16.19



Output Set: MSC/NASTRAN Case 8, Deformed(110.9): Total Translation, Contour: Beam EndA Max Comb Stress

Fig. 16.16: FEM result - horizontal beam 1 - Max Comb stress



Output Set: MSC/NASTRAN Case 13, Deformed(284.3): Total Translation, Contour: Rod Axial Force

Fig. 16.17: FEM result - ROD 1 and 4 - Rod axial tensile force

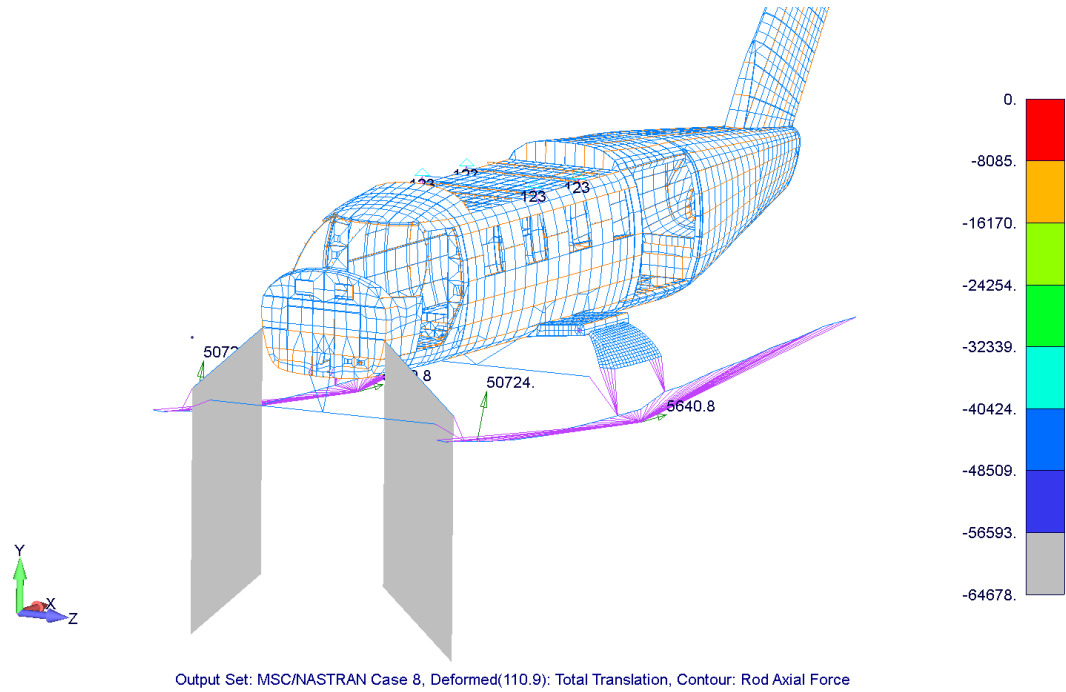


Fig. 16.18: FEM result - ROD 1 and 4 - Rod axial compressive force

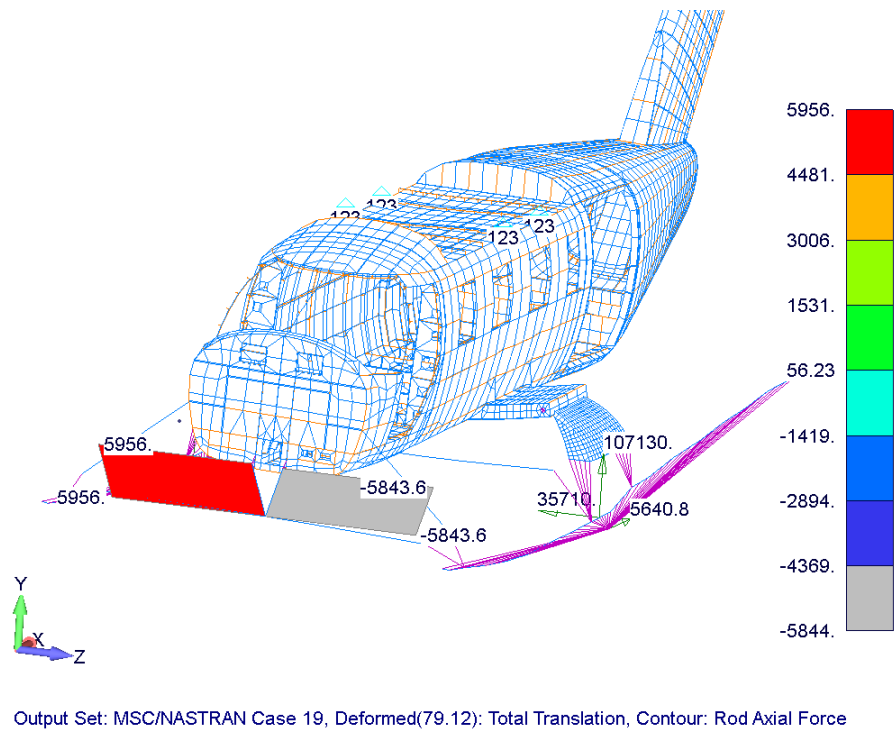


Fig. 16.19: FEM result - ROD 2 and 3 - Rod tensile and compressive force

Check of the Horizontal beam 1

Reserve factor for horizontal beam 1 for ultimate load and limit load is given by ratio between yield strength or ultimate tensile strength and maximal combined stress determined from FEM model - 16.16:

$$R.F.HB1,UL = \frac{R_m}{\sigma_{max}} = \frac{427}{72.22} = \mathbf{5.91} \quad (16.1a)$$

$$R.F.HB1,UL > 1 \rightarrow \text{COMPLY} \quad (16.1b)$$

$$R.F.HB1,LL = \frac{R_{p0.2}}{\sigma_{max}} = \frac{310}{72.22} = \mathbf{4.29} \quad (16.2a)$$

$$R.F.HB1,LL > 1 \rightarrow \text{COMPLY} \quad (16.2b)$$

Check of the Rod 1 and 4

Tensile stress is computed as follows:

$$\sigma_{tmax} = \frac{F_{xmax}}{A} = \frac{72312}{892.2} = 81.1 \text{ MPa} \quad (16.3)$$

where A is cross-section area in accordance with Table 16.7 and F_{xmax} is axial tensile force in accordance with Figure 16.17. Reserve factors for ultimate and limit loads are:

$$R.F.ROD1,4,UL,tensile = \frac{R_m}{\sigma_{tmax}} = \frac{427}{81.1} = \mathbf{5.26} \quad (16.4a)$$

$$R.F.ROD1,4,UL,tensile > 1 \rightarrow \text{COMPLY} \quad (16.4b)$$

$$R.F.ROD1,4,LL,tensile = \frac{R_{p0.2}}{\sigma_{tmax}} = \frac{310}{81.1} = \mathbf{5.73} \quad (16.5a)$$

$$R.F.ROD1,4,LL,tensile > 1 \rightarrow \text{COMPLY} \quad (16.5b)$$

Check of the Rod 2 and 3

Same formulas as previous are used:

$$\sigma_{tmax} = \frac{F_{xmax}}{A} = \frac{5956}{183.8} = 32.4 \text{ MPa} \quad (16.6)$$

where A is cross-section area in accordance with Table 16.7 and F_{xmax} is axial tensile force in accordance with Figure 16.19. Reserve factors for ultimate and limit loads

are:

$$R.F._{ROD2,3,UL,tensile} = \frac{R_m}{\sigma_{tmax}} = \frac{427}{32.4} = \mathbf{13.17} \quad (16.7a)$$

$$R.F._{ROD2,3,UL,tensile} > 1 \rightarrow \text{COMPLY} \quad (16.7b)$$

$$R.F._{ROD2,3,LL,tensile} = \frac{R_{p0.2}}{\frac{\sigma_{tmax}}{1.5}} = \frac{310}{\frac{32.4}{1.5}} = \mathbf{14.35} \quad (16.8a)$$

$$R.F._{ROD2,3,LL,tensile} > 1 \rightarrow \text{COMPLY} \quad (16.8b)$$

Check of the Lugs L_{R1} , L_{R2} , L_{R3} , L_{R4} and L_{HB1}

Lugs are checked in accordance with literature [17]. Because lugs are parts of the joints, paragraph *CS 23.572* is fulfilled. The ultimate load is multiplied by a factor of 1.15. Geometry of the lugs is shown in Figure 16.20 and in Table 16.9. Material properties are stated in Table 16.10

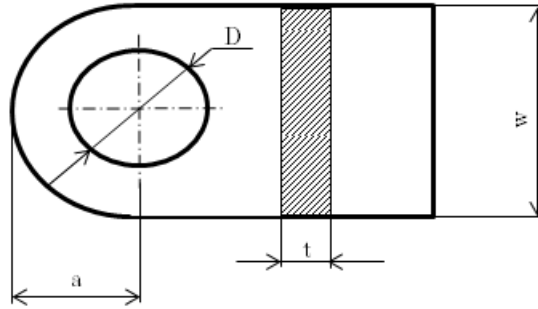


Fig. 16.20: Geometrical properties - lugs for Rods 1, 2, 3, 4 and HB1

Tab. 16.9: Geometrical properties of the lugs

Geometrical properties of the lugs L_{R1} - L_{R4} and L_{HB1}						
Label	unit	L_{R1}	L_{R2}	L_{R3}	L_{R4}	L_{HB1}
D	[mm]	13	6	6	13	13
w	[mm]	40	22	22	40	40
a	[mm]	20	11	11	20	20
t	[mm]	8	5	5	8	8

Tab. 16.10: Material properties of the lugs [23]

Alloy steel AISI 4130		
E	200000	MPa
G	76923	MPa
ρ	7800	$kg \cdot m^{-3}$
$R_{m,L}$	960	MPa
$R_{m,LT}$	960	MPa
$R_{m,ST}$	960	MPa
$R_{p0.2,L}$	830	MPa
$R_{p0.2,LT}$	830	MPa
$R_{p0.2,ST}$	830	MPa

Tensile force is dominant, as regards lug analysis. Failure in tension, failure by shear tear out and failure by bearing of bushing on plate are considered in accordance with literature [17] and [3]. Excel program developed in Evektor using previously mentioned sources was used. Summary of tensile and compressive loads are stated in Table 16.11.

Tab. 16.11: Summary of tensile and compressive force action on front frame

	tensile force	compressive force
Label	[N]	[N]
R1	72312	-64678
R2	5956	-5844
R3	5956	-5844
R4	72312	-64678
HB1	53381	-70289

For those where the compressive force is higher than tensile force, failure by bearing of bushing on plate will be caused just by this compressive force. This is considered during computation and reserve of factor is determined for compressive loads instead of tensile.

Reserve factors are stated in following Table 16.12:

Tab. 16.12: Reserve factors of lugs from front frame

RF			
Label	Allowable load	Deformation	Allowable bearing load
	[-]	[-]	[-]
L_{R1}	1.78	1.44	1.20
L_{R2}	6.81	5.37	4.19
L_{R3}	6.81	5.37	4.19
L_{R4}	1.78	1.44	1.20
L_{HB1}	2.42	1.95	1.48

Check of the pins P_{R1} - P_{R4} and P_{HB1}

There is used method from [2]. This method assumes acting forces on the pin in accordance with Figure 16.21.

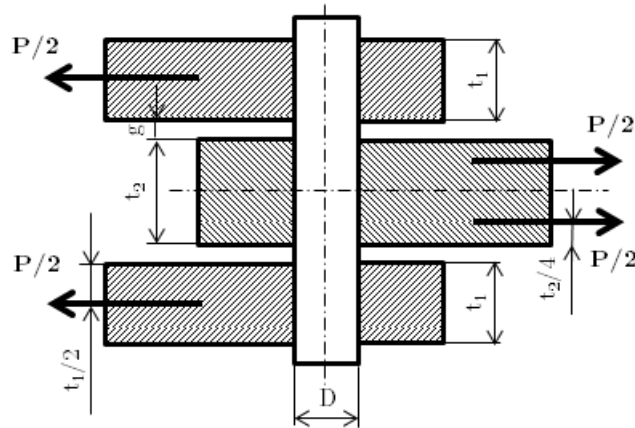


Fig. 16.21: Force position on the pin

The force P from Figure 16.21 corresponds to maximal force F_{max} from Equation 16.3 and 16.6. Geometrical properties of the joints are stated in Table 16.13.

Tab. 16.13: Geometrical and material properties of the joints - front frame

		P_{R1}	P_{R2}	P_{R3}	P_{R4}	P_{HB1}
t_1	mm	10	5	5	10	10
t_2	mm	8	5	5	8	8
g	m	0.5	0.5	0.5	0.5	0.5
D	mm	13	6	6	13	13
A	mm^2	132.7	28.3	28.3	132.7	132.7
$J_y = J_z$	mm^4	1402.0	63.6	63.6	1402.0	1402.0
Material		PH13-8Mo H1150				
E	MPa	197000	197000	197000	197000	197000
G	MPa	75769	75769	75769	75769	75769
R_m	MPa	930	930	930	930	930
$R_{p0.2}$	MPa	620	620	620	620	620

The Shear diagram and bending moment diagram look as follows:

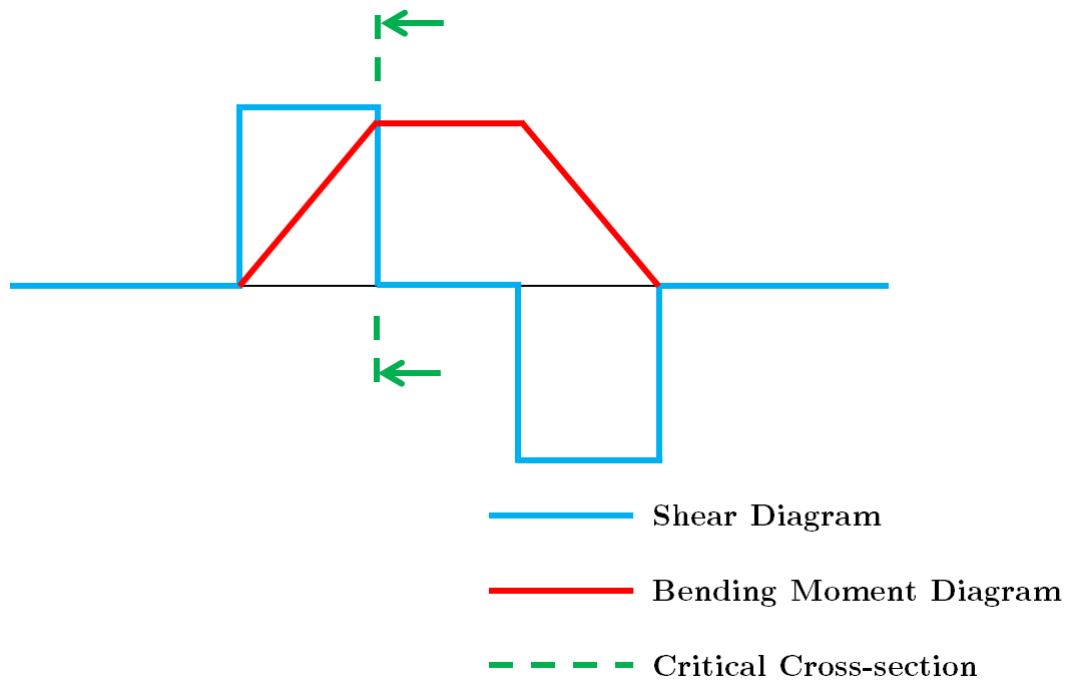


Fig. 16.22: Shear and Bending Moment Diagram of the pin

Then, shear stress is

$$\tau = \frac{T}{A} \quad (16.9)$$

where τ is a shear stress, T is shear force at critical cross-section and A is the area of critical cross-section of the pin.

Bending stress is expressed as

$$\sigma_B = \frac{M_B \cdot \frac{D}{2}}{J_y \cdot K} \quad (16.10)$$

where σ_B is a bending stress, M_B is bending moment at critical cross-section, J_y is moment of inertia and K is section factor of 1.7 for circular cross-section in accordance with literature [2].

Mises equivalent tensile stress is:

$$\bar{\sigma} = \sqrt{\sigma_B^2 + 3 \cdot \tau^2} \quad (16.11)$$

Reserve factor is:

$$R.F.PIN,UL = \frac{R_m}{\bar{\sigma}} \quad (16.12a)$$

$$R.F.PIN,LL = \frac{R_{p0.2}}{\frac{\bar{\sigma}}{1.5}} \quad (16.12b)$$

Reserve factors RF for each pin of front frame are stated in following Table 16.14.

Tab. 16.14: Reserve factors of the pins - front frame

Label	$P/2$	A	τ	σ_B	$\bar{\sigma}$	$R.F.PIN,UL$	$R.F.PIN,LL$
	[N]	[mm ²]	[MPa]	[MPa]	[MPa]	[-]	[-]
P_{R1}	36156	132.7	272.5	741.3	878.8	1.06	1.06
P_{R2}	2978	28.3	105.3	351.9	396.4	2.35	2.35
P_{R3}	2978	28.3	105.3	351.9	396.4	2.35	2.35
P_{R4}	36156	132.7	272.5	741.3	878.8	1.06	1.06
P_{HB1}	35145	132.7	264.8	720.6	854.2	1.09	1.09

Buckling of loaded elements - front frame

Critical compressive force is determined in accordance with LETOV 93 procedure. Geometrical data are described in Figure 16.23 and for front frame are stated in Table 16.15. Critical force F_{crit} is expressed as:

$$F_{crit} = \varphi \cdot \frac{\pi^2 \cdot E \cdot J}{L^2} \quad (16.13)$$

where E is the Young's modulus of the middle part of the rod, J is the minimum moment of inertia of cross-section, L is the length of the rod and φ is the bending stiffness coefficient. This coefficient is function of ratio l_1/L and also ratio:

$$\frac{E \cdot \min(J_y, J_z)}{E_1 \cdot J_1} \quad (16.14)$$

where J_y and J_z are moments of inertia of cross-section to its coordination system.



Fig. 16.23: Geometry for buckling

Tab. 16.15: Buckling of the elements - front frame

Label	Unit	R1 and R4	R2 and R3	HB1
L	[mm]	1132	465.5	2790
l_1	[mm]	50	50	50
$\frac{l_1}{L}$	[-]	0.04	0.11	0.02
a	[mm]	100	30	180
b	[mm]	50	15	60
t	[mm]	2.0	1.5	2.0
t_{lug}	[mm]	8	5	8
w	[mm]	40	22	40
J_y	[mm ⁴]	154907	2680	1924965
J_z	[mm ⁴]	456618	8286	3038137
J_1	[mm ⁴]	1707	229	1707
E	[MPa]	72400	72400	72400
E_1	[MPa]	200000	200000	200000
$\frac{E \cdot \min(J_y, J_z)}{E_1 \cdot J_1}$	[-]	32.9	4.2	408.3
φ	[-]	1.00	0.95	1.00
F_{crit}	[N]	86380.8	8395.3	176706.6
$F_{x,max}$	[N]	72312	5956	70289
$R.F._{ROD1-4,HB1,UL,buckling}$	[-]	1.19	1.41	2.51

16.4.3 Aft Frame

There are used completely same methods as for front frame. Therefore, there will not be used so many comments as it has been in previous section.

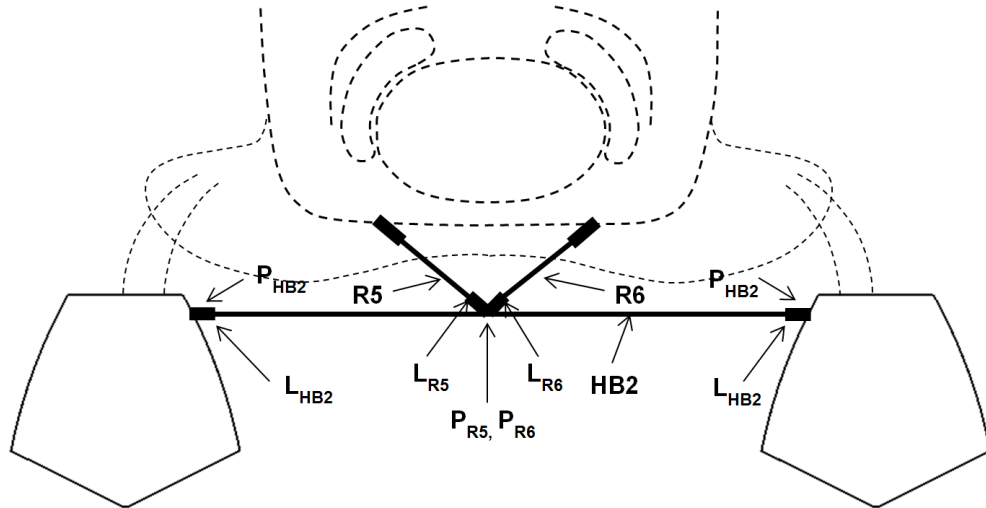


Fig. 16.24: Element description of Front frame

Geometrical and material properties

Cross-sections of the horizontal beam HB2 and Rods R5 and R6 are shown in Figure 16.25. Geometrical properties are stated in Table 16.16 and material properties in Table 16.17 [23].

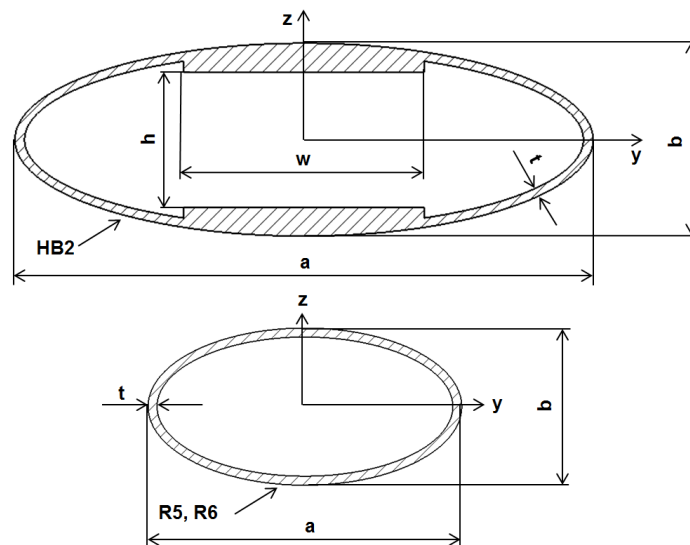


Fig. 16.25: Geometrical description of HB2, R5 and R6

Tab. 16.16: Geometrical properties of HB2, R5 and R6

	Horizontal beam HB2	Rods 5 and 6	
Label	value	value	unit
a	180	60	mm
b	60	30	mm
w	80	-	mm
h	60	-	mm
L	2790	563	mm
t	2.0	1.5	mm
A	1868	395.8	mm^2
J_y	1924965	154907	mm^4
J_z	3038137	456618	mm^4
J	2807613	449493	mm^4

Tab. 16.17: Material properties of HB2, R5 and R6 [23]

	Horizontal beam HB2	Rods 5 and 6	
Label	value	value	unit
Material	2024 T3	2024 T3	-
E	72400	72400	MPa
G	27846	27846	MPa
ρ	2850	2850	$kg \cdot m^{-3}$
R_m	427	427	MPa
$R_{p0.2}$	310	310	MPa

FEM results

Maximal combined stress at horizontal beam 2 is for load case 3 as is shown in Figure 16.26. Maximal tensile force at ROD 5 and 6 is for load case 19 and maximal compressive force also for load case 19. See Figure 16.27.

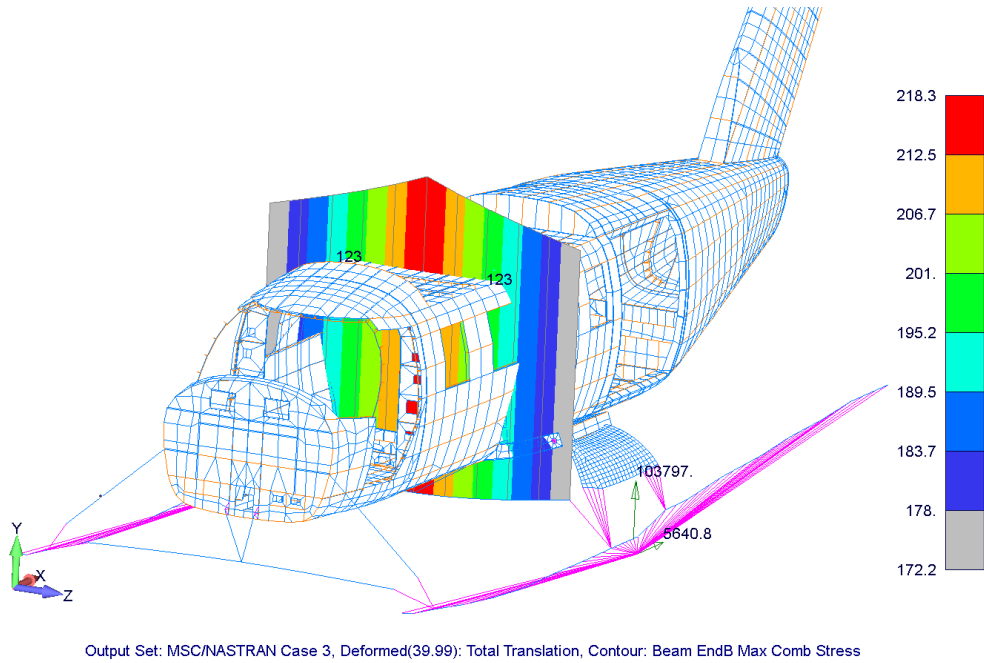


Fig. 16.26: FEM result - horizontal beam 2 - Max Comb stress

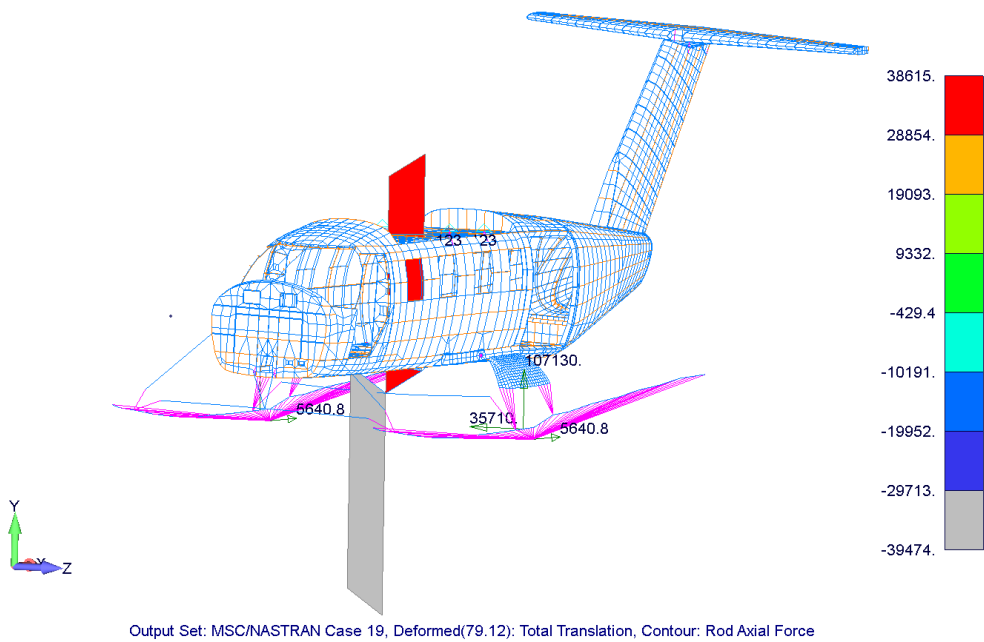


Fig. 16.27: FEM result - ROD 5 and 6 - Rod tensile and compressive force

Check of the Horizontal beam 2

Reserve factor for horizontal beam 2 for ultimate load and limit load is given by ratio between yield strength or ultimate tensile strength and maximal combined stress determined from FEM model - 16.26:

$$R.F.HB2,UL = \frac{R_m}{\sigma_{max}} = \frac{427}{218.3} = \mathbf{1.95} \quad (16.15a)$$

$$R.F.HB2,UL > 1 \rightarrow \mathit{COMPLY} \quad (16.15b)$$

$$R.F.HB2,LL = \frac{R_{p0.2}}{\frac{\sigma_{max}}{1.5}} = \frac{310}{\frac{218.3}{1.5}} = \mathbf{2.13} \quad (16.16a)$$

$$R.F.HB2,LL > 1 \rightarrow \mathit{COMPLY} \quad (16.16b)$$

Check of the Rod 5 and 6

Tensile stress is computed as follows:

$$\sigma_{tmax} = \frac{F_{xmax}}{A} = \frac{38615}{395.8} = 97.6 \text{ MPa} \quad (16.17)$$

where A is cross-section area in accordance with Table 16.16 and F_{xmax} is axial tensile force in accordance with Figure 16.19. Reserve factors for ultimate and limit loads are:

$$R.F.ROD5,6,UL,tensile = \frac{R_m}{\sigma_{tmax}} = \frac{427}{97.6} = \mathbf{4.37} \quad (16.18a)$$

$$R.F.ROD5,6,UL,tensile > 1 \rightarrow \mathit{COMPLY} \quad (16.18b)$$

$$R.F.ROD5,6,LL,tensile = \frac{R_{p0.2}}{\frac{\sigma_{tmax}}{1.5}} = \frac{310}{\frac{97.6}{1.5}} = \mathbf{4.76} \quad (16.19a)$$

$$R.F.ROD5,6,LL,tensile > 1 \rightarrow \mathit{COMPLY} \quad (16.19b)$$

Check of the Lugs L_{R5} , L_{R6} and L_{HB2}

Lugs are checked in accordance with literature [17]. Because lugs are parts of the joints, paragraph *CS 23.572* is fulfilled. The ultimate load is multiplied by a factor of 1.15. Geometry of the lugs is shown in Figure 16.20 and in Table 16.18. Material properties are stated in Table 16.19

Tab. 16.18: Geometrical properties of the lugs L_{R5} , L_{R6} and L_{HB2}

Label	unit	L_{R5}	L_{R6}	L_{HB2}
D	[mm]	10	10	18
w	[mm]	20	20	60
a	[mm]	10	10	30
t	[mm]	8	8	12

Tab. 16.19: Material properties of the lugs [23]

Alloy steel AISI 4130		
E	200000	MPa
G	76923	MPa
ρ	7800	$kg \cdot m^{-3}$
$R_{m,L}$	960	MPa
$R_{m,LT}$	960	MPa
$R_{m,ST}$	960	MPa
$R_{p0.2,L}$	830	MPa
$R_{p0.2,LT}$	830	MPa
$R_{p0.2,ST}$	830	MPa

Tensile force is dominant, as regards lug analysis. Failure in tension, failure by shear tear out and failure by bearing of bushing on plate are considered in accordance with literature [17] and [3]. Excel program developed in Evektor using previously mentioned sources was used. Summary of tensile and compressive loads are stated in Table 16.20.

Tab. 16.20: Summary of tensile and compressive force action on front frame

	tensile force	compressive force
Label	[N]	[N]
R5	38615	-39474
R6	38615	-39474
HB2	143300	-

For those where the compressive force is higher than tensile force, failure by bearing of bushing on plate will be caused just by this compressive force. This is considered during computation and reserve of factor is determined for compressive loads instead of tensile.

Reserve factors are stated in following Table 16.21:

Tab. 16.21: Reserve factors of lugs from aft frame

RF			
Label	Allowable load	Deformation	Allowable bearing load
	[-]	[-]	[-]
L_{R5}	1.65	1.37	1.69
L_{R6}	1.65	1.37	1.69
L_{HB2}	1.95	1.55	1.25

Check of the pins P_{R5} , P_{R6} and P_{HB2}

There is used method from [2]. This method assumes acting forces on the pin in accordance with Figure 16.21. The force P from Figure 16.21 corresponds to maximal force F_{max} from Equation 16.17. Geometrical properties of the joints are stated in Table 16.22.

Tab. 16.22: Geometrical and material properties of the joints - aft frame

Label	Unit	P_{R5}	P_{R6}	P_{HB2}
t_1	<i>mm</i>	8	8	12
t_2	<i>mm</i>	8	8	12
g	<i>m</i>	0.5	0.5	0.5
D	<i>mm</i>	10	10	18
A	<i>mm²</i>	78.5	78.5	254.4
$J_y = J_z$	<i>mm⁴</i>	490.8	490.8	5153
Material		PH13-8Mo H1150		
E	<i>MPa</i>	197000	197000	197000
G	<i>MPa</i>	75769	75769	75769
R_m	<i>MPa</i>	930	930	930
$R_{p0.2}$	<i>MPa</i>	620	620	620

The Shear diagram and bending moment diagram look as follows:

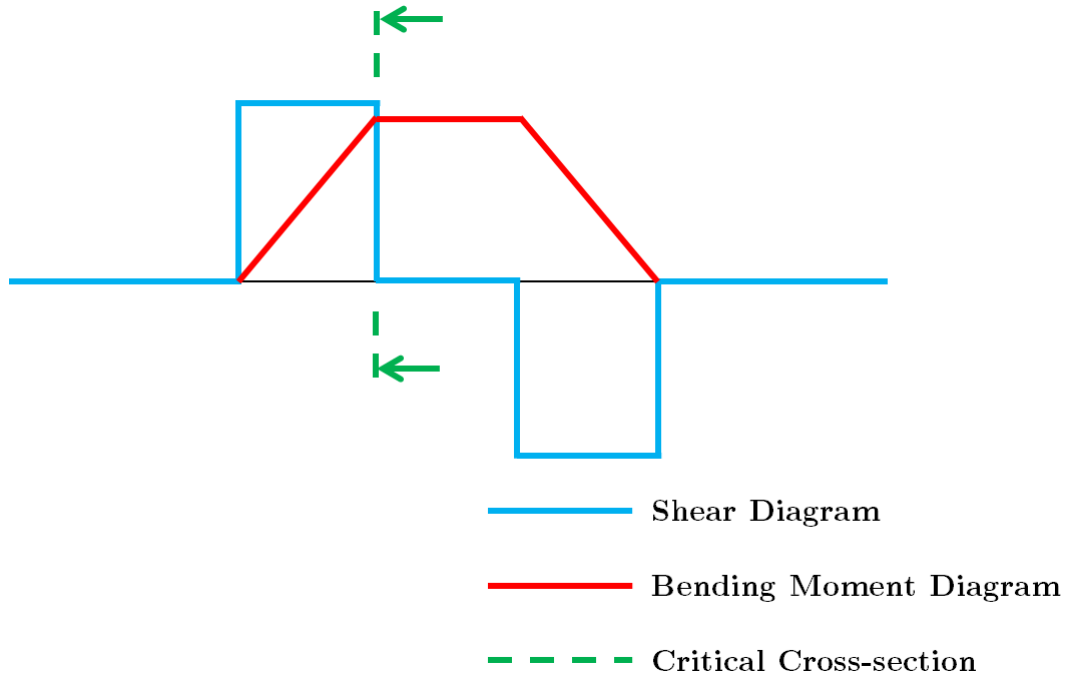


Fig. 16.28: Shear and Bending Moment Diagram of the pin

Then, shear stress is

$$\tau = \frac{T}{A} \quad (16.20)$$

where τ is a shear stress, T is shear force at critical cross-section and A is the area of critical cross-section of the pin.

Bending stress is expressed as

$$\sigma_B = \frac{M_B \cdot \frac{D}{2}}{J_y \cdot K} \quad (16.21)$$

where σ_B is a bending stress, M_B is bending moment at critical cross-section, J_y is moment of inertia and K is section factor of 1.7 for circular cross-section in accordance with literature [2].

Mises equivalent tensile stress is:

$$\bar{\sigma} = \sqrt{\sigma_B^2 + 3 \cdot \tau^2} \quad (16.22)$$

Reserve factor is:

$$R.F.PIN,UL = \frac{R_m}{\bar{\sigma}} \quad (16.23a)$$

$$R.F.PIN,LL = \frac{R_{p0.2}}{\frac{\bar{\sigma}}{1.5}} \quad (16.23b)$$

Reserve factors RF for each pin of front frame are stated in following Table 16.23.

Tab. 16.23: Reserve factors of the pins - aft frame

Label	$P/2$	A	τ	σ_B	$\bar{\sigma}$	$R.F.PIN,UL$	$R.F.PIN,LL$
	[N]	[mm ²]	[MPa]	[MPa]	[MPa]	[–]	[–]
P_{R5}	19737	78.5	251.3	770.5	884.9	1.05	1.05
P_{R6}	19737	78.5	251.3	770.5	884.9	1.05	1.05
P_{HB2}	71650	254.4	281.6	701.0	853.9	1.08	1.08

Buckling of loaded elements - aft frame

Critical compressive force is determined in accordance with LETOV 93 procedure. Geometrical data are described in Figure 16.23 and for front frame are stated in Table 16.24. Critical force F_{crit} is expressed as:

$$F_{crit} = \varphi \cdot \frac{\pi^2 \cdot E \cdot J}{L^2} \quad (16.24)$$

where E is the Young's modulus of the middle part of the rod, J is the minimum moment of inertia of cross-section, L is the length of the rod and φ is the bending stiffness coefficient. This coefficient is function of ratio l_1/L and also ratio:

$$\frac{E \cdot \min(J_y, J_z)}{E_1 \cdot J_1} \quad (16.25)$$

where J_y and J_z are moments of inertia of cross-section to its coordination system.

Tab. 16.24: Buckling of the elements - aft frame

Label	unit	R5 and R6
L	$[mm]$	563
l_1	$[mm]$	50
$\frac{l_1}{L}$	$[-]$	0.09
a	$[mm]$	30
b	$[mm]$	30
t	$[mm]$	1.5
t_{lug}	$[mm]$	8
w	$[mm]$	40
J_y	$[mm^4]$	24449
J_z	$[mm^4]$	72639
J_1	$[mm^4]$	26820
E	$[MPa]$	72400
E_1	$[MPa]$	200000
$\frac{E \cdot \min(J_y, J_z)}{E_1 \cdot J_1}$	$[-]$	5.2
φ	$[-]$	0.96
F_{crit}	$[N]$	52912
$F_{x,max}$	$[N]$	39474
$R.F. \cdot ROD_{5,6,UL,buckling}$	$[-]$	1.34

16.5 Attachment points at the fuselage - front frame

There are compared loads affecting the lugs of front landing gear with data gained from literature [20] dealing with stress analysis of front landing gear attachment in this section. Also, outline of Rod 1 and Rod 4 attachments is done. Description of acting forces is shown in Figure 16.29. Green arrows show resultant force from Rod 2 and Rod 3 and orange arrows represent division of these forces into directions in according to Aeroplane Coordination System.

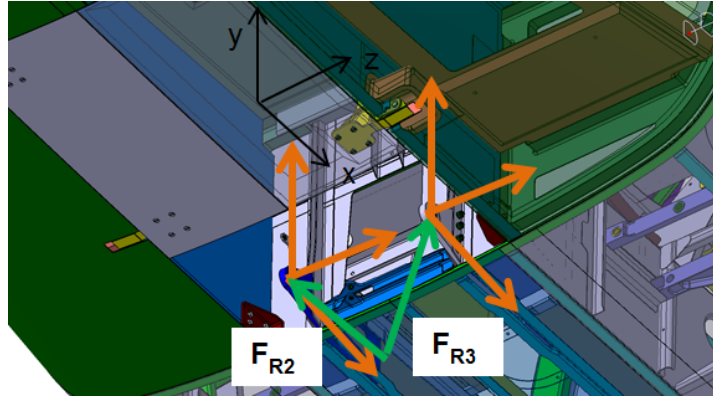


Fig. 16.29: Front Attachment Description

Front frame does not take any longitudinal loads. There are forces only in directions y and z . Forces F_{R2} and F_{R3} divided into the ACS have following components:

Tab. 16.25: Forces - front frame

Load Case 19				
Label	Total Force	x	y	z
[—]	[N]	[N]	[N]	[N]
F_{R2}	5956	0	5664	1840
F_{R3}	5956	0	5664	1840

The lowest R.F. in [20] is 9.33 for force vertical load about 25000N. The loading for our case is about 4 times lower. Therefore this component comply also for the floats. R.F. of two critical cross-sections of longitudinal front landing gear spars for bending moment is 1.27. This value is for $F_z = 10188$. Because the loading for our load case is about 5 times lower, this component comply also for lateral loads.

Loads from ROD 1 and ROD 4 can be also divided to vertical and lateral directions. Maximal forces are stated in following table:

Tab. 16.26: Forces - front frame

Load Case 19				
Label	Total Force	x	y	z
[—]	[N]	[N]	[N]	[N]
F_{R1}	72312	0	49316	52885
F_{R4}	72312	0	49316	52885

As was already mentioned, lateral loads for symmetrical landings does not have any influence on the airframe. This load will be transferred only via lateral stringer that needs to be add to the frame. There is maximal difference for unsymmetrical landing case 19. It is seen in Figure 16.30

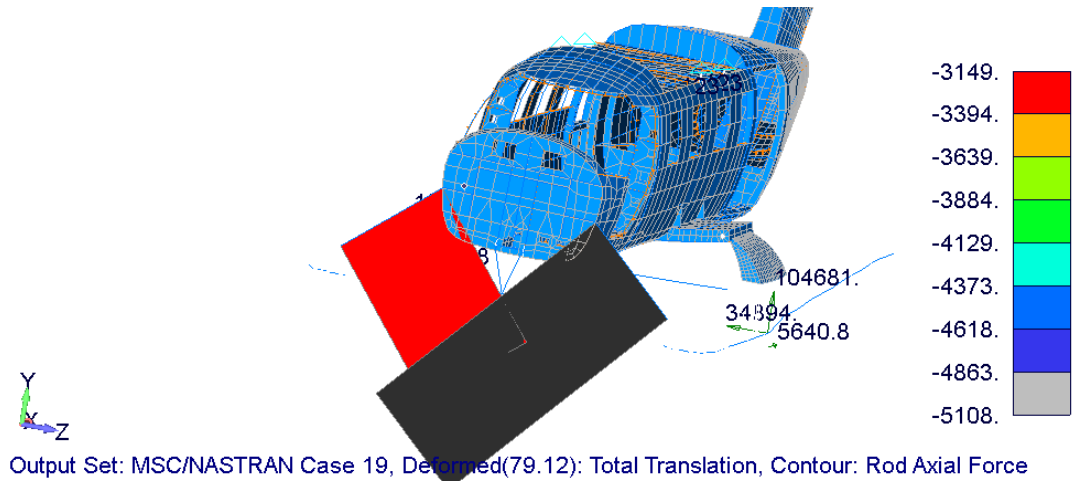


Fig. 16.30: Unsymmetrical landing case 19

The difference is 1336 N in z-direction. It means that this loads needs to be transferred to the bulkhead. This load is very low, there is not done any computation.

16.6 Attachment points at the fuselage - aft frame

16.6.1 Front landing gear spar

Affecting forces F_{R5} , F_{R6} , F_{ML1} and F_{ML3} in Figure 16.31 are taken from FEM model results. These results are stated in Table 16.27. These forces (green colour) are divided to directions corresponding to the Aeroplane Coordination System (orange colour) and also, they are stated in same table. The vertical load about 50000 N will be transferred to the bulkhead via rivets. In accordance with literature [3] single-shear rivet, diameter 5 mm, and thickness of the plate 1.5 mm has ultimate load 5000 N. It means there is necessary to have 10 rivets for every rod.

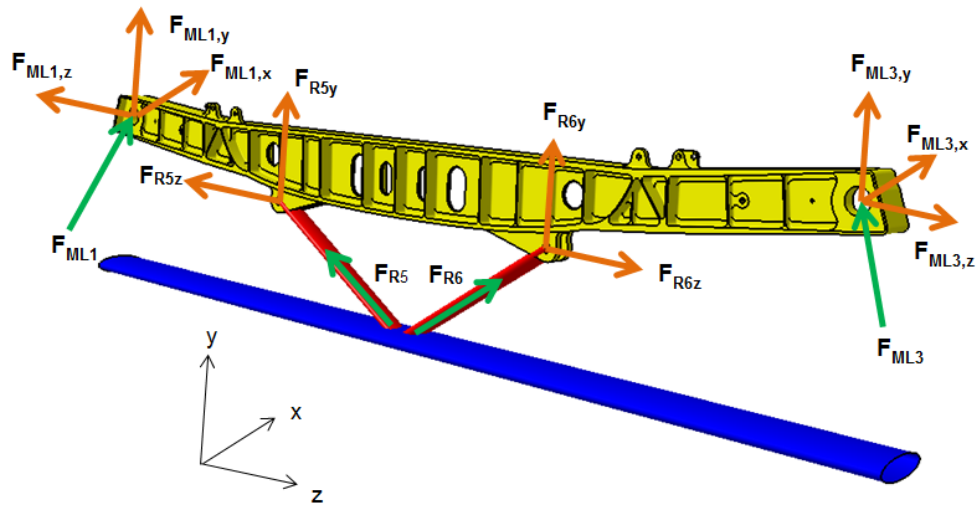


Fig. 16.31: Affecting forces - front spar

Tab. 16.27: Forces - front spar

Load Case 3				
Label	Total Force	x	y	z
[-]	[N]	[N]	[N]	[N]
F_{R5}	-597.3	0	510	-310
F_{R6}	-611.9	0	523	318
F_{ML1}	101108.3	1125.3	57848	-82917
F_{ML3}	101108.3	1125.3	57848	-82917

Load Case 8				
Label	Total Force	x	y	z
	[N]	[N]	[N]	[N]
F_{R5}	-288.3	0	246	-150
F_{R6}	-114.3	0	98	59
F_{ML1}	40839.7	14983	33721	-17501
F_{ML3}	40839.7	14983	33721	-17501

Load Case 18				
Label	Total Force	x	y	z
	[N]	[N]	[N]	[N]
F_{R5}	38547	0	32937	-20026
F_{R6}	-39436	0	-33696	-20488
F_{ML1}	52168.23	13.9	40799	-32511
F_{ML3}	52168.23	13.9	40799	-32511

3D model of landing gear spar is used to determine the constraint forces at lugs 1, 2, 3, 4, 5 and 6. Description of the lugs is shown in Figure 16.32. FEM results are shown in Figures 16.33, 16.34 and 16.35. Load cases with maximal forces F_{ML1} and F_{ML3} and load case for unsymmetrical landing were chosen for analysis.

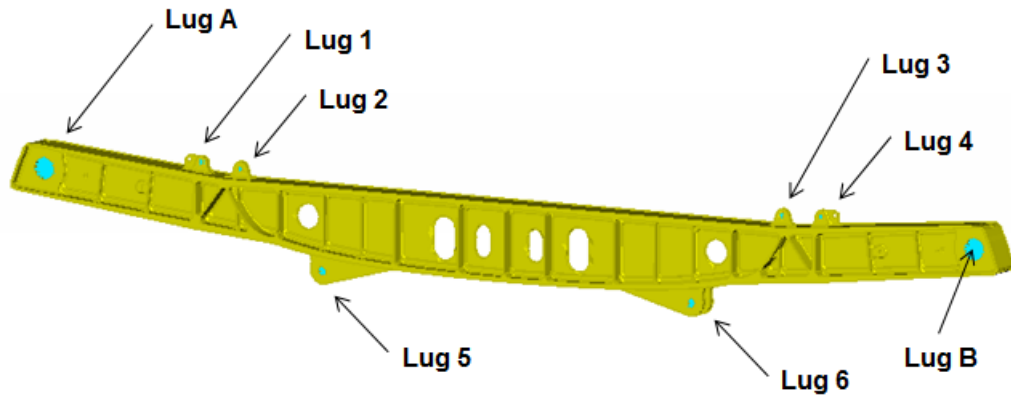


Fig. 16.32: Names of the lugs for front spar

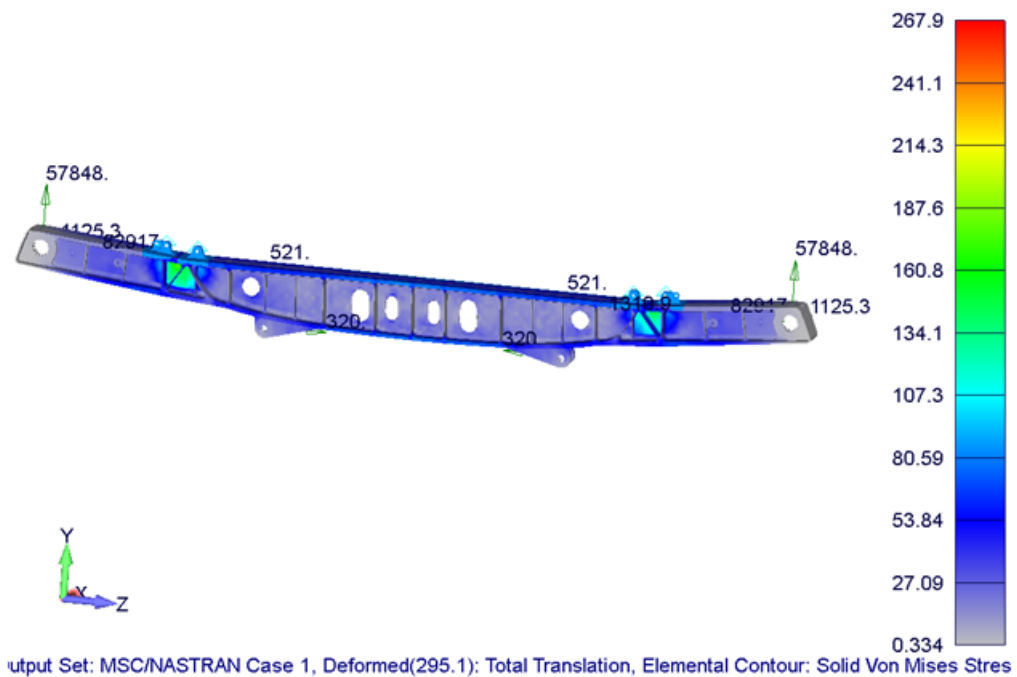


Fig. 16.33: FEM results - Load Case 3

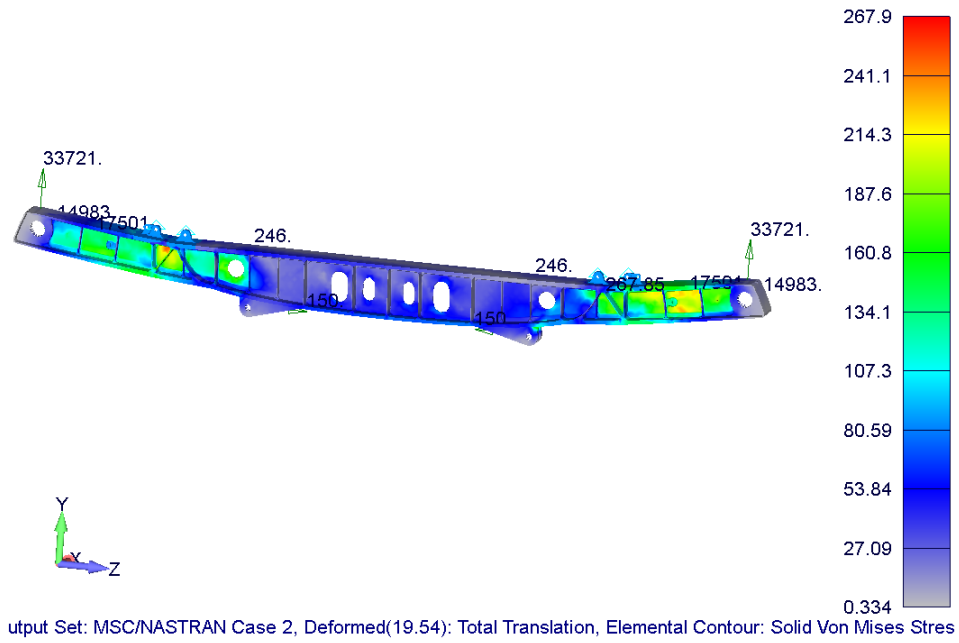


Fig. 16.34: FEM results - Load Case 8

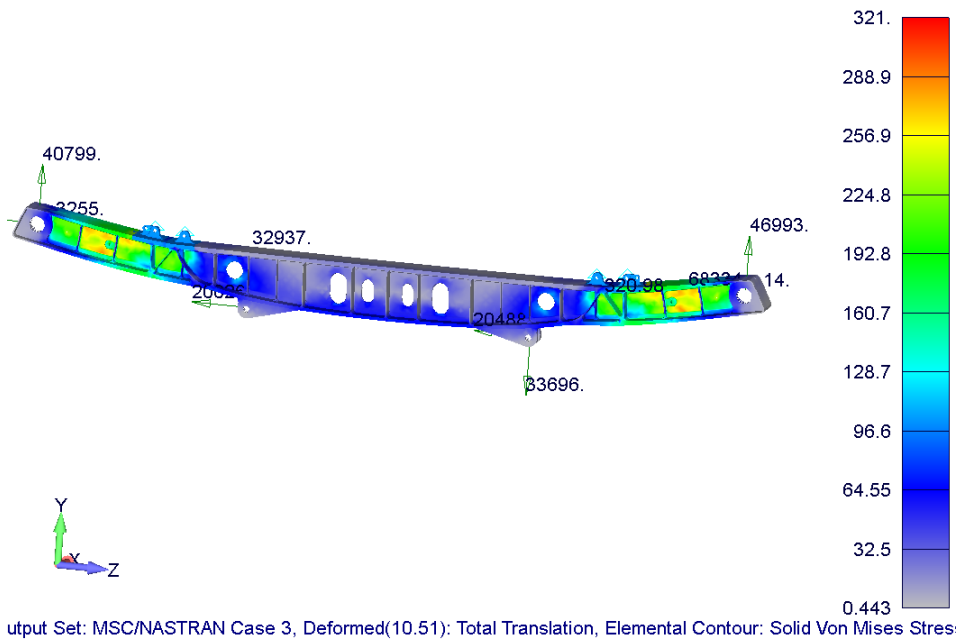


Fig. 16.35: FEM results - Load Case 18

Results from previous Figures are stated in Table 16.28:

Tab. 16.28: Constraint forces at the lugs

Load Case 3			
	F_x	F_y	F_z
	[N]	[N]	[N]
Lug 1	-181	-38796	-11244
Lug 2	-382	-10013	10297
Lug 3	-382	-10013	10297
Lug 4	-181	-38796	-11244
Lug 5	0	-310	510
Lug 6	0	-318	523
Lug A	1125	57848	82917
Lug B	1125	57848	-82917
Load Case 8			
	F_x	F_y	F_z
	[N]	[N]	[N]
Lug 1	-2146	-123526	11215
Lug 2	10254	62520	12015
Lug 3	10955	62520	-12015
Lug 4	-2146	-123526	-11215
Lug 5	0	150	-246
Lug 6	0	59	98
Lug A	14983	33721	17501
Lug B	14983	33721	-17501
Load Case 18			
	F_x	F_y	F_z
	[N]	[N]	[N]
Lug 1	-280	82880	-8972
Lug 2	-887	40237	9063
Lug 3	-976	39616	-8067
Lug 4	-300	83058	-8949
Lug 5	0	20026	-32937
Lug 6	0	-20488	-33696
Lug A	14	40799	-32511
Lug B	3255	46993	-68334

Data from Table 16.28 are transformed in accordance with Figure 16.36 for next

analysis.

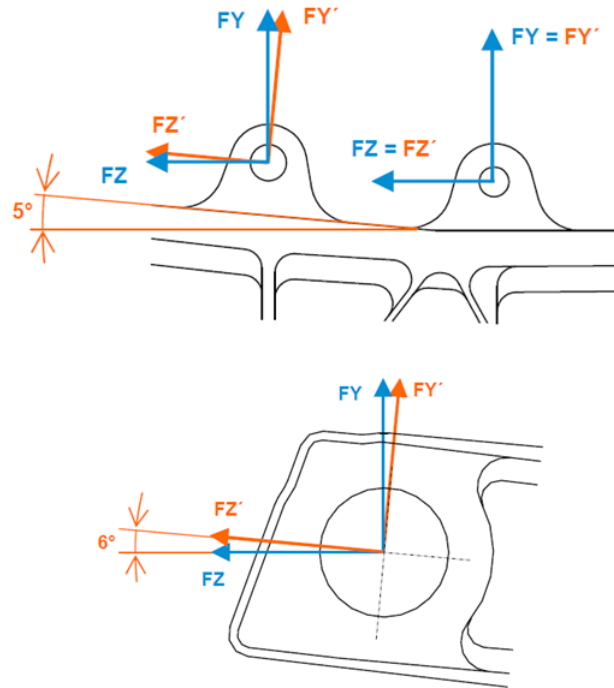


Fig. 16.36: Force transformation [19]

There are determined allowable ultimate loads for axial and transverse tension failure and shear bearing failure in literature [19]. Used procedure is in accordance with literature [17]. These values are compared with data determined in FEM analysis and new reserve factors are set.

Allowable loads for lugs of front landing gear spars in accordance with [19] are:

Tab. 16.29: Allowable loads in accordance with [19]

Label	P_{tu}	P_u	P_{bru}	F_{bru}
[—]	[N]	[N]	[N]	[MPa]
Lug 1 and 4	46538	79027	74637	662
Lug 2 and 3	29120	87360	76160	662
Lug 5 and 6	87996	210865	187533	662
Lug A and B	387072	725760	685440	-

R.F. for tension failure and shear bearing failure in accordance with [17] is ex-

pressed as:

$$R.F. = \frac{1}{(R_a^{1.6} + R_{tr}^{1.6})^{0.625}} \quad (16.26)$$

where:

$$R_a = \frac{F_N}{P_{bru}} \quad (16.27)$$

$$R_{tr} = \frac{F_T}{P_{tu}} \quad (16.28)$$

where F_N is normal force on the lug and F_T is tangent force on the lug. R.F. for bushing in accordance with [17] is expressed as:

$$R.F.\text{-bushing} = \frac{F_{bru} \cdot A_{br}}{F} \quad (16.29)$$

Results for previous equations are stated in Table 16.30.

Tab. 16.30: Reserve factors for front spar lugs

Label	<i>R.F.</i>
[-]	[-]
Lug 1 and 4	1.75
Lug 2 and 3	1.68
Lug 5 and 6	1.12
Lug A and B	4.13

Last thing is to check reserve factor of the spar as a whole. Tensile strength of landing gear spar is 448 MPa [19] and in accordance with Figure 16.35 R.F. can be expressed as:

$$R.F. = \frac{R_m}{\sigma} = \frac{448}{321} = \mathbf{1.39} \quad (16.30)$$

17 FLIGHT PERFORMANCE

17.1 Drag

17.1.1 Floats

It is difficult to determine the drag coefficient without any tunnel testing of the particular floats. Therefore approximate drag coefficient was used from Hoerner's book Fluid-dynamic drag [8]. Drag coefficient related to the main rib at the step is:

$$C_{D_{float}} = 0.220 \quad (17.1)$$

Conversion of the drag coefficient to the wing area is following:

$$C_{D_{float,A}} = 0.220 \cdot \frac{A_{MainRib}}{A_{wing}} \quad (17.2a)$$

$$C_{D_{float,A}} = 0.220 \cdot \frac{0.726489}{25.187} \quad (17.2b)$$

$$C_{D_{float,A}} = 0.006345 \quad (17.2c)$$

Finally, the drag of both floats is:

$$C_{D_{floats,A}} = 2 \cdot C_{D_{float,A}} = 2 \cdot 0.006345 = 0.01269 \quad (17.3)$$

17.1.2 Struts

Friction and wave drag of the struts

The struts have an elliptical shape. Drag coefficient for the ellipse was determined in accordance with literature [24]. ROD1, ROD2, ROD3, ROD4, ROD5, ROD6 have a ratio between semi-major and semi-minor axis equal to 2. In accordance with figure 9.13 from [24], $C_{D_{ellipse}} = 0.6$ and is related to the length of the rod and its semi-minor diameter. Horizontal beams HB1 and HB2 have ratio equal to 3 and $C_{D_{ellipse}} = 0.4$, also related to the length of the beam and its semi-minor diameter. Left and right main legs with fairing have ratio 9 and $C_{D_{ellipse}} = 0.2$. C_D related to the wing of the seaplane can be expressed as follows:

$$C_{D_{strut,A}} = C_{D_{ellipse}} \cdot \frac{b \cdot l}{A_{wing}} \quad (17.4)$$

where $C_{D_{ellipse}}$ is the drag coefficient related to the length of the rod and its semi-minor diameter, A_{wing} is the surface area of the wing projected to the horizontal basic plane, l is the length of a strut or a beam and b is the semi-minor diameter. Ultimate results are stated in following table 17.1:

Tab. 17.1: Drag coefficient of the struts

Label	$C_{D_{ellipse}}$	b	l	$C_{D_{strut,A}}$
[-]	[-]	[mm]	[mm]	[-]
ROD1	0.6	50	1132.0	0.000944
ROD2	0.6	15	465.5	0.000166
ROD3	0.6	15	465.5	0.000166
ROD4	0.6	50	1132.0	0.000944
ROD5	0.6	20	563.0	0.000268
ROD6	0.6	20	563.0	0.000268
HB1	0.4	60	2790.0	0.001772
HB2	0.4	60	2790.0	0.001772
ML left	0.2	200	480.0	0.000762
ML right	0.2	200	480.0	0.000762

Interference drag of the struts

Interference drag can be expressed in accordance with Hoerner's book Fluid-dynamic drag [8] as follows:

$$C_{D_{int,t}} = 0.75 \cdot \frac{b}{a} - \frac{0.0003}{\left(\frac{b}{a}\right)^2} \quad (17.5)$$

where $C_{D_{int,t}}$ is interference drag, b is length of semi-minor axis, a is length of semi-major axis of the strut. This $C_{D_{int,t}}$ is related to the semi-minor axis b . The same coefficient related to the wing area A is expressed by following manner:

$$C_{D_{int,A}} = C_{D_{int,t}} \cdot \frac{t^2}{A_{wing}} \quad (17.6)$$

Because each strut is connected at two points, following can be written:

$$C_{D_{int,A}} = C_{D_{int,t}} \cdot 2 \quad (17.7)$$

Ultimate results are stated in following table 17.2:

Tab. 17.2: Interference drag coefficient of the struts

Label	b	a	$C_{D_{int,t}}$	$C_{D_{int,A}}$
[-]	[mm]	[mm]	[-]	[-]
ROD1	50	100	0.37380	$3.64e^{-5}$
ROD2	15	30	0.37380	$6.68e^{-6}$
ROD3	15	30	0.37380	$6.68e^{-6}$
ROD4	50	100	0.37380	$3.64e^{-5}$
ROD5	20	40	0.37380	$1.19e^{-5}$
ROD6	20	40	0.37380	$1.19e^{-5}$
HB1	60	180	0.24730	$3.14e^{-5}$
HB2	60	180	0.24730	$3.14e^{-5}$
ML left	40	1800	0.05903	$1.88e^{-4}$
ML right	40	1800	0.05903	$1.88e^{-4}$

Total increasing of the drag from each strut is:

$$C_{D_{strut,total}} = C_{D_{strut,A}} + C_{D_{int,A}} \quad (17.8)$$

Total increasing of the drag from each struts together is:

$$C_{D_{struts,A}} = \sum_{i=1}^n C_{D_{strut,total}i} \quad (17.9)$$

where n is number of the struts. Previous equations are summarized in following table:

Tab. 17.3: Total drag of each strut and struts together

label	$C_{D_{strut,total}}$	$C_{D_{struts,A}}$
ROD1	$9.80e^{-4}$	
ROD2	$1.73e^{-4}$	
ROD3	$1.73e^{-4}$	
ROD4	$9.80e^{-4}$	
ROD5	$2.80e^{-4}$	
ROD6	$2.80e^{-4}$	$\sum_{i=1}^n C_{D_{strut,total}i} \quad 8.37e^{-3}$
HB1	$1.80e^{-3}$	
HB2	$1.80e^{-3}$	
ML1	$9.50e^{-4}$	
ML2	$9.50e^{-4}$	

17.1.3 Summary

Total additional drag is composed from drag of the floats, drag of the struts and interference drag between floats, fuselage and struts. Following can be written

$$C_{D_{add,total}} = C_{D_{floats,A}} + C_{D_{strut,A}} + C_{D_{int,A}} \quad (17.10a)$$

$$C_{D_{add,total}} = 0.01269 + 7.826e^{-3} + 5.48e^{-4} \quad (17.10b)$$

$$C_{D_{add,total}} = 2.1064e^{-2} \quad (17.10c)$$

There was determined additional drag coefficient cause by adding floats and struts to the fuselage. Previous drag coefficients were defined for zero angle of attack. To get drag coefficient angle of attack dependency, CFD solution needs to be done. Because flight characteristics, such a range or maximum horizontal speed are flown with angle of attack close to zero, this drag coefficient estimation is sufficient.

17.2 Drag polar

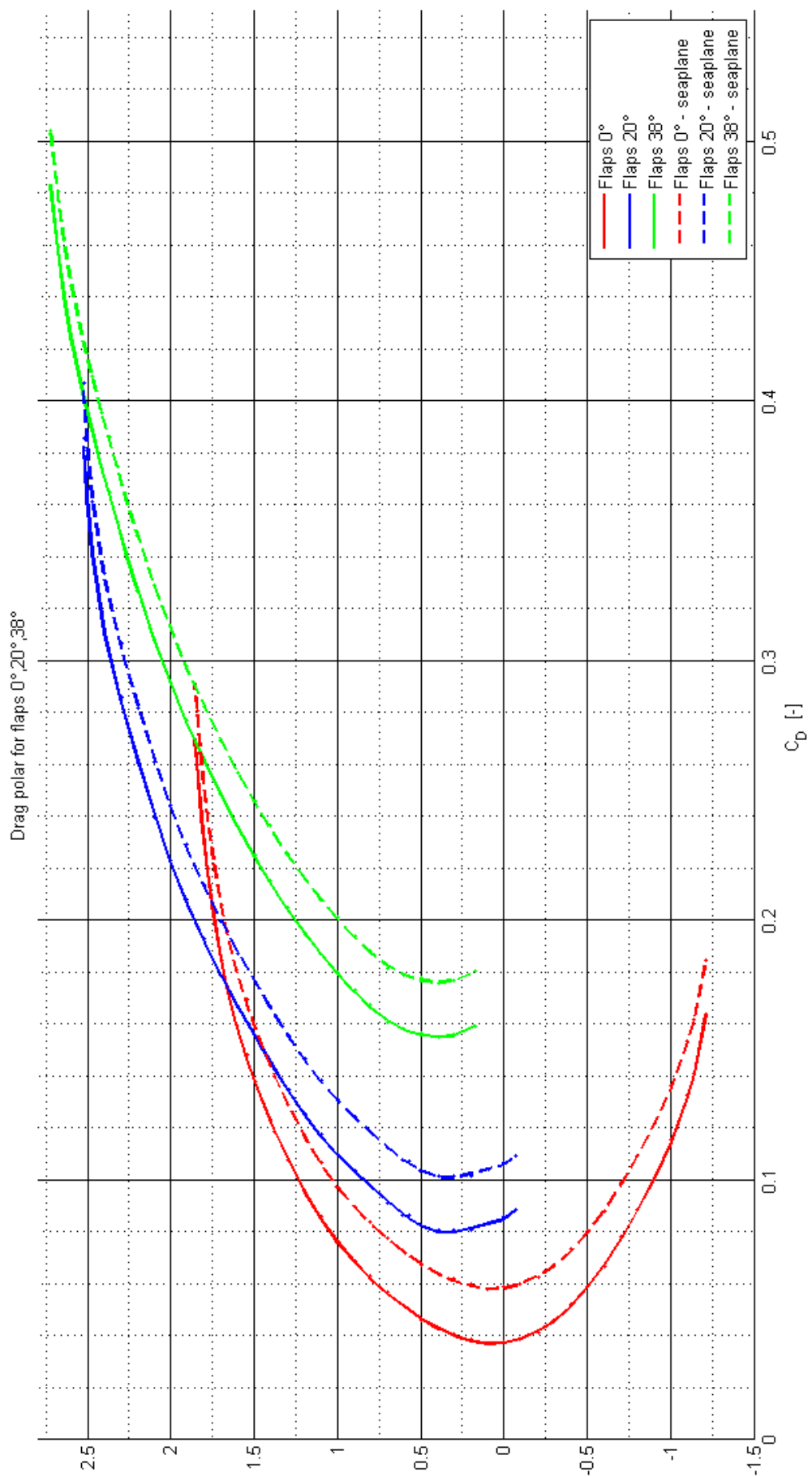
Drag polar data was taken from internal document EV55032-04-AD_verC_ZGAP. In according to flaps position there are three polars for EV-55. Additional drag coefficient has been added. Dashed curves show this reality. All the points were interpolated by tenth polynomial curves. Polynomial coefficients are following:

Tab. 17.4: Polynomial coefficients for terrestrial version

flaps	degree of coefficients										
	10	9	8	7	6	5	4	3	2	1	0
0°	$5.5e^{-3}$	$-1.4e^{-2}$	$-6.0e^{-3}$	$3.2e^{-2}$	$7.2e^{-4}$	$-1.9e^{-2}$	$-4.6e^{-3}$	$-8.5e^{-3}$	$6.2e^{-2}$	$-8.8e^{-3}$	$3.76e^{-2}$
20°	$5.2e^{-2}$	$-6.0e^{-1}$	2.9	-7.8	12.4	-11.7	6.3	-1.6	$1.9e^{-1}$	$-2.6e^{-2}$	$8.51e^{-2}$
38°	$2.0e^{-2}$	$-2.7e^{-1}$	1.5	-5.1	10.5	-13.8	11.7	-6.2	2.0	-0.4	0.19

Tab. 17.5: Polynomial coefficients for seaplane version

flaps	degree of coefficients										
	10	9	8	7	6	5	4	3	2	1	0
0°	$5.5e^{-3}$	$-1.4e^{-2}$	$-6.0e^{-3}$	$3.2e^{-2}$	$7.2e^{-4}$	$-1.9e^{-2}$	$-4.7e^{-3}$	$-8.6e^{-3}$	$6.2e^{-2}$	$-8.8e^{-3}$	$5.87e^{-2}$
20°	$5.2e^{-2}$	$-6.0e^{-1}$	2.9	-7.8	12.4	-11.7	6.3	-1.6	$1.9e^{-1}$	$-2.6e^{-2}$	$1.06e^{-1}$
38°	$2.0e^{-2}$	$-2.7e^{-1}$	1.5	-5.1	10.5	-13.8	11.7	-6.2	2.0	-0.4	0.21



17.3 Maximal horizontal speed

Maximal horizontal speed is determined from power required and power available curves. Their intersections show minimal and maximal horizontal speed for different altitudes. Power required can be computed in following manner:

First, C_L coefficient has to be determined. The C_L is a function of altitude, speed and weight:

$$C_L = \frac{2 \cdot m \cdot g}{\rho \cdot A \cdot V^2} \quad (17.11)$$

For specific C_L coefficient, C_D can be defined from drag polar. It can be done manually from figure 17.1 or by using polynomial functions from table 17.5. The latter method was used in MATLAB. Following can be written:

$$C_D = f(C_L) \quad (17.12)$$

Thrust required is expressed from force equilibrium during horizontal flight:

$$T_{req} = 0.5 \cdot \rho \cdot A \cdot V^2 \cdot C_D \quad (17.13)$$

Power required is thrust required multiplied by speed:

$$P_{req} = T_{req} \cdot V \quad (17.14)$$

where P_{req} is the power required, T_{req} is the thrust required and V is corresponding speed.

Power available is a function of engine power and propeller efficiency.

$$P_{ava} = \frac{P_{engine}}{\eta} \quad (17.15)$$

Power available against speed for different altitudes is shown in Figure 17.2.

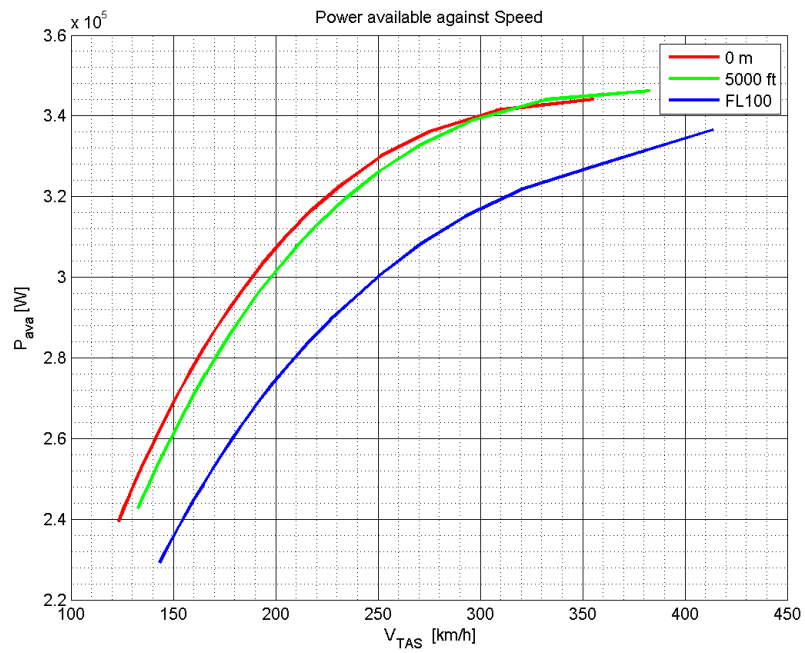


Fig. 17.2: Power available against speed

Propeller efficiency as a function of the speed is shown in Figure 17.3.

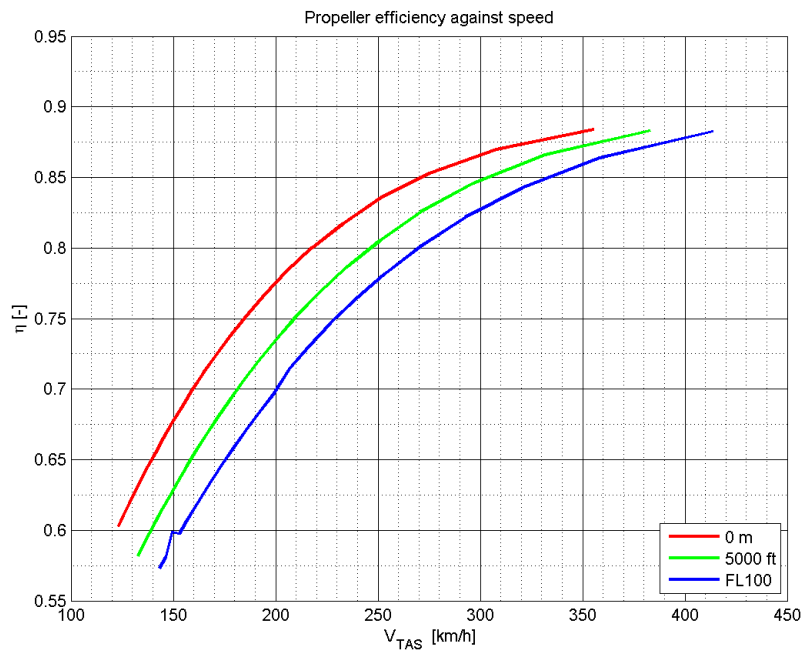


Fig. 17.3: Propeller efficiency against speed

These curves were gained from internal documents for PT6A-21 engine. Power required and Power available curves were computed for altitudes: 0 m, 5000 ft and FL100 and for take-off weight: 3150 kg, 3777 kg and 4600 kg. Power required and Power available curves for different altitudes and different weights are shown in figures 17.4, 17.5 and 17.6.

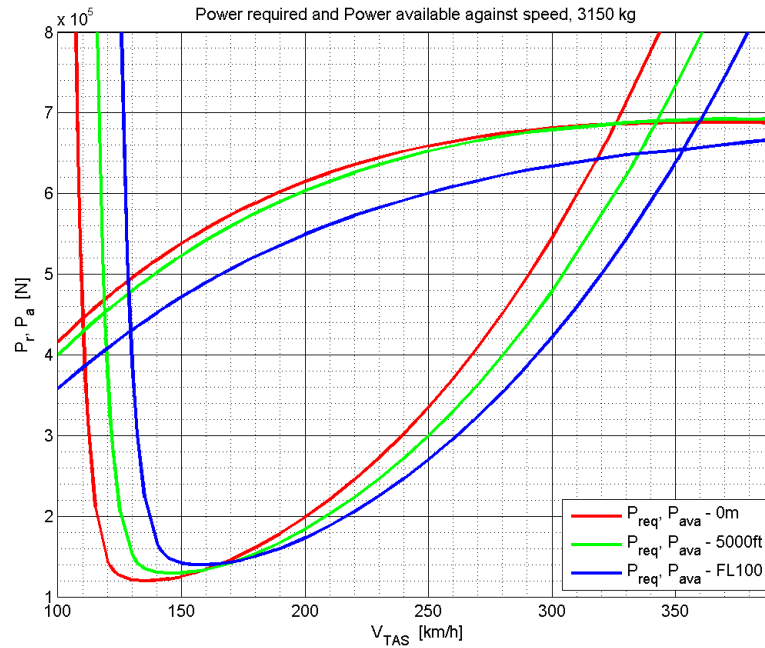


Fig. 17.4: Power required and Power available for 3150 kg

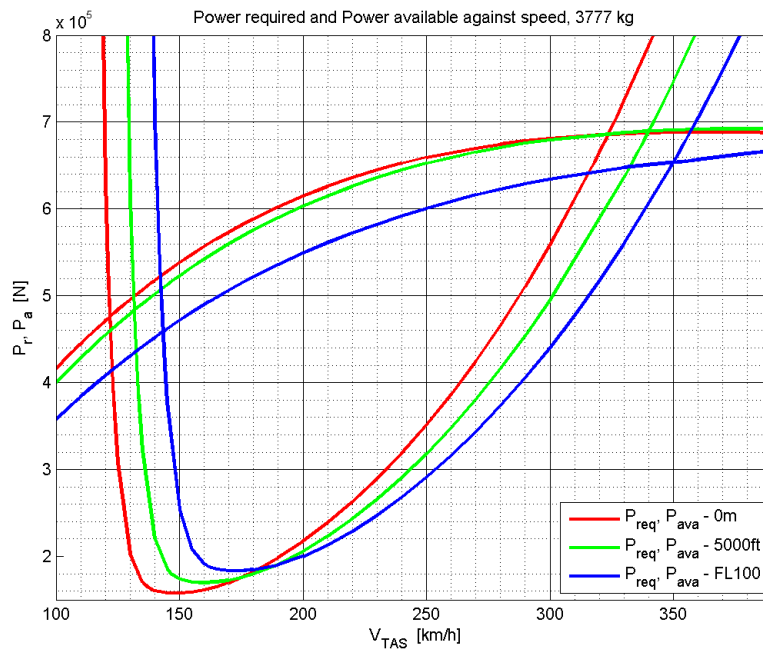


Fig. 17.5: Power required and Power available for 3777 kg

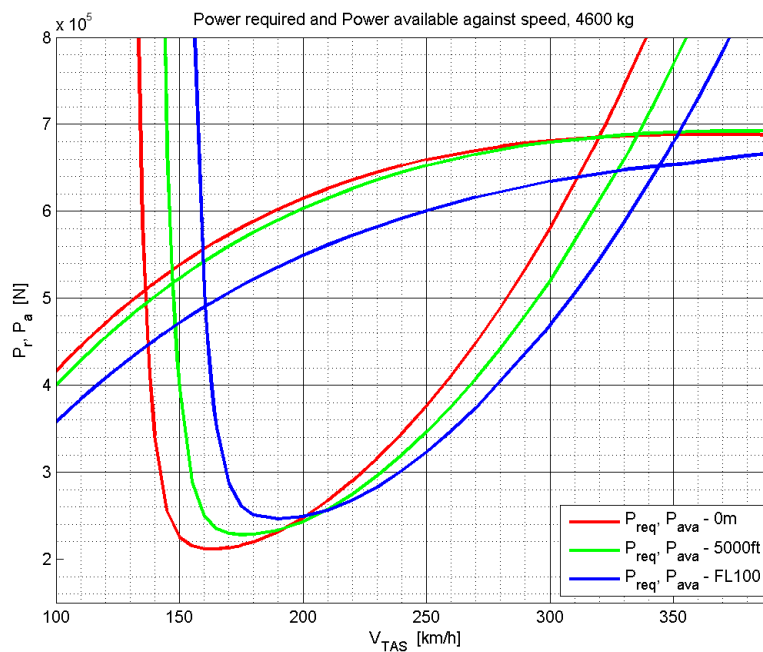


Fig. 17.6: Power required and Power available for 4600 kg

Previous curves are going to be necessary for climbing performance. Intersection

between power available and power required means that these two powers are equal each other. It also means that the maximal speed is reached at this point. From previous figures following can be read:

Tab. 17.6: Maximal horizontal speed

	3150 kg	3777 kg	4600 kg
altitude	V_{max}	V_{max}	V_{max}
	[km/h]	[km/h]	[km/h]
0 m	325	323	330
5000 ft	342	340	335
FL100	353	350	344

17.4 Climbing performance

Vertical speeds for different altitudes and different weights are determined in this section. Vertical speed w is computed from specific excess power for different speeds:

$$w = \frac{\Delta F \cdot V}{G} = \frac{\Delta P}{G} = \frac{\Delta P}{m \cdot g} \quad (17.16)$$

Previous equation is shown in following figures 17.7, 17.8 and 17.9.

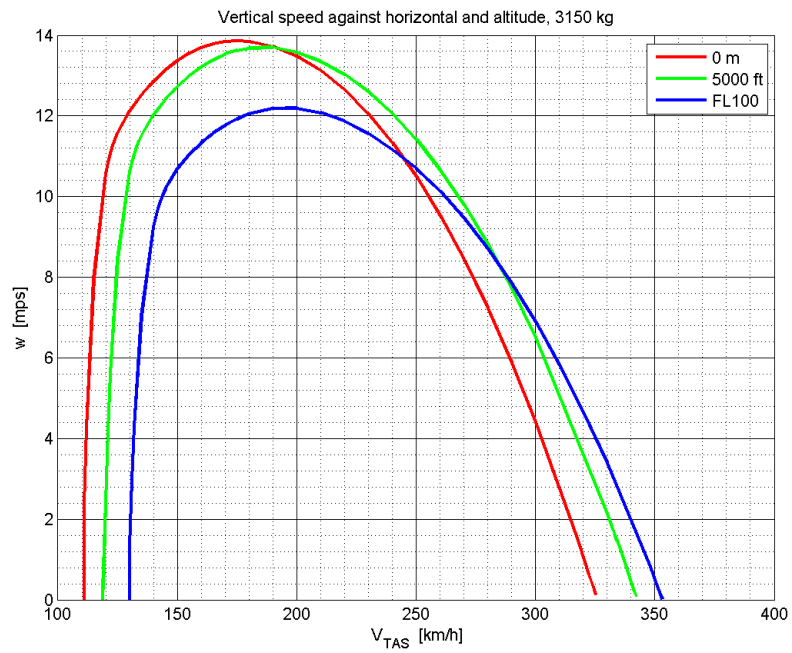


Fig. 17.7: Climbing speed against True air speed for 3150 kg

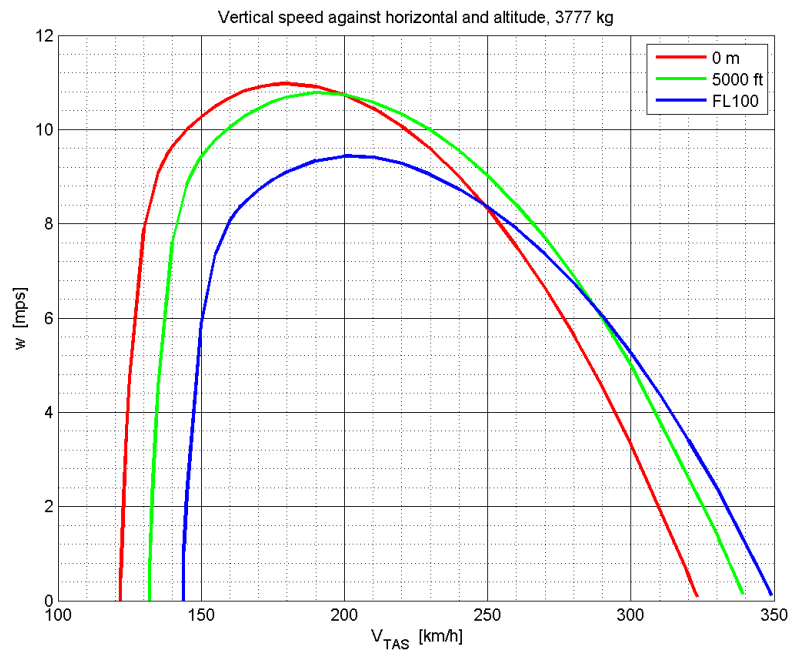


Fig. 17.8: Climbing speed against True air speed for 3777 kg

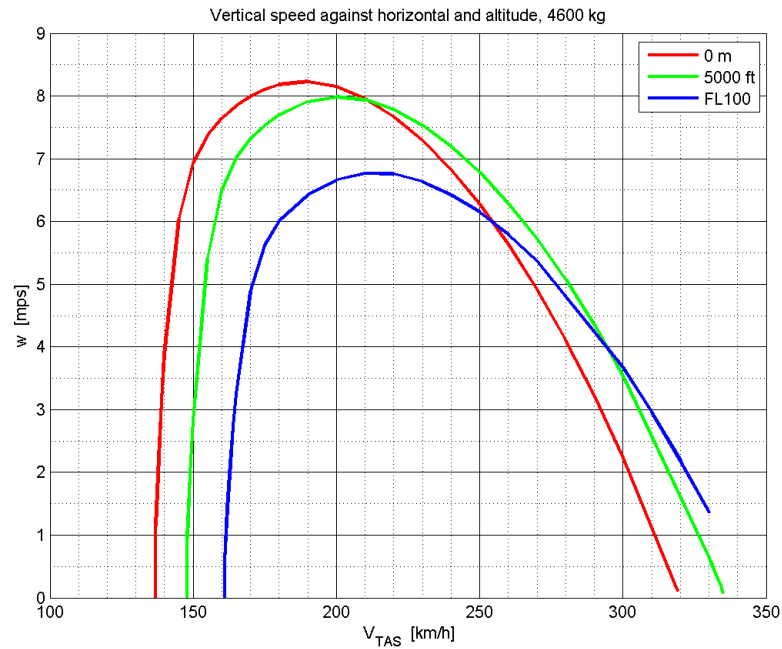


Fig. 17.9: Climbing speed against True air speed for 4600 kg

Important results from previous figures are mentioned in next table 17.7.

Tab. 17.7: Climbing speed

	3150 kg	3777 kg	4600 kg
altitude	w_{max}	w_{max}	w_{max}
	[m/s]	[m/s]	[m/s]
0 m	13.8	11.0	8.2
5000 ft	13.6	10.8	8.0
FL100	12.2	9.4	6.8

17.5 Range and Endurance

Range against true air speed dependency will be create. Also, 'payload - range' diagram will be determined. Following procedure will be used during determination of these curves. Drag polar from figure 17.1 will be used. C_D for given C_L from range

0.3 - 2.5 is read. True air speed is computed using following formula:

$$V_{TAS} = \sqrt{\frac{2 \cdot m_1 \cdot g}{A \cdot \rho \cdot C_L}} \quad (17.17)$$

where V_{TAS} is true air speed, m_1 is take-off weight, g is gravitational acceleration, A is wing area, ρ is density of air for specific altitude and C_L is lift coefficient from range stated in previous paragraph. Fuel weight flow is gained from software for Pratt & Whitney PT6A-21 engine for every V_{TAS} speed and for specific altitudes. 0 m, 5000 ft and FL100 were set as reference altitudes. Specific fuel consumption SFC is expressed as follows:

$$SFC = \frac{C_{hrs} \cdot \eta}{P_{ava}} \quad (17.18)$$

where SFC is specific fuel consumption, C_{hrs} is fuel weight flow and P_{ava} is power available and η is propeller efficiency. Two engines were considered. Speed - SFC dependence for different altitudes is shown in Figure 17.10.

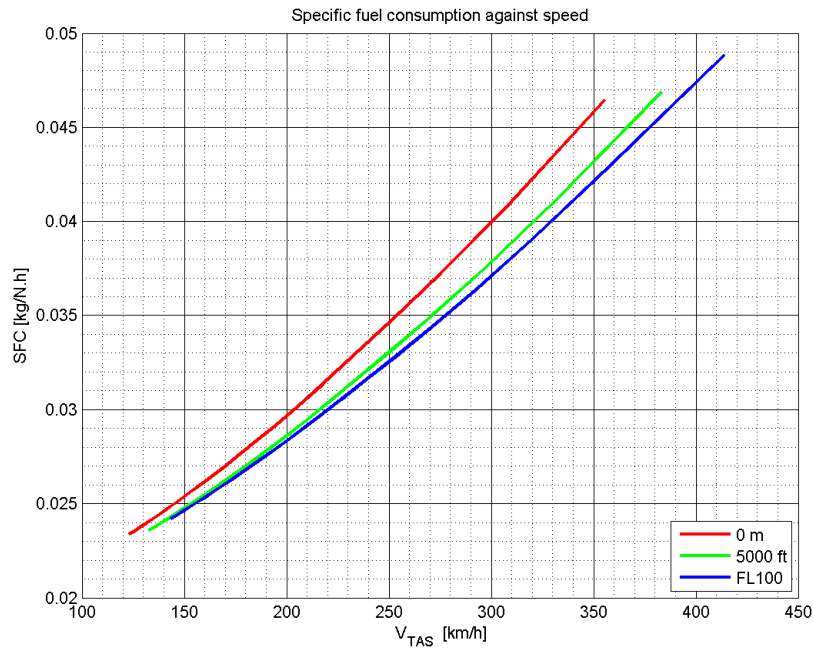


Fig. 17.10: Specific fuel consumption against true air speed

Next step is to determine glide ratio K and its maximal value. It is easily done from following formula:

$$(L/D) = \frac{C_L}{C_D} \quad (17.19a)$$

$$(L/D)_{max} = \left(\frac{C_L}{C_D} \right)_{max} \quad (17.19b)$$

Following non-dimensional ratios needs to be set:

$$\bar{m}_f = 1 - \frac{m_2}{m_1} \quad (17.20)$$

where \bar{m}_f non-dimensional fuel ratio, m_1 is initial weight and m_2 is final weight. Final weight is:

$$m_2 = m_1 - m_f \quad (17.21)$$

where m_f is fuel weight. Fuel weight will be described in next sub-section.

$$\bar{V} = \frac{V}{V_{mD}} \quad (17.22)$$

where \bar{V} is non-dimensional speed, V is true air speed and V_{mD} is minimum drag speed.

17.5.1 Payload configurations

There are considered three payload configurations during range and endurance computations.

Tab. 17.8: Payload configuration 1

Label	value	unit
Operational empty weight	3150	kg
Second pilot	77.1	kg
Passenger 1	77.1	kg
Passenger 2	77.1	kg
Passenger 3	77.1	kg
Passenger 4	77.1	kg
Passenger 5	77.1	kg
Passenger 6	77.1	kg
Passenger 7	77.1	kg
Passenger 8	77.1	kg
Passenger 9	77.1	kg
Cargo	350	kg
Fuel	329	kg
Summary	4600	kg

Tab. 17.9: Payload configuration 2

Label	value	unit
Operational empty weight	3150	kg
Second pilot	0	kg
Passenger 1	0	kg
Passenger 2	0	kg
Passenger 3	0	kg
Passenger 4	0	kg
Passenger 5	0	kg
Passenger 6	0	kg
Passenger 7	0	kg
Passenger 8	0	kg
Passenger 9	0	kg
Cargo	0	kg
Fuel	1450	kg
Summary	4600	kg

Tab. 17.10: Payload configuration 3

Label	value	unit
Operational empty weight	3150	kg
Second pilot	77.1	kg
Passenger 1	77.1	kg
Passenger 2	77.1	kg
Passenger 3	77.1	kg
Passenger 4	77.1	kg
Passenger 5	77.1	kg
Passenger 6	77.1	kg
Passenger 7	77.1	kg
Passenger 8	77.1	kg
Passenger 9	77.1	kg
Cargo	0	kg
Fuel	679	kg
Summary	4600	kg

17.5.2 Range

To compute range, mode where $\rho = const.$ and $V = const.$ was chosen. In accordance with literature [4], range is computed by using following formula:

$$R = \left(\frac{2 \cdot K_{max} \cdot \eta}{g \cdot SFC} \right) \cdot \arctan \left(\frac{\bar{m}_f}{\bar{V}^2 + \frac{1 - \bar{m}_f}{\bar{V}^2}} \right) \quad (17.23)$$

Previous equation is expressed in figures 17.11, 17.12 and 17.13 for different altitudes and payload configurations.

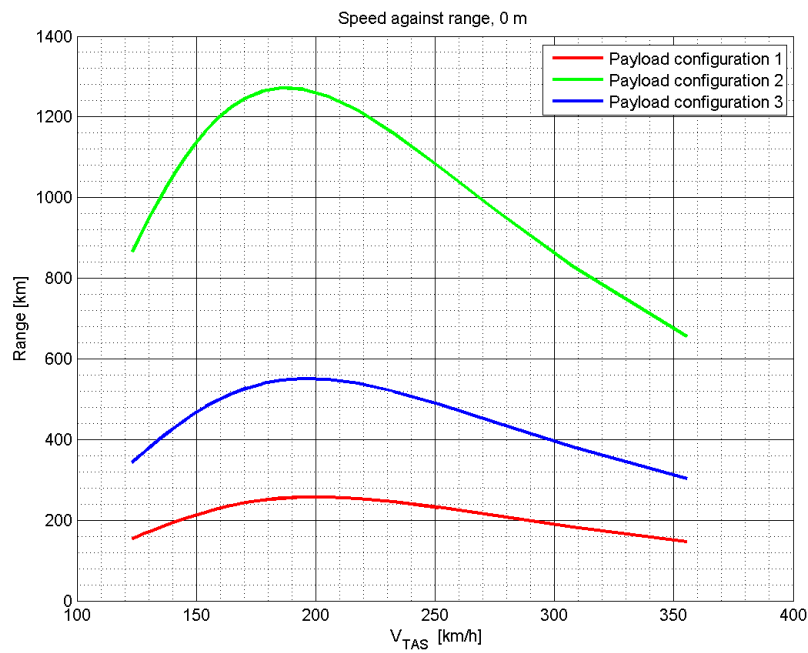


Fig. 17.11: Speed against Range for 0 m

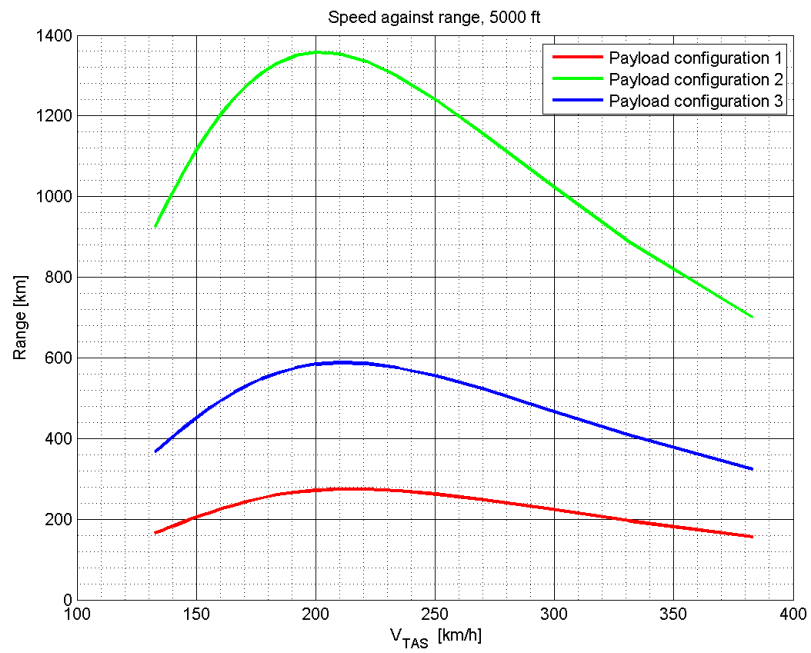


Fig. 17.12: Speed against Range for 5000 ft

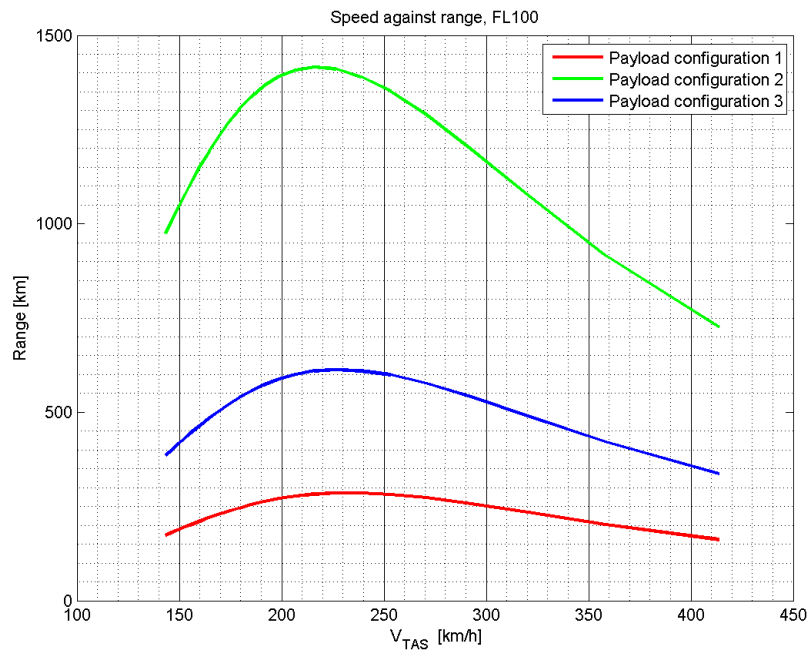


Fig. 17.13: Speed against Range for FL100

'Payload - Range' diagram is built from previous graphs in accordance with

literature [4] for maximal range speed and for maximal horizontal speed.

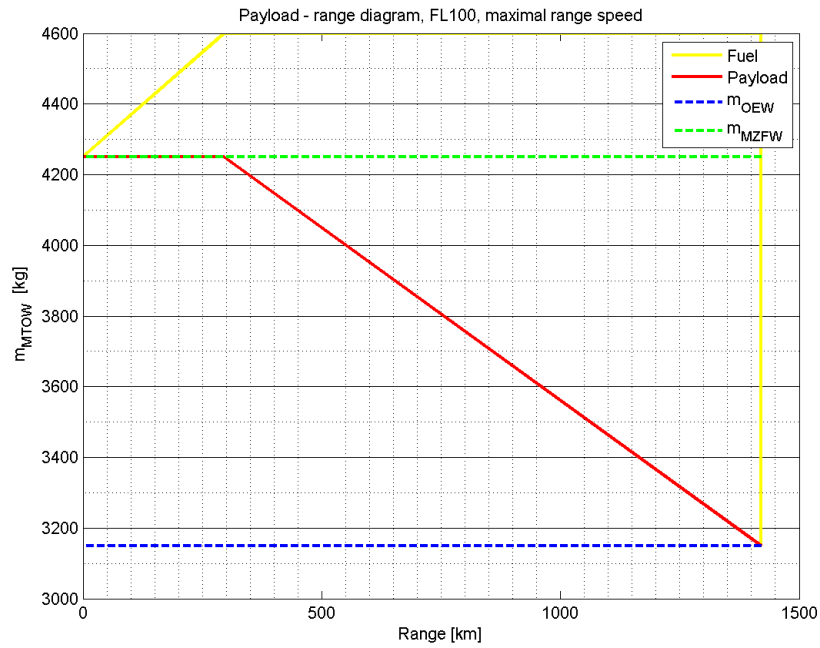


Fig. 17.14: Payload - Range diagram, FL100, maximal range speed

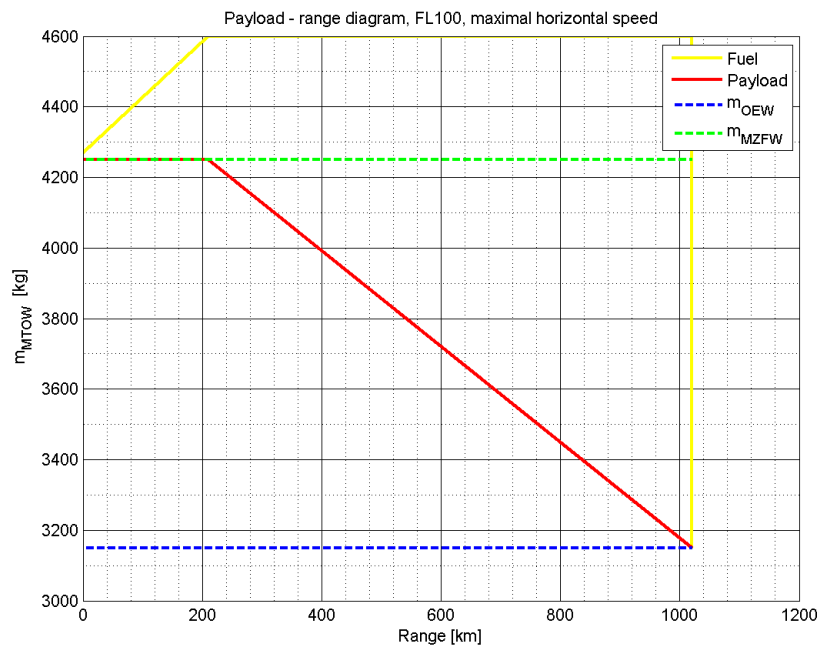


Fig. 17.15: Payload - Range diagram, FL100, maximal horizontal speed

17.5.3 Endurance

Same preconditions are used also for endurance: $\rho = const.$ and $V = const.$. In accordance with literature [4], endurance is computed by using following formula:

$$E = \left(\frac{2 \cdot K_{max} \cdot \eta}{g \cdot SFC \cdot V_{mD}} \right) \cdot \frac{1}{\bar{V}} \cdot \arctan \left(\frac{\bar{m}_f}{\bar{V}^2 + \frac{1-\bar{m}_f}{\bar{V}^2}} \right) \quad (17.24)$$

where

$$V_{mD} = \sqrt{\frac{2 \cdot m \cdot g}{A \cdot \rho \cdot C_{L,K_{max}}}} \quad (17.25)$$

$C_{L,K_{max}}$ is lift coefficient corresponding with C_L for maximal glide ratio (L/D). Previous equation 17.24 is expressed in Figures 17.16, 17.17 and 17.18 for different altitudes and payload configurations.

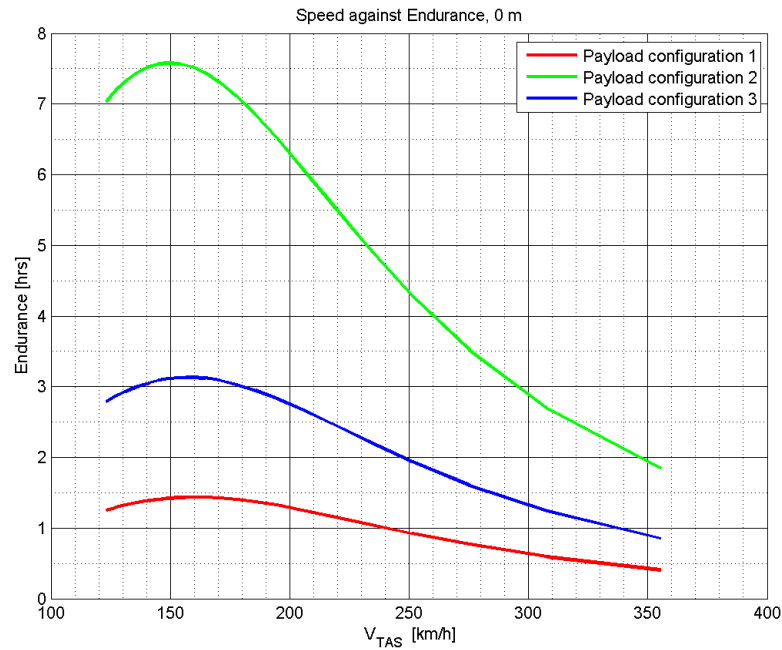


Fig. 17.16: Speed against Endurance for 0 m

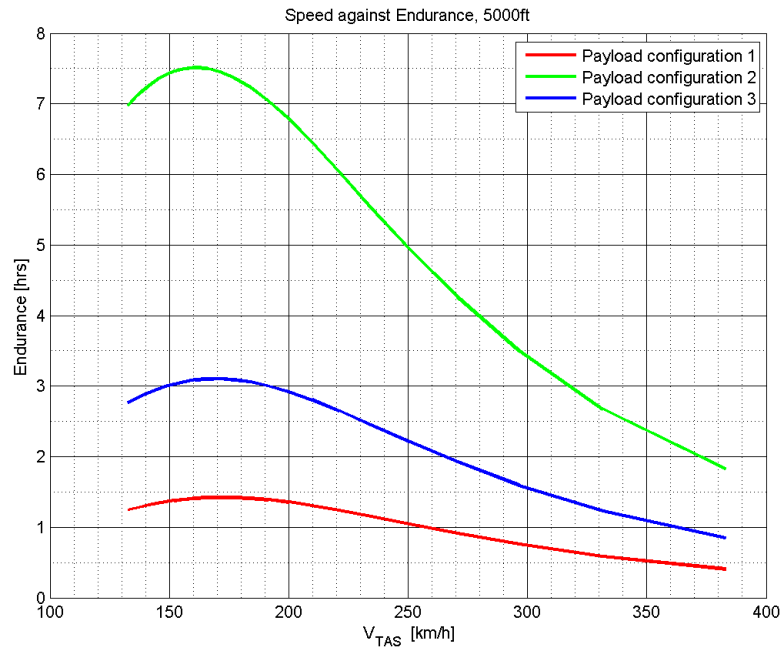


Fig. 17.17: Speed against Endurance for 5000 ft

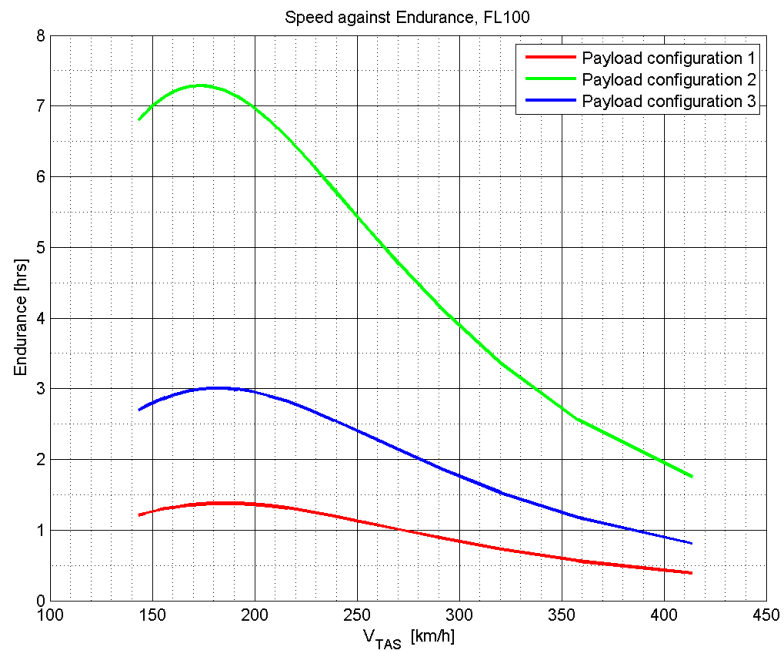


Fig. 17.18: Speed against Endurance for FL100

Previous graphs are summed up in next table:

Tab. 17.11: Summary of Range and Endurance

	Maximal range			Maximal endurance		
	0 m	5000 ft	FL100	0 m	5000 ft	FL100
	[km]	[km]	[km]	[hrs]	[hrs]	[hrs]
Payload config. 1	260	280	295	1.45	1.40	1.40
Payload config. 2	1280	1360	1420	7.25	7.50	7.55
Payload config. 3	555	580	615	3.15	3.10	3.00

18 CONCLUSION

Due to seaplane modification, there are many characteristics which have been changed comparing to the terrestrial version. Compared to the competitors seaplanes, EV-55 has the highest wing loading. Figure 18.1 shows wing loading against maximal horizontal speed. It is seen that EV-55 as a seaplane has the highest cruise speed from all of the competitors seaplanes. The maximal cruise speed is 353 km/h . Compared to the terrestrial version it is about 80 km/h lower.

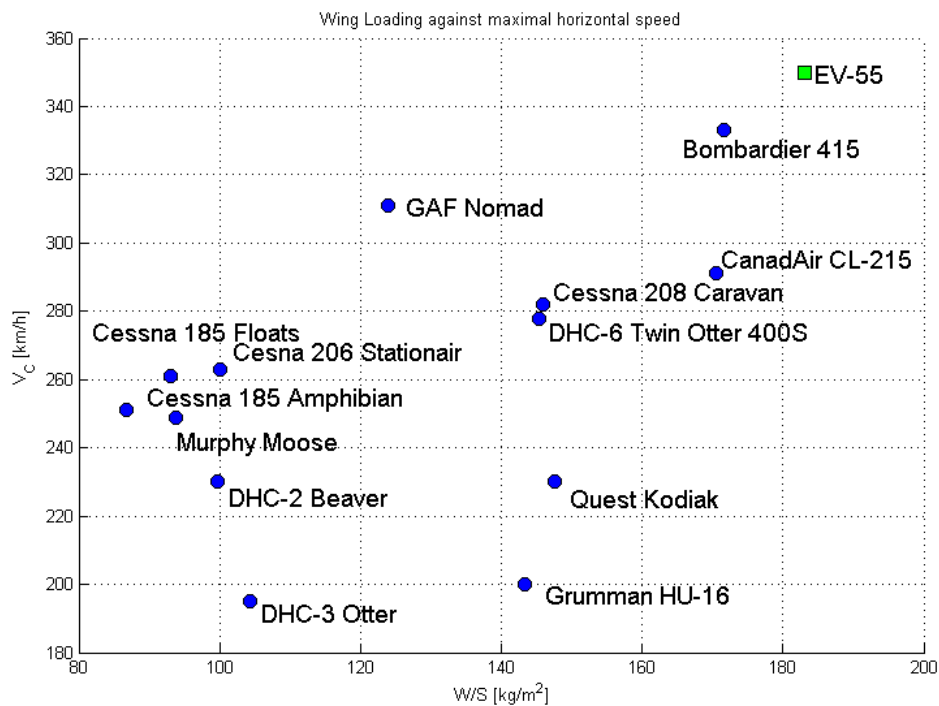


Fig. 18.1: Wing loading against maximal horizontal speed

Figure 18.2 shows wing loading - range dependency. High wing loading is the cause why EV-55 does not have such as high range as other seaplanes.

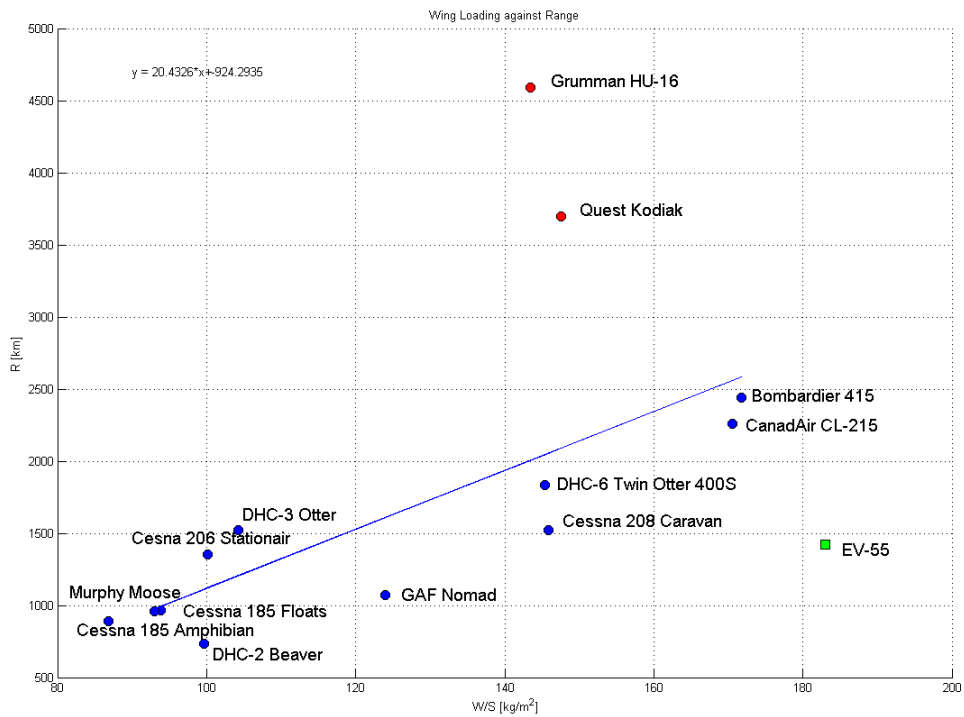


Fig. 18.2: Wing loading against range

Last Figure 18.3 shows wing loading - stall speed dependency. Although EV-55 has the highest wing loading, it does not have highest stall speed. This is caused mainly by used aerofoils and shape of the wing.

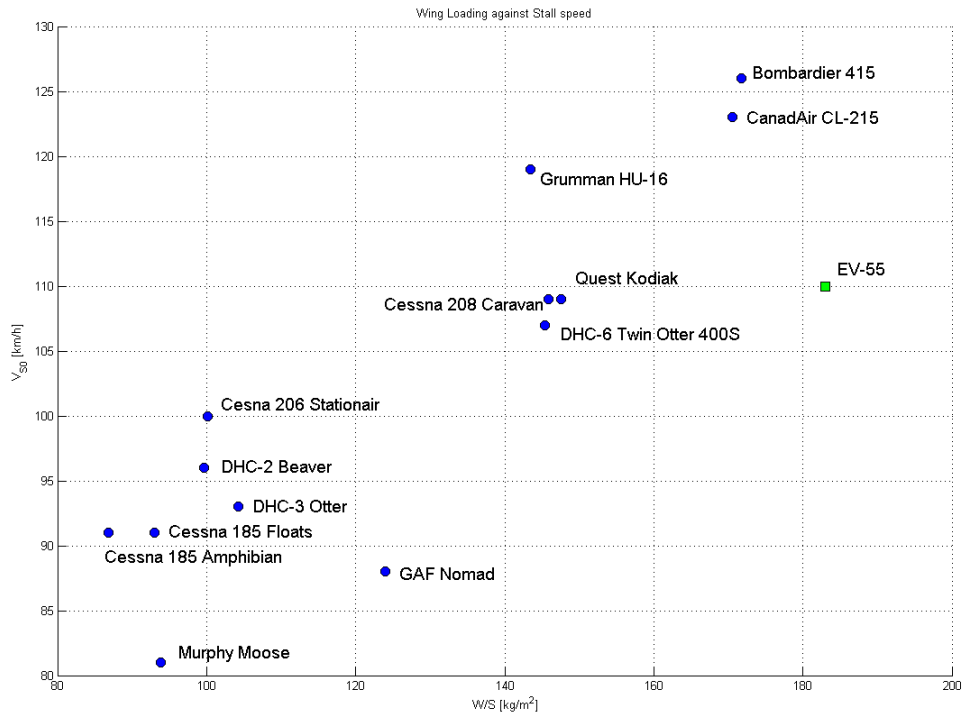


Fig. 18.3: Wing loading against stall speed

Minimum operation weight had to be increased due to floats. Compared to the terrestrial version, the weight increased about 200 *kg*. This has negative effect on the payload that had to be decreased. Second option is to decrease amount of fuel and the range will be decreased, as well. The weight envelope had to be limited from left side and right side. Maximal weight of cargo at front cargo space has been restricted for some of weight configurations. Minimum static margin remains at 8%, maximum static margin was decreased from 35% to 31.4%.

Maximal load factor determined in accordance with [5] is 6.33. For terrestrial version maximal load factor determined for landing cases is 5.58. Load factor for seaplane is higher. This will lead to higher inertia of the elements such a cargo, engines and so on. How this higher inertia affects other element, needs to be determine in next stage of development.

Frame connecting the floats and fuselage has been designed. Stress analysis of horizontal beams and vertical rods was done. Reserve factors were determined and R.F. is higher than one for all of the checked elements. Front spar as an example, was chosen to compare the ground and water loads. Front spar is able to transfer higher loads developed during water level landing. Aft landing gear spar was not checked since the scope of master's thesis is considerable.

Table 18.1 shows comparison of the main characteristics between terrestrial and seaplane version.

Tab. 18.1: Comparison between terrestrial EV-55 and EV-55 Seaplane

	Landplane	Seaplane	unit
Maximal horizontal speed at FL100	443	353	<i>km/h</i>
Maximal range	2300	1420	<i>km</i>
Minimum operational empty weight	3150	2950	<i>kg</i>
Maximum zero fuel weight	4450	4250	<i>kg</i>
Maximum load factor at c.g.	5.58	6.33	–
Minimum static margin	8	8	%
Maximum static margin	35	31.4	%
Maximum vertical speed at 0 m (4600 kg)	8.5	8.3	<i>m/s</i>

EV-55 is suitable for twin-float seaplane modification without any substantial modifications in existing airframe.

BIBLIOGRAPHY

- [1] ANČÍK, Zdeněk - RŮŽIČKA, Pavel - PÍŠTĚCKÝ, Pavel - TEMEL, Tomáš. *Základní geometrické a aerodynamické podklady letounu EV-55*. Internal document from Evektor. 20.3.2008. 169. Print.
- [2] BRUHN, E.F.. *Analysis and Design of Flight Vehicle Structures*. Indianapolis: Jacobs Publishing, INC., 1973. Print.
- [3] ČTVERÁK, J. - MERTL, V. - PÍŠTĚK, A.. *Soubor podkladů pro pevnostní výpočty leteckých konstrukcí*. Brno, 1997.
- [4] DANĚK, Vladimír. *Mechanika letu I*. First edition. Brno: Akademické nakladatelství CERM, s.r.o., 2009, 293. ISBN 978-80-7204-659-1. Print
- [5] European Aviation Safety Agency. *Certification Specifications for Normal, Utility, Aerobatic, and Commuter Category Aeroplanes CS-23*, Amendment 3, 20 July 2012. 405. Print.
- [6] FALTA, Robert. *Pozemní případy zatížení*. Internal document from Evektor. 7.3.2008. 44. Print.
- [7] Federal Aviation Authority. *Federal aviation regulations, Part 23 - AIRWORTHINESS STANDARDS: NORMAL, UTILITY, ACROBATIC, AND COMMUTER CATEGORY AIRPLANES*, 5.12.2013. Print.
- [8] HOERNER, S.F.. *Fluid-dynamic drag*. Brick Town, NJ: Hoerner Fluid Dynamics, 1965. 454. Print.
- [9] HUGHES, Charles H.. *Handbook of ship calculations, construction and operation*. New York: Appleton and company, 1917. 65. Print.
- [10] JANEBA, Ivo - MERTL, Vlastimil. *Plováky pro malý letoun*. Place and year of publication unknown. 14. Print.
- [11] JANÍČEK, P. - ONDRÁČEK, E. - VRBKA, J. - BURŠKA, J.. *Mechanika těles - Pružnost a pevnost I*. Brno: Akademické nakladatelství CERM, s.r.o., Květen 2003. 287. ISBN 80-214-2592-X. Print.
- [12] JOHNSTON, Paul - RAM, Joel - PETRUSKA, Ondrej - SPONER, Jan - HOLLIS, Michal. *TMAL51 Aircraft conceptual design*. Linköping, Sweden: Project work - Linköping University, 2012. 33. Print.
- [13] KIMBERLIN, Ralph D.. *Flight Testing Of Fixed-Wing Aircraft*. Reston, VA: American Institute of Aeronautics and Astronautics, Inc., 2003. Print.

- [14] KOSOUROV, K.F.. *Gidrosamolety ix morechodnost: i rascet*. Leningrad, SSSR: ONTI, 1935. 368. Print.
- [15] MOHR, Benedikt - SCHÖMANN, Joachim. *Seaplane Data Base*. Garching, Germany: Technical University Munich, 2010. 68. Print.
- [16] NELSON, William. *Seaplane design*. First Edition, New York and London: McGraw-Hill Book Company, Inc., 1934. 273. Print.
- [17] NIU, Michael C.Y.. *Airframe Structural Design*. Ninth printing. Burbank, California: Lockheed Aeronautical Systems Company, 1997, 612. ISBN 962-7128-04-X. Print.
- [18] ROSENTHAL, L.W.. *The Weight of Seaplanes Floats*. Royal Aeronautical Society Journal, September 1949.
- [19] STEJSKAL, Jiří. *Kontrola nosníků podvozku a trupu mezi přepážkami 10 a 12 pod podlahou*. Internal document from Evekto. 30.6.2010. 91. Print.
- [20] STEJSKAL, Jiří. *Zástavba předového podvozku*. Internal document from Evekto. 13.5.2011. 131. Print.
- [21] TEMEL, Tomáš. *Projekční hmotový rozbor letounu EV-55*. Internal document from Evekto. 21.12.2007. 31. Print.
- [22] TICHÝ, Jaroslav - PATEK, Peter. *Teória lode*. Bratislava: Slovenská technická univerzita v Bratislave, 2006. 355. Print.
- [23] VLACHYNSKÝ, J.. *Kovové materiály*. Internal document from Evekto. 1.2.2007. 183. Print.
- [24] YOUNG, D.F. - MUNSON, B.R. - OKIISHI, T.H.. *A Brief Introduction to Fluid Mechanics*. New York: John Wiley & Sons, 1997. Print.
- [25] WIPAIRE Inc. *Wipline 8750 Floats*. [online]. ©2014 [retrieved 30.1.2014] Available from: <<http://www.wipaire.com/wipline-floats/8750.php>>.

LIST OF FIGURES

3.1	Seaplane manufacturing timeline [15]	19
4.1	Three-view drawing of the EV-55 Outback	21
5.1	Basic parts of the float	23
5.2	Dependence between hydrodynamic drag D_{HD} and forward speed V [10]	24
5.3	Dependence between hydrodynamic drag D_{HD} and forward speed V [10]	25
5.4	Dependence between hydrodynamic drag D_{HD} and forward speed V [10]	26
7.1	EV-55 as a flying boat with auxiliary floats	32
7.2	EV-55 as a flying boat with widened fuselage	33
7.3	EV-55 as a flying boat with widened fuselage - blade-strike	34
7.4	EV-55 as a flying boat with widened fuselage and top-wing mounted engines	34
7.5	Single/Twin-float design	36
7.6	Stability of EV-55 as a flying boat with widened fuselage	38
8.1	Wing Loading against Range	39
8.2	Maximum take-off weight against Empty weight	40
8.3	Wing Loading against Capacity	40
8.4	Wing Loading against Cruise speed	41
8.5	Wing Loading against Stall speed	41
9.1	Aeroplane and float coordination system - side view	42
9.2	Aeroplane and float coordination system - front view	43
9.3	Centre of gravity coordination system - side view	43
10.1	Front and aft attachment points	44
11.1	Basic buoyancy condition	46
11.2	Stable buoyant condition	46
11.3	Stable buoyant condition - floats	47
11.4	Metacentric height \overline{GM} versus a and b variables	49
11.5	Contour lines of metacentric height \overline{GM}	50
11.6	Geometric data measured in CATIA V5	51
11.7	Waterline position and stabilizing moment ($m_{TOW} = 3150kg$)	53
11.8	Waterline position and stabilizing moment ($m_{TOW} = 3777kg$)	54
11.9	Waterline position and stabilizing moment ($m_{MTOW} = 4600kg$)	55
11.10	Forces acting during take-off	56
11.11	Reed's diagram	58
11.12	Wind gust	59

12.1	Weight of the floats versus volume of the floats	61
12.2	Weight envelope of the terrestrial version	62
12.3	Weight envelope of the seaplane version	64
12.4	Weight envelope of seaplane version - modified	65
12.5	Weight envelope of the terrestrial version, the seaplane version, and the seaplane - modified	66
14.1	Position of applied resultant water load for step landing	72
14.2	Dead rise angle position	73
14.3	Position of applied resultant water load for bow landing	74
14.4	K_1 factor against x_f coordinate - weight configuration 1	75
14.5	Position of applied resultant water load for stern landing	77
14.6	Position of applied resultant water load for unsymmetrical landing case	79
15.1	Front and aft attachment points	84
15.2	Front attachment points	85
15.3	Front attachment points - solution	85
15.4	Aft attachment points	86
16.1	General description of loaded elements	92
16.2	EV55-v7-00-03 version of FEM model	92
16.3	Clean model of the fuselage	93
16.4	FEM model of the EV-55 Seaplane	93
16.5	FEM model of the floats - side view	94
16.6	FEM model of the floats - top view	94
16.7	FEM model of the rods	95
16.8	FEM model of the horizontal beams	95
16.9	FEM model of the RBE2 and RBE3 elements	96
16.10	FEM model of the main legs	97
16.11	Action forces at connection point CP1, Load Case 3	98
16.12	Action forces at connection point CP2, Load Case 8	99
16.13	Action forces at connection point CP3, Load Case 13	99
16.14	Element description of Front frame	101
16.15	Geometrical description of HB1, R1, R2, R3 and R4	101
16.16	FEM result - horizontal beam 1 - Max Comb stress	103
16.17	FEM result - ROD 1 and 4 - Rod axial tensile force	103
16.18	FEM result - ROD 1 and 4 - Rod axial compressive force	104
16.19	FEM result - ROD 2 and 3 - Rod tensile and compressive force	104
16.20	Geometrical properties - lugs for Rods 1, 2, 3, 4 and HB1	106
16.21	Force position on the pin	108
16.22	Shear and Bending Moment Diagram of the pin	109
16.23	Geometry for buckling	111

16.24	Element description of Front frame	112
16.25	Geometrical description of HB2, R5 and R6	112
16.26	FEM result - horizontal beam 2 - Max Comb stress	114
16.27	FEM result - ROD 5 and 6 - Rod tensile and compressive force	114
16.28	Shear and Bending Moment Diagram of the pin	118
16.29	Front Attachment Description	121
16.30	Unsymmetrical landing case 19	122
16.31	Affecting forces - front spar	123
16.32	Names of the lugs for front spar	124
16.33	FEM results - Load Case 3	124
16.34	FEM results - Load Case 8	125
16.35	FEM results - Load Case 18	125
16.36	Force transformation [19]	127
17.1	Polars for different flaps deflection	134
17.2	Power available against speed	136
17.3	Propeller efficiency against speed	136
17.4	Power required and Power available for 3150 kg	137
17.5	Power required and Power available for 3777 kg	138
17.6	Power required and Power available for 4600 kg	138
17.7	Climbing speed against True air speed for 3150 kg	140
17.8	Climbing speed against True air speed for 3777 kg	140
17.9	Climbing speed against True air speed for 4600 kg	141
17.10	Specific fuel consumption against true air speed	142
17.11	Speed against Range for 0 m	145
17.12	Speed against Range for 5000 ft	146
17.13	Speed against Range for FL100	146
17.14	Payload - Range diagram, FL100, maximal range speed	147
17.15	Payload - Range diagram, FL100, maximal horizontal speed	147
17.16	Speed against Endurance for 0 m	148
17.17	Speed against Endurance for 5000 ft	149
17.18	Speed against Endurance for FL100	149
18.1	Wing loading against maximal horizontal speed	151
18.2	Wing loading against range	152
18.3	Wing loading against stall speed	153
A.1	Competitors aeroplanes	164
B.1	K_1 factor against x_f coordinate - weight configuration 1	165
B.2	K_1 factor against x_f coordinate - weight configuration 2	166
B.3	K_1 factor against x_f coordinate - weight configuration 3	166
B.4	K_1 factor against x_f coordinate - weight configuration 4	167

B.5	K_1 factor against x_f coordinate - weight configuration 5	167
D.1	Complete breakdown	169
D.2	Complete breakdown	170
E.1	Moment of inertia	171

LIST OF TABLES

4.1	Flight performance of EV-55	22
7.1	The pros and cons	35
7.2	The pros and cons	37
11.1	Chosen variables a and b	50
11.2	Data for Figure 11.7	53
11.3	Data for Figure 11.8	54
11.4	Data for Figure 11.9	55
11.5	Change of waterline angle ϕ with a full thrust	57
11.6	Final angle ϕ_{total} between longitudinal axis and water level	57
12.1	Mass, c.g. and inertia characteristic for each group	60
12.2	c.g. position and moment of inertia from SAVLE	63
12.3	Summary of the weight configurations	66
12.4	c.g. position and moment of inertia for seaplane	68
13.1	Weight corrected calibrated stalling speed	70
13.2	Centre of gravity correction	71
13.3	Centre of gravity correction	71
14.1	Load factors n_{w_A} for step landings	73
14.2	Reaction forces F_{Rw_A} for symmetrical step landings	74
14.3	K_1 factor for different weight configuration	76
14.4	Load factors n_{w_B} for bow landings	76
14.5	Reaction forces F_{Rw_B} for symmetrical bow landings	77
14.6	K_1 factor for different weight configuration	78
14.7	Load factors n_{w_C} for stern landings	78
14.8	Reaction forces F_{Rw} for symmetrical bow landings	79
14.9	Reaction forces $F_{Rw_{D,y}}$ and $F_{Rw_{D,z}}$ for unsymmetrical step landings	80
14.10	Load factors n_{w_E} for take-off	81
14.11	Reaction forces F_{Rw} for take-off	81
14.12	Hydrostatic drag D_{HS} and hydrodynamic drag D_{HD}	82
16.1	Limit and Ultimate reaction forces for step landing	88
16.2	Limit and Ultimate reaction forces for bow landing	89
16.3	Limit and Ultimate reaction forces for stern landing	90
16.4	Limit and Ultimate reaction forces for unsymmetrical landing	91
16.5	RBE2 and RBE3 elements	97
16.6	Reaction forces at connection points CP1, CP2 and CP3	100
16.7	Geometrical properties of HB1, R1, R2, R3 and R4	102
16.8	Material properties of HB1, R1, R2, R3 and R4 [23]	102
16.9	Geometrical properties of the lugs	106

16.10	Material properties of the lugs [23]	107
16.11	Summary of tensile and compressive force action on front frame	107
16.12	Reserve factors of lugs from front frame	108
16.13	Geometrical and material properties of the joints - front frame	109
16.14	Reserve factors of the pins - front frame	110
16.15	Buckling of the elements - front frame	111
16.16	Geometrical properties of HB2, R5 and R6	113
16.17	Material properties of HB2, R5 and R6 [23]	113
16.18	Geometrical properties of the lugs L_{R5} , L_{R6} and L_{HB2}	116
16.19	Material properties of the lugs [23]	116
16.20	Summary of tensile and compressive force action on front frame	116
16.21	Reserve factors of lugs from aft frame	117
16.22	Geometrical and material properties of the joints - aft frame	117
16.23	Reserve factors of the pins - aft frame	119
16.24	Buckling of the elements - aft frame	120
16.25	Forces - front frame	121
16.26	Forces - front frame	121
16.27	Forces - front spar	123
16.28	Constraint forces at the lugs	126
16.29	Allowable loads in accordance with [19]	127
16.30	Reserve factors for front spar lugs	128
17.1	Drag coefficient of the struts	130
17.2	Interference drag coefficient of the struts	131
17.3	Total drag of each strut and struts together	132
17.4	Polynomial coefficients for terrestrial version	133
17.5	Polynomial coefficients for seaplane version	133
17.6	Maximal horizontal speed	139
17.7	Climbing speed	141
17.8	Payload configuration 1	143
17.9	Payload configuration 2	144
17.10	Payload configuration 3	144
17.11	Summary of Range and Endurance	150
18.1	Comparision between terrestrial EV-55 and EV-55 Seaplane	154
C.1	Summary of the reaction forces caused by water loads	168
F.1	Input data - PBEAM elements - floats	172
G.1	Input data - PROD elements	173
G.2	Input data - PBEAM elements	173

LIST OF APPENDICES

A	Competitive seaplanes	164
B	K_1 factor graphs	165
C	Summary of the water loads	168
D	Complete weight breakdown	169
E	Moments of inertia	171
F	Input data-PBEAM elements-floats	172
G	Input data - PROD and PBEAM elements - struts and horizontal beams	173

A COMPETITIVE SEAPLANES

List of competitive seaplanes														
Airplane	Crew	Capacity	Length	Wingspan	Height	Wing Area	Empty weight	MTOW	Cruise speed	Stall speed	Range	Service ceiling	Rate of climb	Wing loading
	[-]	[-]	[m]	[m]	[m]	[m ²]	[kg]	[kg]	[km/h]	[km/h]	[nm]	[m]	[m/s]	[kg/m ²]
Units														
GAF Nomad	1	12	12,6	16,5	5,5	31,1	2150	3855	311	88	1074	6400	7,4	124,0
Bombardier 415	2	8	19,8	28,6	8,9	100,0	12880	17170	333	126	2443	4500	8,1	171,7
CanadAir CL-215	2	18	18,8	28,6	9,0	100,3	12065	17100	291	123	2260	4450	5,0	170,5
DHC-2 Beaver	1	6	9,2	14,6	2,7	23,2	1361	2313	230	96	732	5486	5,2	99,7
DHC-6 Twin Otter 400S	1	20	15,8	19,8	5,9	39,0	3121	5670	278	107	1832	8138	8,1	145,4
Murphy Moose	1	5	7,1	11,0	2,0	16,9	816	1587	249	81	965	4575	7,6	93,8
DHC-3 Otter	1	10	12,8	17,7	3,8	34,8	2010	3629	195	93	1520	5730	4,3	104,3
Grumman HU-16	4	10	19,2	29,5	7,9	96,2	10401	13797	200	119	4589	6550	7,4	143,4
Cessna 208 Caravan	1	9	12,7	15,9	4,3	26,0	2598	3792	282	109	1519	2000	3,9	145,8
Quest Kodiak	1	9	10,2	13,7	4,7	22,3	1710	3291	230	109	3700	7620	7,0	147,6
Cessna 185 Amphibian	1	5	8,4	10,9	3,9	16,2	982	1406	251	91	893	4700	4,9	86,8
Cessna 206 Stationair	1	5	8,6	11,0	2,8	16,3	987	1632	263	100	1352	4785	5,0	100,1
Cessna 185 Floats	1	5	8,2	10,9	3,7	16,2	866	1506	261	91	957	5000	4,9	93,0
EV-55 Seaplane	2	9	14,35	16,1	4,66	25,187	3150	4600	353	118	883	-	9,2	182,6

Fig. A.1: Competitors aeroplanes

B K_1 FACTOR GRAPHS

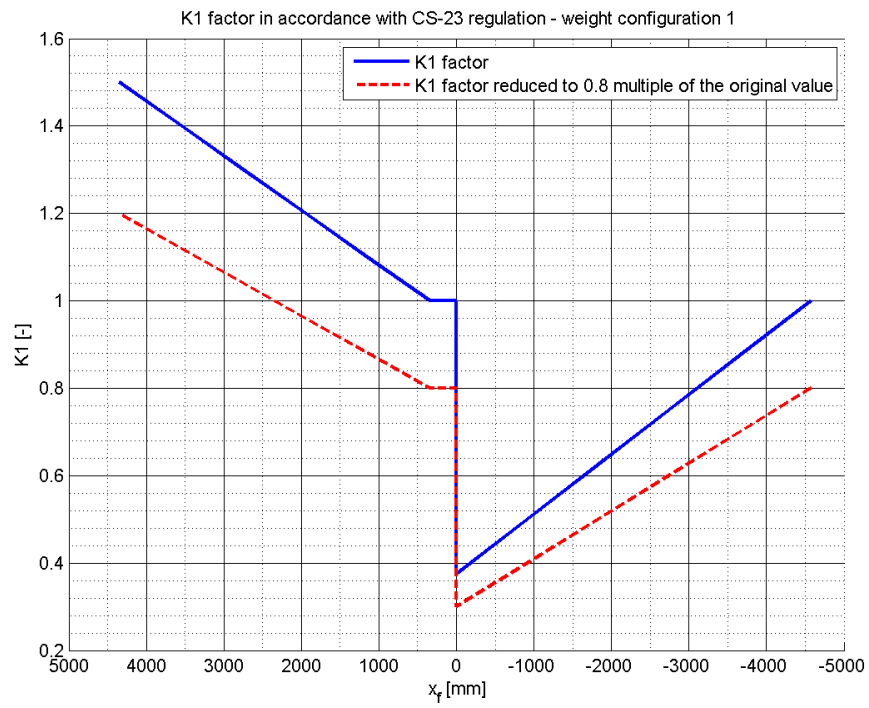


Fig. B.1: K_1 factor against x_f coordinate - weight configuration 1

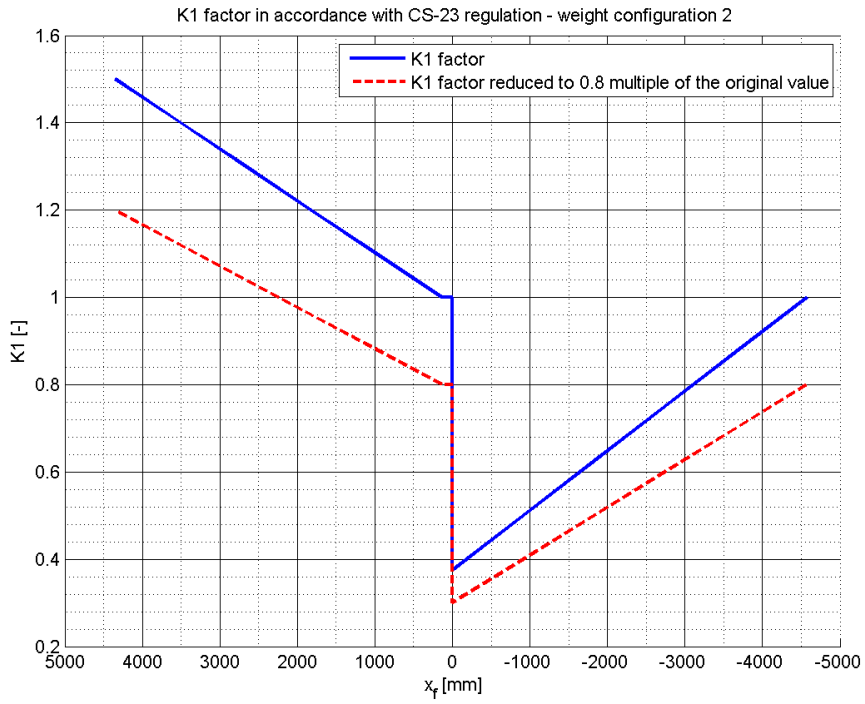


Fig. B.2: K_1 factor against x_f coordinate - weight configuration 2

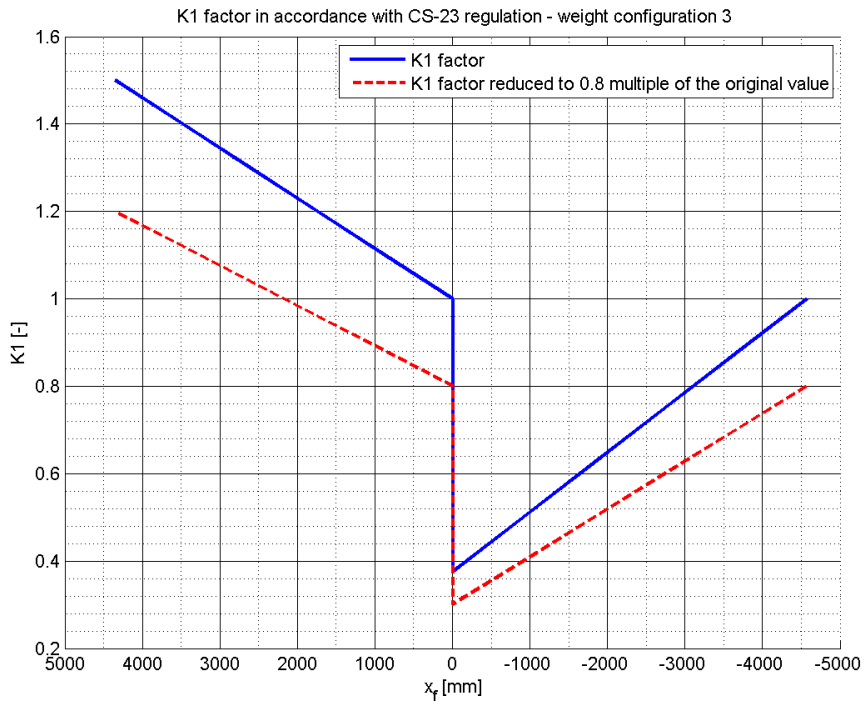


Fig. B.3: K_1 factor against x_f coordinate - weight configuration 3

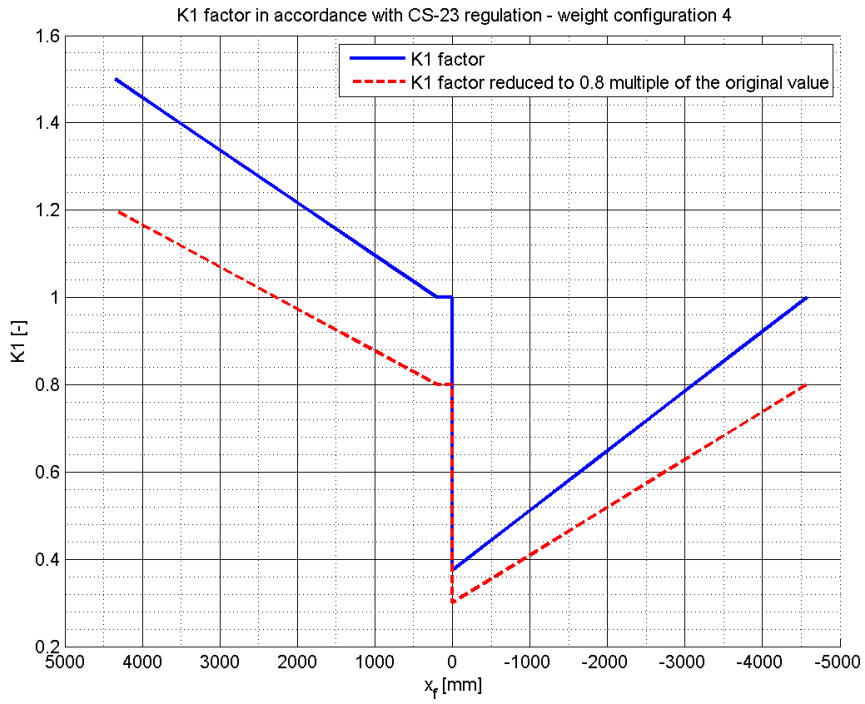


Fig. B.4: K_1 factor against x_f coordinate - weight configuration 4

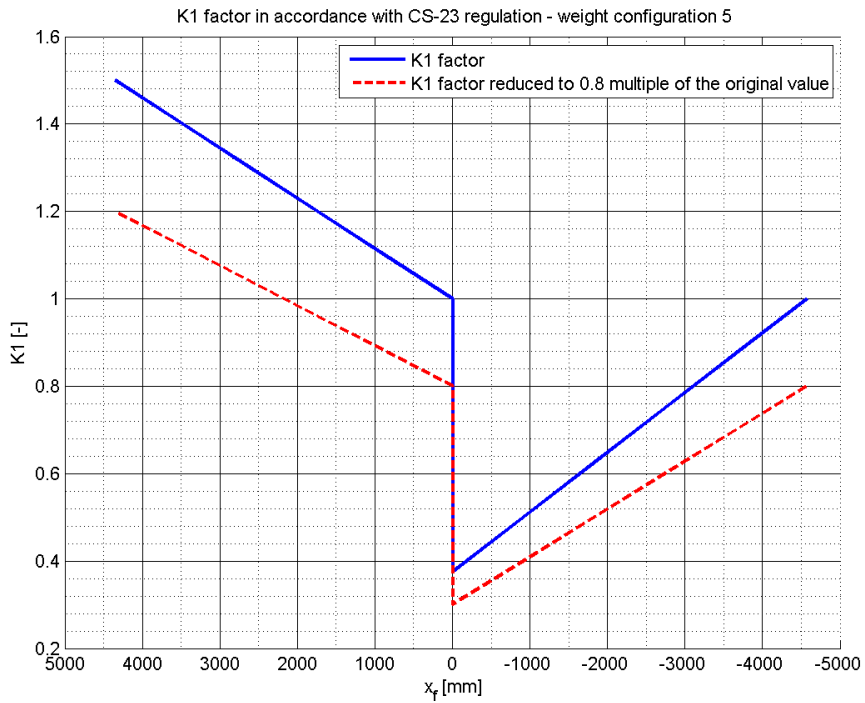


Fig. B.5: K_1 factor against x_f coordinate - weight configuration 5

C SUMMARY OF THE WATER LOADS

Tab. C.1: Summary of the reaction forces caused by water loads

Case	Weight configuration	Position of result force	Resultant force		
		x_f	$F_{Rw_A,x}$	$F_{Rw_A,y}$	$F_{Rw_A,z}$
[-]	[-]	[m]	[N]	[N]	[N]
Step landing	1	0.37	0	108881	0
	2	0.16	0	105338	0
	3	0.011	0	138395	0
	4	0.23	0	190452	0
	5	0.0	0	186099	0
Bow landing	1	3.48	53983	50397	50397
	2	3.48	53621	50060	50060
	3	3.48	67632	63140	63140
	4	3.48	84069	78486	78486
	5	3.48	81706	76279	76279
Stern landing	1	-3.86	6736	49495	0
	2	-3.86	6642	48804	0
	3	-3.86	8318	61124	0
	4	-3.86	10313	75779	0
	5	-3.86	10004	73513	0
Unsym. landing	1	0.37	0	81661	13276
	2	0.16	0	79004	12844
	3	0.011	0	103796	16875
	4	0.23	0	142840	23222
	5	0.0	0	139574	22692

D COMPLETE WEIGHT BREAKDOWN

Weight breakdown								
Serial Number	Name of the weight item	Weight m [kg]	Distance of C.G. of weight item from the beginning of the			Static moment		
			x [m]	y [m]	z [m]	m*x [kg.m]	m*y [kg.m]	m*z [kg.m]
Landing gear down								
1	Main landing wheel L	7,490	6,899	-0,965	-0,736	51,674	-7,228	-5,513
2	Main landing wheel R	7,490	6,899	-0,965	0,736	51,674	-7,228	5,513
3	Break L	12,600	6,899	-0,917	-0,730	86,927	-11,554	-9,198
4	Break R	12,600	6,899	-0,917	0,730	86,927	-11,554	9,198
5	Pneumatic L	9,660	6,898	-0,954	-0,735	66,635	-9,216	-7,100
6	Pneumatic R	9,660	6,898	-0,954	0,735	66,635	-9,216	7,100
7	Landing leg with dumper L	39,700	6,569	-0,767	-1,014	260,789	-30,450	-40,256
8	Landing leg with dumper R	39,700	6,569	-0,767	1,014	260,789	-30,450	40,256
9	cover control unit of main landing gear L							
10	Long rod	0,363	6,484	-0,697	-0,857	2,354	-0,253	-0,311
11	Rod 1	0,107	6,484	-0,875	-0,495	0,694	-0,094	-0,053
12	Inner rod	0,130	6,534	-0,947	-0,559	0,849	-0,123	-0,073
13	Outer rod	0,125	6,484	-0,912	-1,229	0,811	-0,114	-0,154
14	Straight lever	0,177	6,486	-0,749	-0,505	1,148	-0,133	-0,089
15	Angled lever	0,396	6,515	-0,892	-0,353	2,580	-0,353	-0,140
16	cover control unit of main landing gear R							
17	Long rod	0,363	6,484	-0,697	0,857	2,354	-0,253	0,311
18	Rod 1	0,107	6,484	-0,875	0,495	0,694	-0,094	0,053
19	Inner rod	0,130	6,534	-0,947	0,559	0,849	-0,123	0,073
20	Outer rod	0,125	6,484	-0,912	1,229	0,811	-0,114	0,154
21	Straight lever	0,177	6,486	-0,749	0,505	1,148	-0,133	0,089
22	Angled lever	0,396	6,515	-0,892	0,353	2,580	-0,353	0,140
23	Nose landing wheel L	4,400	2,250	-0,611	-0,125	9,900	-2,688	-0,550
24	Nose landing wheel R	4,400	2,250	-0,611	0,125	9,900	-2,688	0,550
25	Nose landing gear leg cover control unit of nose landing gear R	27,200	2,582	-0,660	-0,003	70,230	-17,952	-0,082
26								
27	Horizontal bar	0,862	2,602	-0,512	0,000	2,243	-0,441	0,000
28	Rod L	0,150	2,432	-0,650	-0,184	0,365	-0,098	-0,028
29	Rod R	0,150	2,432	-0,650	0,184	0,365	-0,098	0,028
30	Long rod	0,300	2,432	-0,650	0,184	0,730	-0,195	0,055
31	Spring L	0,250	2,622	-0,655	-0,204	0,656	-0,164	-0,051
32	Spring R	0,250	2,622	-0,655	0,204	0,656	-0,164	0,051
33	Brick L	0,006	2,421	-0,760	-0,196	0,015	-0,005	-0,001
34	Brick R	0,006	2,421	-0,760	0,196	0,015	-0,005	0,001
RESULT		179,470	5,817	-0,800	0,000	1043,993	-143,531	-0,026
Anti blocking system ABS								
35	Control Unit ABS L	1,000	5,300	-0,780	-0,390	5,300	-4,134	-0,390
RESULT		1,000	5,300	-4,134	-0,390	5,300	-4,134	-0,390
Hydraulics - Landing gear up								
36	Cylinder of main landing gear L	5,600	6,064	-0,860	-0,750	33,958	-4,816	-4,200
37	R	5,600	6,064	-0,860	0,750	33,958	-4,816	4,200
38	Cylinder of nose landing gear	5,600	3,230	-0,778	0,000	18,088	-4,357	0,000
RESULT		16,800	5,119	-0,833	0,000	86,005	-13,989	0,000

Fig. D.1: Complete breakdown

Hydraulic items								
39	Hydraulic control distributor	1,000	1,944	-0,665	0,401	1,944	-0,665	0,401
40	Reverse valve	0,030	1,838	-0,652	0,319	0,055	-0,020	0,010
41	Hydraulic control distributor	1,500	2,572	-0,664	0,463	3,858	-0,996	0,695
42	Reverse valve	0,030	2,460	-0,622	-0,305	0,074	-0,019	-0,009
43	Electronic items	0,700	3,267	-0,100	0,000	2,287	-0,070	0,000
44	Hydraulic control distributor	0,100	2,590	-0,612	0,580	0,259	-0,061	0,058
45	Three-way manual valve	0,200	4,063	-0,311	-0,042	0,813	-0,062	-0,008
46	Reducing valve	0,800	2,044	-0,579	0,520	1,635	-0,463	0,416
47	Control valve of brakes L	0,500	2,793	-0,529	0,599	1,397	-0,265	0,300
48	Control valve of brakes R	0,500	2,793	-0,477	0,599	1,397	-0,239	0,300
49	Aeroshell 31 tank	0,200	1,627	-0,412	0,480	0,325	-0,082	0,096
50	ABS valve L	0,400	2,466	-0,580	0,598	0,986	-0,232	0,239
51	AVS valve R	0,400	2,465	-0,512	0,633	0,986	-0,205	0,253
52	Brake valve L	0,300	2,245	-0,555	0,574	0,674	-0,167	0,172
53	Brake valve R	0,300	2,245	-0,502	0,601	0,674	-0,151	0,180
54	Pressure indicator	0,150	1,672	-0,330	0,191	0,251	-0,050	0,029
55	Pressure indicator	0,150	1,672	-0,330	0,117	0,251	-0,050	0,018
56	Emergency brake valve	0,800	3,970	-0,384	-0,047	3,176	-0,307	-0,038
57	Hydraulic unit	7,200	1,535	-0,519	0,298	11,052	-3,737	2,146
58	Filter	0,500	1,656	-0,325	0,405	0,828	-0,163	0,203
59	Accumulator 1 liter	4,600	1,567	-0,307	-0,084	7,208	-1,412	-0,386
60	Combined safety valve	0,120	1,416	-0,456	-0,381	0,170	-0,055	-0,046
61	Reverse valve	0,030	1,672	-0,284	0,268	0,050	-0,009	0,008
62	Pressure indicator	0,150	1,672	-0,330	0,041	0,251	-0,050	0,006
63	Accumulator 2,5 liter	6,800	1,567	-0,323	-0,173	10,656	-2,196	-1,176
64	Pressure indicator	0,150	1,672	-0,330	-0,308	0,251	-0,050	-0,046
65	Pressure indicator	0,150	1,672	-0,330	-0,233	0,251	-0,050	-0,035
66	Combined safety valve	0,120	1,554	-0,434	-0,383	0,186	-0,052	-0,046
67	Reverse valve	0,030	1,671	-0,283	-0,156	0,050	-0,008	-0,005
68	Distributive valve	0,080	1,672	-0,342	-0,108	0,134	-0,027	-0,009
69	flaps cylinder	1,800	7,044	0,991	-0,108	12,679	1,784	-0,194
70	Hydraulic control distributor	1,500	2,152	-0,664	0,434	3,228	-0,996	0,651
71	Reverse valve	0,030	2,054	-0,622	0,305	0,062	-0,019	0,009
72	Hydraulic control distributor	0,700	2,402	-0,664	0,519	1,681	-0,465	0,363
73	Dumping valve	0,200	2,352	-0,668	0,436	0,470	-0,134	0,087
74	Three-way manual valve	0,200	4,127	-0,311	-0,042	0,825	-0,062	-0,008
75	Hydraulic liquid	6,800	1,680	-0,530	0,298	11,424	-3,604	2,026
76	Hosepipe	0,800	5,327	-0,259	-0,013	4,262	-0,207	-0,010
77	Fittings	1,800	3,070	-0,550	0,204	5,526	-0,990	0,367
78	Handle of accumulator	1,200	1,614	-0,301	-0,033	1,937	-0,361	-0,040
79	Nitrogen 8MPa / 4 litres	0,600	1,487	-0,446	-0,146	0,892	-0,268	-0,088
80	Pipelines	5,800	3,869	-0,615	0,325	22,440	-3,567	1,885
RESULT		49,420	2,379	-0,421	0,177	117,554	-20,797	8,772
TOTAL RESULT								
		246,690	5,079	-0,740	0,034	1252,851	-182,451	8,355

Fig. D.2: Complete breakdown

E MOMENTS OF INERTIA

Weight configuration				1	2	3	4	5
SAVLE configuration				404	1753	2011	509	1812
Total	c.g. terrestrial version	XTG	[mm]	6124,1	6403,4	6555,3	6283,7	6555,5
		YTG	[mm]	327,5	284,5	224,1	393,3	110,5
		ZTG	[mm]	9,3	1,0	25,0	12,0	1,1
		%MAC	[-]	8,0	25,5	35,0	18,0	35,0
	Inertia moments - terrestrial version	IxG	[kg.m2]	12415,3	12250,1	12733,0	20041,4	13204,7
		IyG	[kg.m2]	26486,7	26035,6	28754,2	34539,7	26726,2
		IzG	[kg.m2]	18220,1	18350,3	20489,4	19490,7	18811,0
Removable item	Landing gear	XTG	[mm]	5817,0	5817,0	5817,0	5817,0	5817,0
		YTG	[mm]	-800,0	-800,0	-800,0	-800,0	-800,0
		ZTG	[mm]	0,0	0,0	0,0	0,0	0,0
		IxG	[kg.m2]	228,2	211,2	188,4	255,6	149,0
		IyG	[kg.m2]	16,9	61,8	98,0	39,1	98,1
		IzG	[kg.m2]	245,1	272,8	286,1	294,6	246,7
		Removable item	ABS	XTG	[mm]	5300,0	5300,0	5300,0
YTG	[mm]			-780,0	-780,0	-780,0	-780,0	-780,0
ZTG	[mm]			-390,0	-390,0	-390,0	-390,0	-390,0
IxG	[kg.m2]			1,4	1,3	1,2	1,5	1,0
IyG	[kg.m2]			0,8	1,4	1,8	1,1	1,8
IzG	[kg.m2]			1,9	2,4	2,6	2,3	2,4
Removable item	Hydraulic cylinders			XTG	[mm]	5119,0	5119,0	5119,0
		YTG	[mm]	-833,0	-833,0	-833,0	-833,0	-833,0
		ZTG	[mm]	0,0	0,0	0,0	0,0	0,0
		IxG	[kg.m2]	22,6	21,0	18,8	25,3	15,0
		IyG	[kg.m2]	17,0	27,7	34,7	22,8	34,7
		IzG	[kg.m2]	39,6	48,7	53,4	48,1	49,6
		Addable item	Left float	XTG	[mm]	6020,0	6020,0	6020,0
YTG	[mm]			-1640,0	-1640,0	-1640,0	-1640,0	-1640,0
ZTG	[mm]			1750,0	1750,0	1750,0	1750,0	1750,0
IxG	[kg.m2]			1295,2	1269,6	1211,8	1342,2	1151,2
IyG	[kg.m2]			581,1	611,6	622,0	590,2	637,4
IzG	[kg.m2]			736,7	730,9	714,4	796,2	638,4
Addable item	Right float			XTG	[mm]	6020,0	6020,0	6020,0
		YTG	[mm]	-1640,0	-1640,0	-1640,0	-1640,0	-1640,0
		ZTG	[mm]	-1750,0	-1750,0	-1750,0	-1750,0	-1750,0
		IxG	[kg.m2]	1306,4	1286,9	1250,8	1361,6	1174,9
		IyG	[kg.m2]	592,3	628,9	661,0	609,7	661,0
		IzG	[kg.m2]	736,7	730,9	714,4	796,2	638,4
		Addable item	Struts	XTG	[mm]	4677,6	4677,5	4677,5
YTG	[mm]			-1265,0	-1265,0	-1265,0	-1265,0	-1265,0
ZTG	[mm]			0,0	0,0	0,0	0,0	0,0
IxG	[kg.m2]			329,7	312,2	288,4	357,5	246,1
IyG	[kg.m2]			272,0	387,3	458,6	335,4	458,7
IzG	[kg.m2]			601,7	699,4	746,7	692,9	704,5
Total	c.g. seaplane			XTG	[mm]	6123,5	6334,4	6485,6
		YTG	[mm]	121,3	82,0	26,9	181,3	-76,7
		ZTG	[mm]	7,4	23,4	32,1	16,5	32,1
		%MAC	[-]	8,0	21,2	30,6	17,4	31,4
	Inertia moments - seaplane	IxG	[kg.m2]	14781,5	14527,4	14869,9	22476,0	15186,1
		IyG	[kg.m2]	28031,3	27716,6	30499,0	36153,7	28469,8
		IzG	[kg.m2]	20142,5	20331,7	22460,5	21572,8	20614,7

Fig. E.1: Moment of inertia

F INPUT DATA-PBEAM ELEMENTS-FLOATS

Tab. F.1: Input data - PBEAM elements - floats

Name	PID	MID	A	I1	I2	J
[-]	[-]	[-]	[mm ²]	[mm ⁴]	[mm ⁴]	[mm ⁴]
Front part						
PBEAM_1	1010	4	3532	4.50E7	3.74E7	9.17E7
PBEAM_2a	2	4	5570	1.83E8	1.43E8	9.17E7
PBEAM_2b	3	4	6596	3.38E8	2.26E8	9.17E7
PBEAM_3	4	4	7306	5.00E8	3.20E8	5.00E8
PBEAM_4	5	4	8083	7.46E8	4.27E8	5.00E8
PBEAM_5	6	4	8370	8.28E8	4.81E8	5.00E8
PBEAM_6	1012	4	8430	8.18E8	4.94E8	2.00E9
PBEAM_7	1013	4	8431	8.29E8	4.95E8	2.00E9
PBEAM_8	1014	4	8431	8.29E8	4.95E8	2.00E9
PBEAM_9a	1015	4	8431	8.29E8	4.95E8	2.00E9
PBEAM_9b	1017	4	8431	8.29E9	4.95E9	2.00E9
PBEAM_9c	1018	4	8431	8.29E9	4.95E9	2.00E9
PBEAM_9d	1019	4	8431	8.29E9	4.95E9	2.00E9
PBEAM_9e	1020	4	8431	8.29E9	4.95E9	2.00E9
Aft part						
PBEAM_10	15	4	7648	5.13E8	3.92E8	1.80E8
PBEAM_11	1021	4	7328	4.49E8	3.53E8	1.70E8
PBEAM_12	1022	4	6837	3.28E8	2.98E8	1.60E8
PBEAM_13	1023	4	6273	2.35E8	2.42E8	1.50E8
PBEAM_14	1024	4	5817	1.62E8	2.03E8	1.40E8
PBEAM_15	1025	4	5382	1.15E8	1.68E8	1.30E8
PBEAM_16	1026	4	4947	7.01E7	2.38E8	1.15E8
PBEAM_17	1027	4	4407	4.74E7	1.04E8	1.10E8

G INPUT DATA - PROD AND PBEAM ELEMENTS - STRUTS AND HORIZONTAL BEAMS

Tab. G.1: Input data - PROD elements

Name	PID	MID	A	J
[-]	[-]	[-]	$[mm^2]$	$[mm^4]$
PROD_1	1016	4	465.5	114828
PROD_2	1028	4	183.8	85363
PROD_3	1031	4	183.8	85363
PROD_4	1032	4	465.5	114828
PROD_5	1033	4	254.5	114828
PROD_6	1034	4	254.5	114828

Tab. G.2: Input data - PBEAM elements

Name	PID	MID	A	I1	I2	I12	J
[-]	[-]	[-]	$[mm^2]$	$[mm^4]$	$[mm^4]$	$[mm^4]$	$[mm^4]$
PBEAML_HorStrut_f	1030	4	832	6.9E5	1.9E5	0.12	4.2E5
PBEAML_HorStrut_a	1029	4	832	6.9E5	1.9E5	0.12	4.2E5